"I hereby declare that I have read through this report entitle "*Analysis on Passive Vehicle Suspension System*" and found that it has comply the partial fulfillment for awarding the degree of Bachelor of Electrical Engineering (Control, Instrumentation and Automation)"
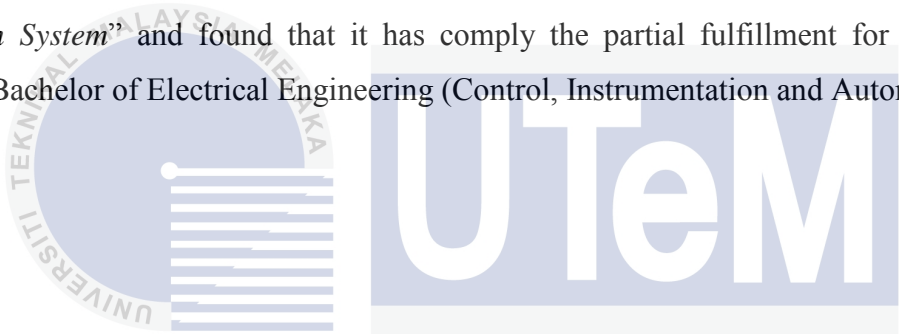
Signature   :
………………………………….

Supervisor name   :   Dr. Aliza Bte Che Amran
…………………………………….

Date   :   18/6/2014
…………………………………….

ANALYSIS ON PASSIVE VEHICLE SUSPENSION SYSTEM

CHIN FEN YING

A report submitted in partial fulfillment of the requirements for the degree of Bachelor in Electrical Engineering (Control, Instrumentations and Instrumentations)

Faculty of Electrical Engineering

UNIVERSITI TEKNIKAL MALAYSIA MELAKA

2014

I declare that this report entitle "*Analysis on Passive Vehicle Suspension System*" is the result of my own research except as cited in references. The report has not been accepted for any degree and is not concurrently submitted in candidature of any other degree.

Signature : ……………………………………….

Name : Chin Fen Ying
……………………………………….

Date : 17/6/2014
……………………………………….

ACKNOWLEDGMENT

It is a pleasure to thank those who made this thesis possible. I would like to acknowledge and extend my heartfelt gratitude to my supervisor, Dr Aliza Binti Che Amran for her vital encouragement and support. This thesis would not have been possible to be completed if without her valuable guidance regarding the production of this thesis. Her ideas, suggestions, advices and guidance have really helped me to improve and understand more on the objectives of the thesis.

In addition, I would like to say thanks for all master students of Motion Control Lab who taught me about OriginPro 8, Matlab Simulink and MicroBox 2000/2000C. Last but not least, I would also like to thank my course mates, for the help and inspiration extended during the whole period. They have made available their support in a number of ways. For instance, they had been constantly given suggestions and assistance for the completion of the thesis.

ABSTRACT

Vehicle suspension system plays an important role in automobile industry in order to guarantee good ride quality of vehicle. Basically, traditional suspension system which is passive suspension system consists of springs, shock absorbers and linkages that connect a vehicle body to its wheels. However, passive suspension system is an open loop system which does not contain any controllers to control the performance of the vehicle suspension system when passing through bumpy on the road. In this report, construction of an experiment setup to represent passive vehicle suspension system for quarter car model is considered. Experimental setup for passive suspension system is important because proper modeling of vehicle suspension system could lead to good controller design and hence improve the performance of the vehicle suspension system. This report primarily focuses on the two-degree-of freedom quarter-car model to represent passive suspension system. Semi-active and active suspension system will not be covered in this project A number of experiments have been carried out using the experiment setup in order to identify the characteristic of this experimental setup. Experiments with different vehicle body mass, different period for one pulse and different pulse width of input pressure of the road excitation have been conducted. The experiments results are evaluated based on the vehicle body displacement and tire displacement of the experimental setup. However, experiments give different results when three parameters are varied. Experiment results show that the pulse width of the input pressure is directly affected the characteristic of this passive suspension system experimental setup. Lastly, simple simulation has been done in order to compare the simulation and experiments results. The amplitude and shape of the simulation and experimental results are evaluated in this report.

ABSTRAK

Sistem kenderaan memainkan peranan penting bagi menjamin kualiti perjalanan kenderaan yang baik. Pada asasnya, sistem suspensi tradisional yang merupakan sistem suspensi pasif terdiri daripada spring, penyerap henjutan yang menghubungkan kenderaan dan roda . Walau bagaimanapun, sistem suspensi pasif ialah sistem gelung terbuka yang tidak mengandungi apa-apa pengawal untuk mengawal prestasi sistem kenderaan apabila melalui permukaan jalan raya yang beralun. Oleh itu, pembinaan sebuah setup eksperimen untuk mewakili sistem kenderaan pasif untuk suku model kereta telah dipertimbangkan. Penyediaan eksperimen sistem pasif adalah penting kerana pemodelan baik sistem suspensi kenderaan boleh membawa kepada reka bentuk pengawal yang baik dan dengan itu meningkatkan prestasi sistem penggantungan kenderaan. Laporan ini memberi tumpuan terutama kepada dua darjah kebebasan model suku – kereta untuk mewakili sistem suspensi pasif. Sistem suspensi separuh–aktif dan aktif tidak akan termasuk dalam projek ini Beberapa eksperimen telah dijalankan dengan menggunakan setup eksperimen untuk mengenal pasti ciri setup eksperimen ini. Eksperimen dengan jisim kereta yang berbeza dan tekanan input berbeza lebar denyut telah dijalankan. Keputusan eksperimen dinilai berdasarkan anjakan badan kenderaan dan anjakan tayar. Tetapi, keputusan eksperimen akan berubah apabila tiga parameter berdasarkan eksperimen set dimanipulasi. Saiz input tekanan secara langsung memberi kesan kepada ciri bagi sistem suspensi pasif persediaan eksperimen ini.. Akhir sekali, simulasi telah dilakukan untuk membandingkan keputusan simulasi dan eksperimen. Amplitud dan bentuk keputusan simulasi dan eksperimen telah dinilai dalam laporan ini

TABLE OF CONTENTS

UNIVERSITI TEKNIKAL MALAYSIA MELAKA

LIST OF TABLES

LIST OF FIGURES

LIST OF ABBREVIATIONS

M_s	-	Mass of vehicle body (sprung mass)
M_{us}	-	Mass of the wheel and tire (unsprung mass)
k_s	-	Spring constant of the suspension system
k_t	-	Spring constant of the tire
b_s	-	Dashpot constant (shock absorber)
r	-	Vertical displacement of road input
X_s	-	Vertical displacement of sprung mass
X_{us}	-	Vertical displacement of unsprung mass

LIST OF APPENDICES

CHAPTER 1

INTRODUCTION

The purpose of this chapter is to provide an introduction about the project carried out in this course. First of all, an overview of vehicle suspension system is being introduced. Then, problem statement of this project is explained. Next, project objectives and scopes are discussed at the end of this chapter.

1.1   Research Background

Nowadays, condition of local roads in Malaysia is getting worst. Roads are full of potholes, improper road shoulders and bumps. This condition causes a lot of problems especially damage to vehicles' parts and system where the potential damage includes tire puncture, premature wear on shocks and struts, wheel rim damage, suspension damage, steering system misalignment and engine damage. Moreover, those dreadful road conditions will affect drive stability, steering and braking which will lead to road accident. For example, a broken shock or strut which caused by severe hitting of a deep pothole could alter the steering and handling of the vehicle and create dangerous driving. This situation highlights that quality of road surface is very important in ensuring safe driving on the road. Besides that, good suspension system will increase the protection of vehicles from bad road conditions and hence decreases the rate of accidents in our country. In the above mentioned case, good suspension system will helps the vehicle to "absorb" the impact of the pothole thus the driving quality is not interrupted by bad road surfaces. Figure 1.1shows the road conditions in Malaysia.

(a)   (b)

Figure 1.1: (a) Bad road quality in Malaysia [19] and (b) Pothole on the road surface in

Malaysia [18]

Vehicle suspension system plays an important role in automobile industry in order to guarantee good quality of car. A good vehicle suspension system provides high vehicle handling, good drive stability, ensures the comfort of passengers, and good isolation from road noise, road shocks and vibration. Suspension system consists of springs, shock absorbers and linkages that connects a vehicle to its wheels and allows relative motion between the two [16]. In other words, the suspension system separates the car body and the car wheel. The shock absorber dissipates shock energy received from road bump without causing undue oscillation in the vehicle. However, the spring absorbs the shock energy received from road bump and converts it into potential energy of spring. Figure 1.2 shows an example of a spring and shock absorber.

(a)   (b)

Figure 1.2: (a) Diagram of spring and shock absorber [20], and (b) How absorber and spring

are attached to a vehicle [21]

The suspension systems can be divided into three types which are passive, semi-active, and active suspension system. The passive suspension system is an open-loop control system that does not contain any external energy sources and only consists of passive elements which are spring and shock absorber. Due to open-loop control system characteristic, the performance of the passive suspension system cannot be adjusted to achieve the desired performance. Passive suspension system has the ability to store energy via a spring and dissipate it via a shock absorber. However, passive suspension system does not have the function of supplying energy to the system. The performance of the passive suspension system can be improved by adding active components to the system.

Semi-active suspension system is modified from passive suspension system by changing the shock absorber to a variable shock absorber [4]. The damping coefficient of the shock absorber can be adjusted in order to follow the road conditions. Active suspension system is a closed-loop control system that consists of external energy source. It is modified by adding force actuator to the system. The performance of the active suspension system can be adjusted due to its closed-loop control system characteristic. Besides that, it has the ability to store, dissipate and to introduce energy to the system. At the moment the sensor of the system detects the changes of the road surface, the data of the road surface will be sent to the controller. Then the controller will calculate amount of energy need to be added or dissipated from the system in order to keep the tire in touch with the road and thus improve the handling quality and ride comfort [2]. Figure 1.3 shows the schematic of passive, semi-active and active suspension system. Schematic of Figure 1.3 is suggested by D.S.Joo et al. [8].
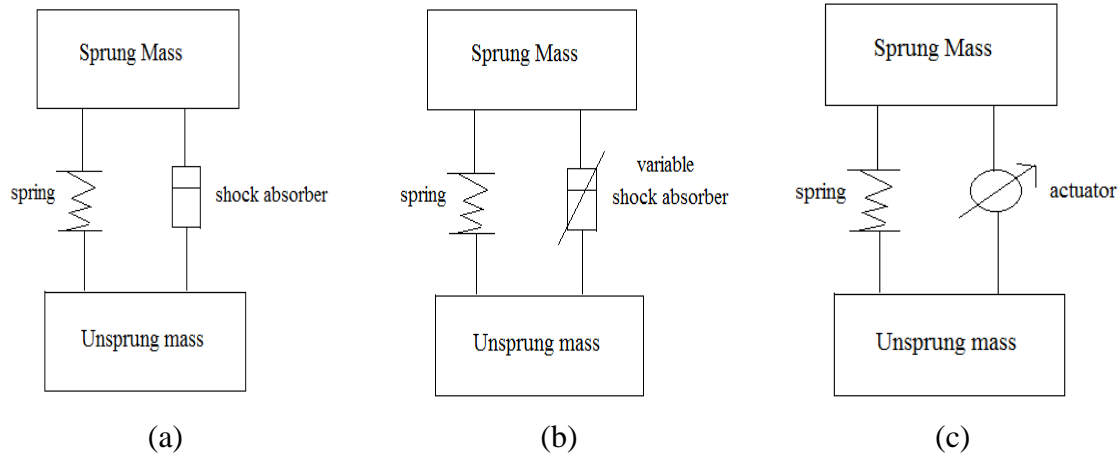
Figure 1.3: (a) Passive suspension system [8], (b) Semi-active suspension system [8], and (c) Active suspension system [8]

1.2   Research Motivation

At present, vehicle suspension system plays an important role in order to guarantee good performance of car. Vehicle suspension system aims to provide passenger with ride comfort while maintaining the safety and stability of the vehicle [3]. However, most of the vehicles are using traditional passive suspension system which has very limited performances and not able to provide good performance of vehicle. When a wheel passes through a bump, there is a vertical force and energy is transferred to the spring which makes it to oscillate vertically. Oscillation of the wheel causes the wheel and the car's frame to move upwards and thus the wheel loses contact with the road surface. Then, the wheel will move downwards back to the ground due to the gravity. When the oscillation of the wheel is large, the suspension travel and the wheel deflection of car are large. Suspension travel is the measured distance between the sprung mass with the unsprung mass. Wheel deflection is the measured distance between unsprung mass with the road profile. Sprung mass are parts of the vehicle supported on the spring such as car body, the frame, the engine, and associated parts. Unsprung mass are parts of vehicle that are not supported by spring, the wheels, tires, and brake assemblies. Figure 1.4 shows the explanation of suspension travel and wheel deflection in picture.
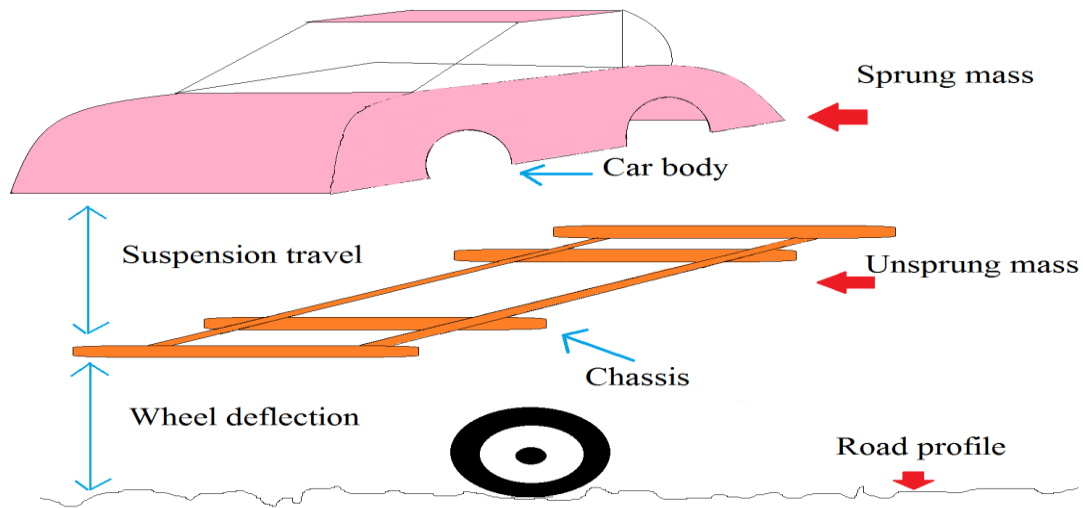
Figure 1.4: Suspension travel and wheel deflection

Therefore, large oscillation between sprung mass and unsprung mass (suspension travel) cause passengers to feel bumpy on the road and bad drive stability. Besides that, passengers will feel the same condition if large oscillation occurs between unsprung mass with road profile (wheel deflection). Passengers feel insecure and not comfortable when sitting inside the car. In long run, bad suspension system could affect the backbone of the passengers and may cause serious injuries.

Thus, analysis on passive suspension system is conducted in order to determine the characteristic of the vehicle suspension system. Proper modeling of vehicle suspension system could lead to good controller design and hence improve the performance of the vehicle suspension system. Vehicle suspension system with controller or active suspension system will be conducted by future final year student. This research will carry out study and analysis on passive suspension system only which represents the open loop system of active suspension system.

1.3   Objectives

- To construct a prototype to represent passive suspension system based on modeling of quarter-car suspension system
- To run open-loop experiments and identify the characteristics of the prototype in terms of the vehicle body and tire positions
- To observe the difference between passive suspension system simulations and experiments in terms of the vehicle body and tire positions

1.4   Scope of Research

This report will primarily focus on the two-degree-of freedom quarter-car model to represent passive suspension system. Semi-active and active suspension system will not be covered in this project. In this report, the simulation and the experiment setup will carry out at the same time. The modeling of the system is simulated by using MATLAB. The performances covered in this project are the vehicle body displacement and tire deflection of vehicle. If the model represents the system well, then the research could be continued on designing a controller. Therefore, vehicle suspension system with controller or active suspension system will be conducted by future final year student.

CHAPTER 2

LITERATURE REVIEW

In previous chapter, a brief introduction about this project has been provided. Now, this chapter will explain more about the vehicle suspension system. Besides that, techniques used to improve vehicle suspension system which have been proposed by other researches will be presented in this chapter.

2.1   Basic Principles

As mentioned in Chapter 1, vehicle suspension system plays an important role in automobile industry in order to guarantee good quality of vehicle. Good suspension system ensures safe ride of passengers and good handling performance by making sure the wheels of vehicle follow the road condition. In addition, suspension system isolates the vehicle body from road shocks and vibration generated by the road surface for comfortable ride [4]. Basically, vehicle suspension system consists of spring, shock absorber and linkages that connect a vehicle to its wheel [16]. There are three types of vehicle suspension system commonly used in the markets which are passive, semi-active, and active suspension system.

2.1.1 Passive Suspension System

Passive suspension system is a traditional suspension system which consists of spring and shock absorber only. The parameters of spring and shock absorber are fixed and cannot be adjusted. Passive suspension system has the ability to store energy via a spring and dissipate it via shock absorber. However, passive suspension system does not have the function of supplying energy to the system [2]. The performance of the passive suspension system can be improved by adding active components to the system.

2.1.2 Semi-active Suspension System

Semi-active suspension system is quite similar with passive suspension system but it is modified by changing the shock absorber to a variable shock absorber [4]. The damping coefficient of the shock absorber can be adjusted in order to ensure the wheel of vehicle keep in touch to the ground.

2.1.3 Active Suspension System

Active suspension system is modified from passive suspension system by adding force actuator parallel to the spring and shock absorber. Active suspension system has the ability to store, dissipate and introduce energy to the system [2]. Schematic of passive, semi-active and active suspension system can be referred from Figure 1.3.

2.1.4   Advantages and Disadvantages of Each Suspension System

When comparing the advantages of semi-active and active suspension system, it can be found that semi-active suspension has simpler design, low implantation cost, uses less power, and more reliable. However, semi-active suspension system does have disadvantage. The damper of the semi-active suspension system is resisted hence the performance is not as good as active suspension system [5]. Even though active suspension system has higher power consumption, more complex design, more expensive, and heavy weight as compared to semi-active suspension system, yet it has wider range of force and no force-velocity constraint [6]. Therefore, active suspension system can achieve better performance as compared to semi-active suspension system. Even though passive suspension system cannot provide better performance as compared to semi- active and active suspension system, it is a reliable system, inexpensive and does not require power consumption. As a result, passive suspension system is popular in automobile industry [17].

2.2   Others Research and Studies

Nowadays, numerous of research projects using different types of active and semi-active suspension system has been proposed. Armin Barouz et al. [2] have proposed a Linear Quadratic Control (LQR) controller for active suspension system by using a quarter car model. Quarter car model has been chosen as it is simple and able to detect important characteristics of full car model. In addition, LQR controller is used because the factors of the performance index can be weighted according to the designer's desires. In this research, the performance of the active suspension system is evaluated using different types of road profile. At the end of the research, it is found that the suspension travel of active suspension system has reduced more than half of the value of passive suspension system hence improves the ride comfort and road handling of vehicle.

At present, many researches proposed two degree-of freedom quarter car model in their project [2, 4, 7, 8, and 13]. However, L.J.Yue et al. [3] has proposed a five-degree-of

freedom half-body car model using Fuzzy Logic Controller. Five-degree-of freedom half body model has been selected since it can capture the vertical movement of the four wheels and the body center of gravity, pitching movement of the body and the most important data which is the response of passenger. As compared to five-degree-of freedom half-body car model, a two-degree-of freedom quarter body model only can capture the vertical movement of vehicle body. Therefore, it can be seen that five-degree-of freedom half-body car model has more advantages than a two-degree-of freedom quarter body model.

Besides that, Y.Zheng [4] has proposed a Fuzzy logic Controller for active suspension system. The advantage of this controller is it does not require precise mathematical model of a system because it is a special form of knowledge-based control. Moreover, the mathematical control strategy can be translated into linguistic control strategy by using fuzzy logic controller. Basically, there are three steps need to be carry out by using fuzzy logic controller. Those steps are fuzzification, reasoning using the fuzzy rule base, and defuzzification [3]. In this research, body acceleration and the body velocity are the two linguistic variables used in the system. According to the results obtained in this project, sprung mass acceleration and the tire deflection of the active suspension system are significantly lower than the passive suspension system. Thus, the performance of the vehicle is greatly improved by using fuzzy logic controller as active suspension system.

Furthermore, J.Sun et al. [6] has conducted an experimental study on using three different types of controllers for active suspension system. The controllers are sky-hook control, generalized adaptive control, and least means squares (LMS) adaptive control. Generalized adaptive control is a control course during which the response of the vehicle system is generally used to adjust suspension's damper to optimization step by step. By comparing the three different types of controllers, it can be concluded that the LMS adaptive control strategy shows big improvement in the performance of suspension system. The acceleration PSD (power spectral density) using LMS adaptive control strategy decreases sharply for 8-10 times in high or low frequency resonance band as compared to passive suspension system.

Y.Ai et al. [12] has carried out their research by combining Neural Network (NN) with self-adapted control in semi-active control system. In this research, neural network toolbox is used to design NN recognizer and NN controller. Artificial neural network is a system simulating human brain message process mechanism. Learning is one of main characters of NN. The combination of NN with self -adaptation control allow controller to acquire greater adaptive ability to work in complicated circumstance. In addition, combination of NN with self-adapted control the car body acceleration better than fuzzy control. However, the result of the wheel speed for NN with self-adapted control is worse than fuzzy control.

Even though numerous of research projects using different types of active and semi-active suspension system has been proposed, there are some research projects studied about the passive suspension system. Y.P.Kuo et al. [17] has proposed a passive vehicle suspension system design using evolutionary algorithm. In this research, Evolutionary Programming (EP) is used to determine the optimum set of nonlinear system parameters for the nonlinear passive suspension system. Besides that, better exploitation of the optimal passive suspension system parameters can be achieved using evolutionary programming with dynamic step size. In this research, researchers first determine the frequency responses of the front tire deflection and body acceleration using different spring stiffness and damper coefficients. It is found that the resonance frequencies are greatly influenced by the variations parameter of the spring and damper. Therefore, the body acceleration and tire deflection can be reduced by selecting an optimum set of damper and spring parameters using evolutionary programming. The fitness function is calculated using an equation. As the fitness function increases, the overall performance of the passive suspension system is improved as well. According to the results obtained in this research, it can be seen that system with proposed evolutionary programming with dynamic step size has larger fitness values as compared to system without using evolutionary programming. Thus, the performance of the passive suspension system has greatly improved by using evolutionary programming.

Recently, researches starting to focus more on developing prototype by applying vehicle suspension system approach. S.J.Huang et al. [23] has proposed an quarter car active suspension system using hydraulic actuator. Due to the nonlinear and time-varying behavior of

the hydraulic actuator, adaptive sliding controller with self-tuning fuzzy compensation is used to overcome the problem. This adaptive sliding controller with self-tuning fuzzy compensation is different with the conventional model-based sliding controller as try and error fuzzy tuning parameters has been carried out in this research. At the end of the research, results show that the proposed controller has greatly improved the performances of the suspension system. The oscillation amplitude of the sprung mass using proposed controller is much lower than the conventional model-based sliding controller.

Besides that, G.Priyandoko et al. [24] has carried out a research on quarter car suspension system using Active Force Control (AFC) with iterative learning algorithm for active suspension system. In addition, pneumatic actuator, pressure sensor, current sensor, accelerometer, LVDT, and programmable logic controller (PLC) are used for the experimental setup. Basically, this proposed control system consists of three feedback control loops where PI controller is used to track the force of pneumatic actuator; AFC with IL algorithm is used to compensate the disturbances and lastly PID controller is used for the calculation of the desired force. According to the results obtained from this research, the acceleration and displacement of the vehicle body using proposed controller have been reduced by comparing to the PID controller. Hence, this shows that AFC with IL algorithm is a better controller than the PID controller.

2.3   Summary of review

After going through other researches projects, it can be found that different types of controllers are used in semi-active and active suspension system. Those controllers applied to active or semi-active suspension system have greatly improved the performances of the suspension system as compared to conventional passive suspension system. Therefore, semi-active and active suspension systems are getting more popular in automotive industry.

Besides that, most of the research projects proposed active suspension system by using model in Figure 2.1 [2, 4, 6, 7, and 10]. However, modeling of passive suspension system is

not shown in their projects. Therefore, modeling of the passive suspension system is taken from the model proposed by P.Alexandru et al. [10] as shown in Figure 3.2.
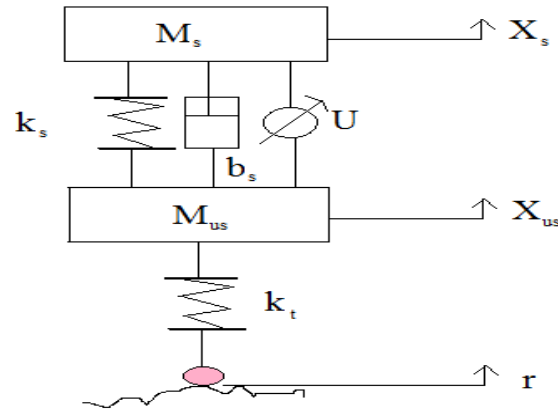
Figure 2.1: Active suspension system [10]

A good model for passive suspension system is very important in a research as it represents the open loop system of active suspension system. This means that the passive suspension system does not include any controller to adjust the performances in order to achieve desired performances. As a result, proper modeling of passive suspension system could help to design good controller on active suspension system and therefore improve the performance of the vehicle suspension system.

CHAPTER 3

METHODOLOGY

In this chapter, the processes of constructing the experimental setup of the research are explained. List of components used in the experiment setup and the calibration process of the components are discussed in Section 3.1. Besides that, the steps used to obtain the modeling of passive suspension system that has been studied through literature review are covered in Section 3.2. During this research, the experiment setup and the simulation of the passive suspension system were carried out in parallel.

3.1 Experimental Hardware and Setup

The purpose of developing this experimental setup is to construct a prototype which can represent the quarter car passive suspension system. Since vehicle passive suspension system is an open loop system therefore this prototype will not involve any controller to control the dynamic behavior of the of quarter car suspension model.

This quarter car passive suspension system experimental setup consists of fourteen bearings, three Infrared sensors (IR-sensor), one gas spring, one double acting cylinder, two flow control valve, one pressure regulator, one 5/2 way valve and two springs with different spring coefficient. Apart from these items, the setup also consists of a laptop, a set of Micro-Box 2000/2000C. Figure 3.1 shows the schematic view of experimental setup while Figure 3.2 shows the experimental setup itself. Table 3.1 shows a short summary about the dimensions of the experimental setup.

Table 3.1: Dimensions of the experimental setup

Hardware	Dimensions (mm)
Base	342 x 342 x8
Plate	200 x 200 x 8
Shaft	1000 x 10
Height of experimental setup	1000

By referring to Figure 3.1 shown below, the green line represents the compressed air supply from the small air compressor to the double acting cylinder. The air supplied is passing through the pressure regulator and 5/2 way valve before reaching the double acting cylinder. The red line is the analog signal that sends from IR-sensors to the Micro-Box. The analog signal received by the Micro-Box is stored and display using software Matlab 2009a. The cyan line represents the output signal sent from Micro-Box which is used to control the operation of the double acting cylinder. Lastly, yellow line is the Ethernet line that connects laptop and the Micro-Box for communication purpose.
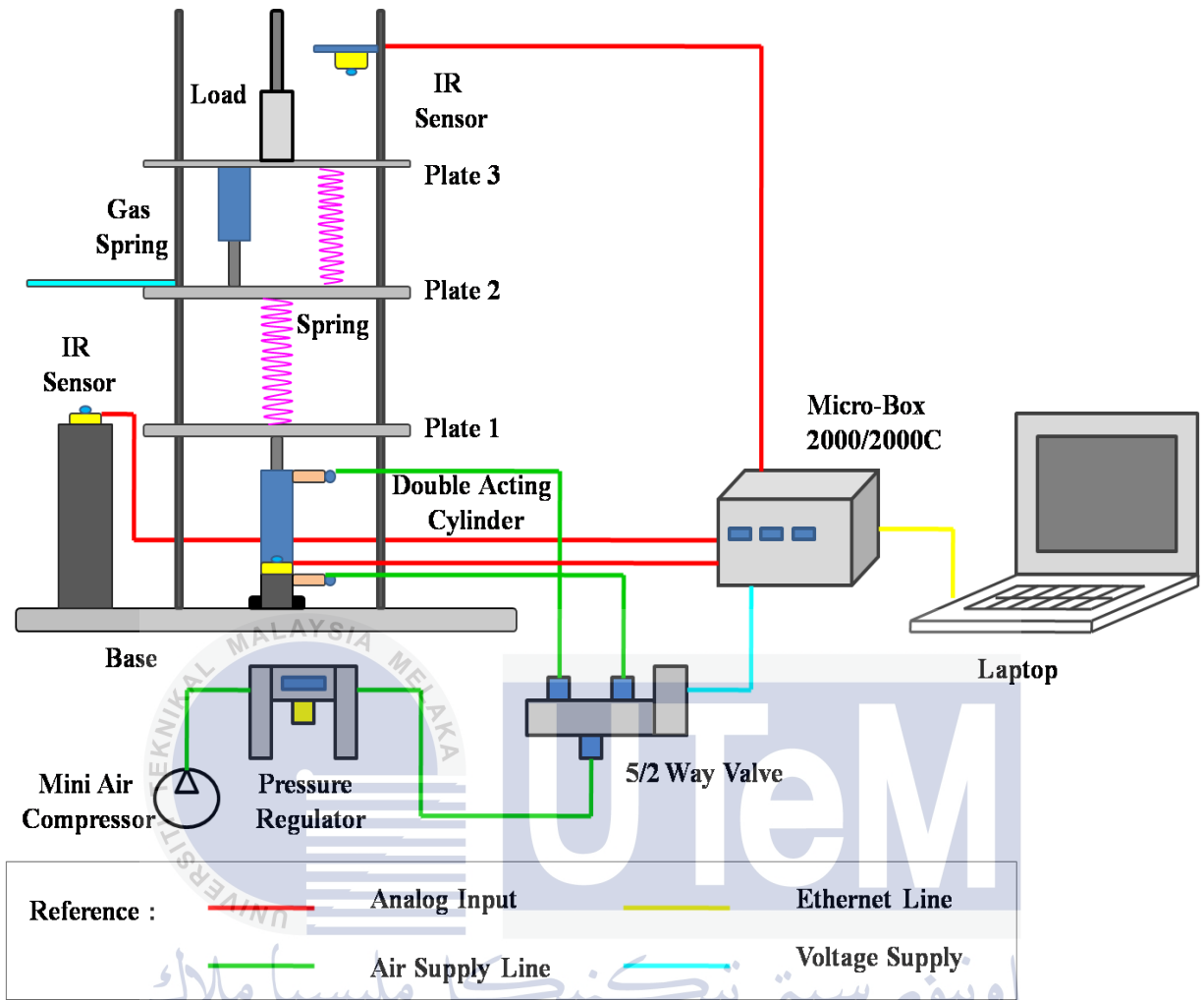
Figure 3.1: Schematic diagram of experimental setup
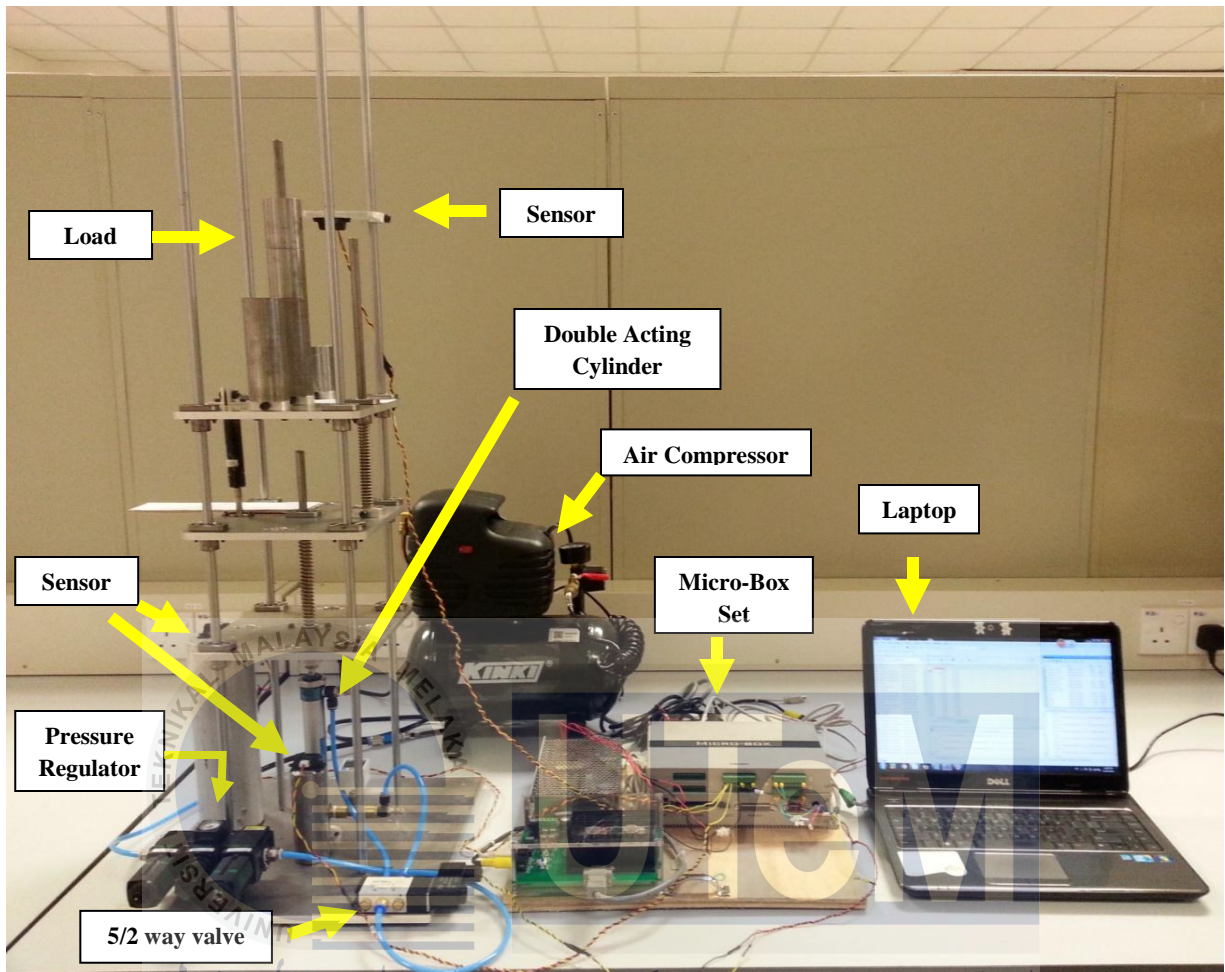
Figure 3.2: Experimental setup

In order to ensure the validity and reliability of the obtained results, the experiment equipments need to be calibrated each time before the experiments being conducted. The IR-sensor and gas spring are calibrated because the characteristic of equipments is affected by the environment of the place of carrying out the experiment. Table 3.2 shows the equation of the equipments that have been calibrated. These calibration expressions are derived in Section 4.1 of this report.

Table 3.2: Calibration equation of equipments used in experimental setup

Experimental Equipments	Calibration Equation
IR-Sensor	Voltage (V) = 111.19943*Displacement (mm) + 0.04301
Gas Spring	Force (N) = -9.57296*Velocity (m/s) + 39.24
Spring places between mass of vehicle body and mass of tire	Force (N) = 2411.41282*Length (m) + 6.73551
Spring represents the air pressure inside tire	Force (N) = 1245.99381*Length (m) – 2.76877

3.1.1 Equipments Used In Experiment Setup

3.1.1.1 Micro-Box 2000/2000C

A set of Micro-Box 2000/2000C is used to communicate with the laptop through serial port and TCP/IP communication interface. This Micro-Box is I/O expandability where it is equipped with AD/DA, Encoder, CAN, and Counter (PWM) modules. Besides that, Micro-Box works perfectly with MATLAB®, Simulink®, xPC Target and Real-Time Workshop (RTW). Hence, it allows engineers to perform real-time modeling and simulation of control system. In addition, Matlab software version 2009a was installed in laptop in order to send signal to Micro-Box. Figure 3.3 shows the photograph of Micro-Box 2000/2000C.

Figure 3.3: Micro-Box 2000/2000C

3.1.1.2 Arduino Mega 2560 R3

Arduino Mega 2560 R3 (Supplier: Cytron Technologies Sdn. Bhd. and model: MD0002356) is used to calibrate the infrared sensors. Arduino Mega 2560 is a microcontroller board based on the ATmega2560. It consists of 54 digital I/O pins where 15 of it provide PWM output, 16 of it are analog input pins. In addition, Arduino Mega has flash memory of 256KB for storing code. Arduino Mega can easily get started by connecting it to laptop using a USB cable. Besides that, MATLAB Support Package was installed in order to communicate with Arduino. Simulink block diagram was build to interface with the Arduino. Photograph of Arduino Mega 2560 R3 can be found in Figure 3.4.
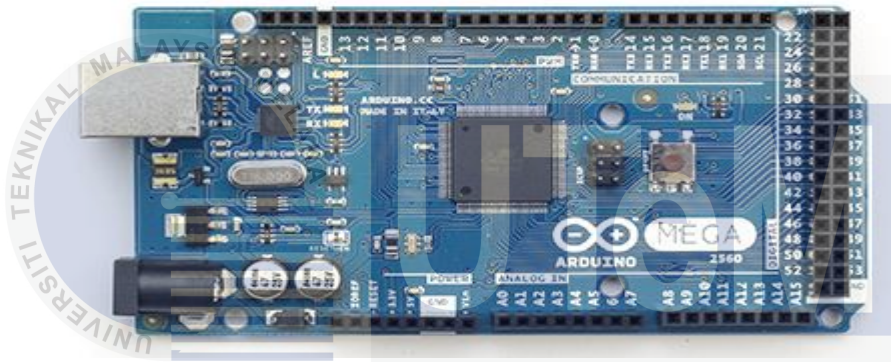
Figure 3.4: Arduino Mega 2560 R3

3.1.1.3 Ball Bearing

Twelve bearings (Supplier: Nam See Bee Sdn. Bhd. and model: LMH10UU) are used in this experiment setup to reduce the friction of the linear movement between the shafts and the plates. These bearings are attached on the plates of the experiment setup. This model LMH10UU means that the inner diameter of the bearing is 10mm. Basically, a bearing consists of balls, smooth inner and outer metal surface for the balls to rotate. Since the shafts of the experiment setup is fixed, the first two plates of the experiment setup which represent the vehicle body mass and wheel and tire mass will move upwards and downwards when the piston of the double acting cylinder starts to extract and retract to give the input signal as road profile. Metal balls inside the bearing causes the plates and shafts to roll over each other hence

reduce the coefficient of friction. Low coefficient of friction will greatly improve the efficiency, accuracy and speed of operation of the experiment setup. Photograph of bearing is shown in Figure 3.5. Figure 3.6 shows the way of attaching bearings on plate.
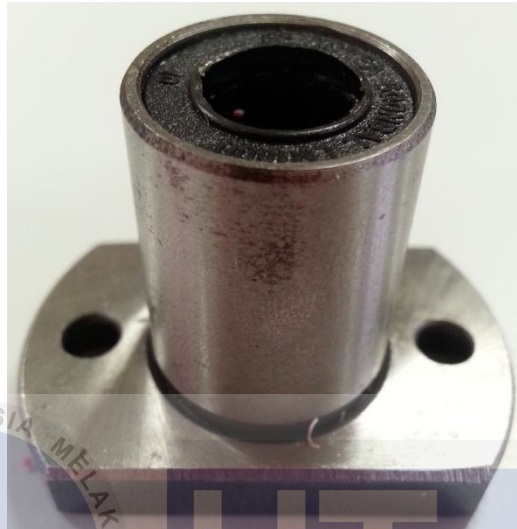
Figure 3.5: A bearing
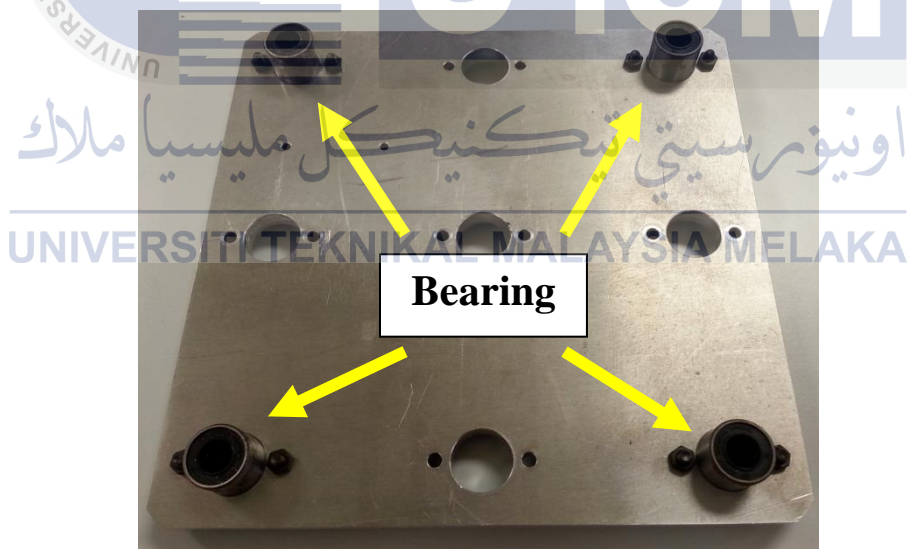
Figure 3.6: Bearing assembly on one of the plates

3.1.1.4 Infrared Sensor (IR-sensor)

Two infrared sensors (Supplier: Cytron Technologies Sdn. Bhd. and model: GP2D120XJ00F) are used in the experiment setup in order to measure the displacement of the plates which represent the vehicle body mass and mass of wheel and tire respectively. This infrared sensor is a sharp analog distance sensor which has valid sensing range from 4cm to 30cm. Therefore, the output of the sensor is not stable if the distance sensed is out of the sensing range. Besides that, the analog output voltage of the sensor is non-linear against the distance of the object being measured. When the sensor detects the movement of an object, it will send signal to MATLAB through the Micro-Box 2000/2000C. In addition, the resolution of this sensor is 0.01 volts per step from the ADC and the distance measuring range for the sensor is 38.3ms with tolerance of $\pm$9.6ms.

Even though the datasheet did provide the graph of analog output voltage against the distance of an object, it is necessary to recalibrate the characteristic of the infrared sensor as the environment and temperature of the place carry out the experiment will affect the characteristic of a sensor. The calibration of sensor is made in order to verify the accuracy of the sensor. Ruler and vernier caliper were used to measure the distance between the sensor and the plate in the calibration process of the sensor. Firstly, the sensor was placed at 1cm away from the plate. Then, the distance between the sensor and the plate was increased by 1cm each time until it reached 30cm. Figure 3.7 shows the photograph of infrared sensor. Figure 3.8 shows the experiment setup used for the calibration of the sensor. The calibration data of the infrared sensor using Arduino Mega 2560R3 is shown in Table A1 in Appendix A. Figure 3.9 shows the Simulink block diagram used to display the reading of the output voltage when the sensor is adjusted to a certain displacement. Since Arduino Mega 2560R3 is an analog-to-digital (A/D) converter which has 10bit of resolution, the digital data received by the infrared sensor was then converted to analog signal which is the output voltage by using the formula shown in the gain of Figure 3.9.
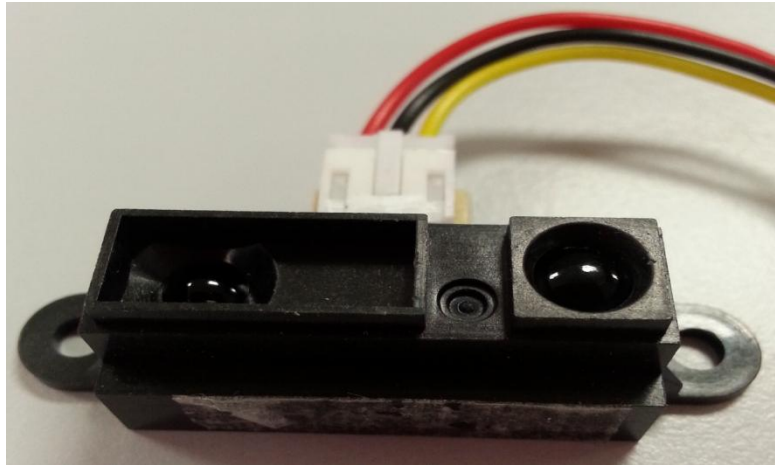
Figure 3.7: Infrared sensor

| (a) | (b) |
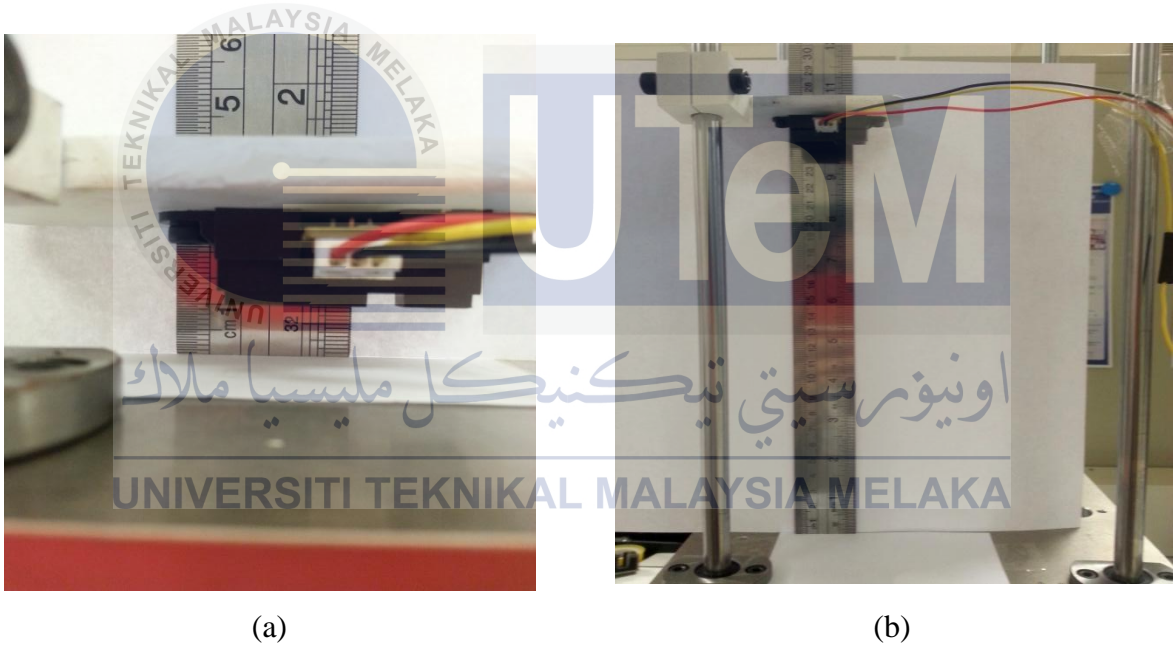
Figure 3.8: Setup for the sensor calibration (a) calibration of sensor at 1cm and (b) calibration of sensor at 23cm
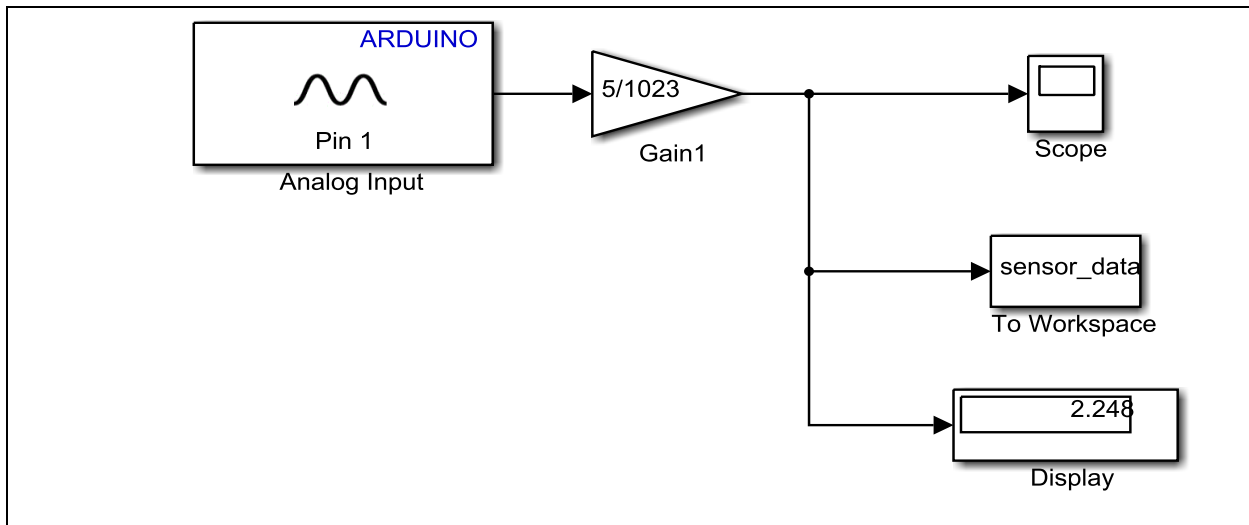
Figure 3.9: Simulink block diagram used to display the reading of the output voltage when the sensor is adjusted to certain displacement

After the calibration of the infrared sensor, the data collected is plotted using OriginPro 8. The graph of output voltage (V) versus displacement (mm) which represents the characteristic of infrared sensor can be found in Figure 4.1. Furthermore, the graph of output voltage (V) versus the inverse number of displacement (mm) shown in Figure 4.2 is plotted in order to get the equation that describes the characteristic of the sensor.

3.1.1.5 Spring

Two springs (Supplier: Teck Heng Spring Enterprise) with different spring constant are used in this experiment setup. A spring with lower spring constant is placed between the mass of vehicle body and the mass of wheel and tire. This spring is used to support the plate which represents the weight of the vehicle so that the vehicle will not directly hit the ground when passing over road bumps. When vehicle passing through bumps, the tire will move upwards causes the spring to be compressed and energy is stored inside the spring. Then the spring will retract back and the tire will move downwards to keep in touch with the road surface after the energy stored inside spring is being released. Besides that, there is another stiffer spring connected between the mass of tire and the road profile. This spring is used to

represent the high air pressure inside the tire. The air pressure must be high enough to support the total weight of the vehicle so that the vehicle will not slam down.

However, the spring rates of the springs are undefined because these two springs were bought based on the diameter of the wire and diameter of the coil. Therefore, the spring constant of springs are calculated based on the Hooke's Law where the equation is as following:

$$F = kx \tag{3.1}$$

Where

F = force needed to compress/ extend a spring (N)

k = stiffness of a spring/ spring constant (Nm^{-1})

x = distance of spring when it is stretched/ compressed away from the rest position (m)

Figure 3.10 shows the schematic diagram of how to determine the distance of spring when it is compressed away from the rest position (x) while Figure3.11 shows experimental setup used to get the spring constant of a spring.
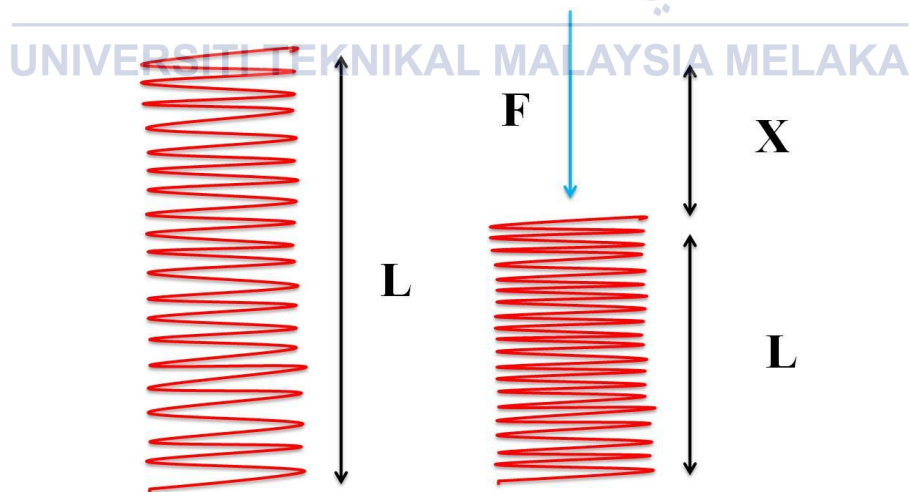
Figure 3.10: Schematic diagram of how to determine the length of spring when it is compressed away by force (F)
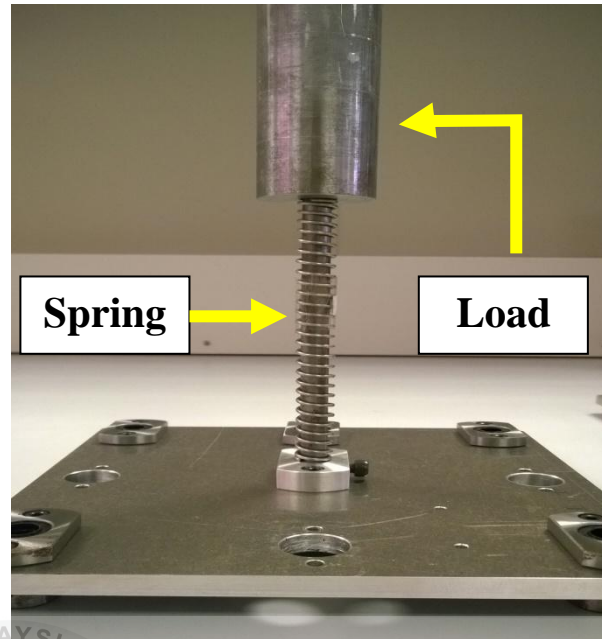
Figure 3.11: Experimental setup used to get the spring constant of a spring

According to Figure 3.11, a load of mass 1kg is placed on top of the spring. When a load is added on it, the length of spring being compressed is recorded. The load is added one by one until the spring is fully compressed. After that, the force applied to the spring is calculated using Newton's Second Law of Motion. The formula is shown below:

$$F = ma \tag{3.2}$$

Where

F = force applied on the object

m = mass of the object

a = acceleration of the object

Now, two springs are used in this experimental setup. For the first spring which places between mass of vehicle body and mass of tire has a total length of 140mm and the diameter of the wire used for this spring is 1.58mm. Besides that, the no of coil of this spring is 28 and the inner diameter of the coil is 10.45mm. After experiment has been conducted for this spring,

all the data is collected and shown in Table A4 in Appendix A. The force applied to the spring is calculated using Equation (3.2) and shown in Table A4 in Appendix A. The data shown in Table A3 is then used to plot a graph which shows the relationship between force in N and the length of spring being compressed in cm. The graph is shown in Figure 4.4.

For the second spring which represents the air pressure inside tire, the total length of spring is 150.13mm and the diameter of the wire used for this spring is 2.0mm. Besides that, the no of coil of this spring is 27 and the inner diameter of the coil is 10.83mm. The force applied to the spring is calculated using Equation (3.2) and all the data collected is shown in Table A5. The data shown in Table is then used to plot a graph which shows the relationship between force in N and the length of spring being compressed in cm. The graph can be found in Figure 4.5.

3.1.1.6 Gas Spring

Gas spring (Impresstech Engineering (Melaka) Sdn. Bhd.) is used to control the motion of the spring. Basically, gas spring is one of the types of shock absorber. It is a pressure tube which consists of high compressed nitrogen and small amount of oil. Nitrogen is chosen as compressed air used in gas spring because nitrogen and oil will not react in high pressure. When the piston rod of the gas spring is compressed, the cross-sectional area inside the gas spring decreases and hence increases the pressure of nitrogen. As a result, force is produced to give the piston rod in an extension direction. The oil inside the gas spring slows down the speed of the extended piston and therefore damping effect is occurred.

In this research, gas spring is placed in parallel with a spring between the plate which represents the mass of the vehicle body and the plate which represents the mass of the tire and wheel. The placement of the spring and gas spring in parallel is acting as the vehicle suspension system. By referring to the working principle of the gas spring shown above, since the speed of the extended piston rod is slow, hence the gas spring will damp the oscillation of the spring in order to prevent the spring from oscillating too much. Over oscillation of the

spring causes passengers inside the car feel uncomfortable. So, gas spring plays an important role in controlling the oscillation of the vehicle body.

This gas spring is customized based on the force to be supported by it. Hence, the damping coefficient of the gas spring is undefined and experiments were carried out in order to get the damper coefficient. The equation used to determine the damping coefficient is shown below:

$$F = cv \qquad (3.3)$$

$$F = c\frac{x}{t} \qquad (3.4)$$

Where

F = force applied to the gas spring (N)

c = damping coefficient (Ns/m)

v = velocity of the piston rod to be extended or compressed (m/s)

x = displacement of the piston rod of gas spring (m)

t = time taken for the piston rod to be extended or compressed (s)

In order to achieve the requirement in the Equation (3.4) for calculation of damping coefficient, two different experiments are carried out to obtain the time taken for piston rod to be extended or compressed and to obtain the length of the piston rod when load is added to the gas spring. For the first experiment which is to determine the time taken for piston rod to be extended or compressed, the piston is fixed on table and camera is used to record down the time taken for the piston rod of gas spring to extend after being compressed. After the time taken had been recorded, the video is then opened using the Windows Movie Maker to slow play the video in order to get the exact time taken for the piston rod to extend. The time taken obtained will be used in Equation (3.4) for calculation of damping coefficient. Figure3.12 shows the experiment setup to record the time taken for the piston rod of gas spring to extend after being compressed.
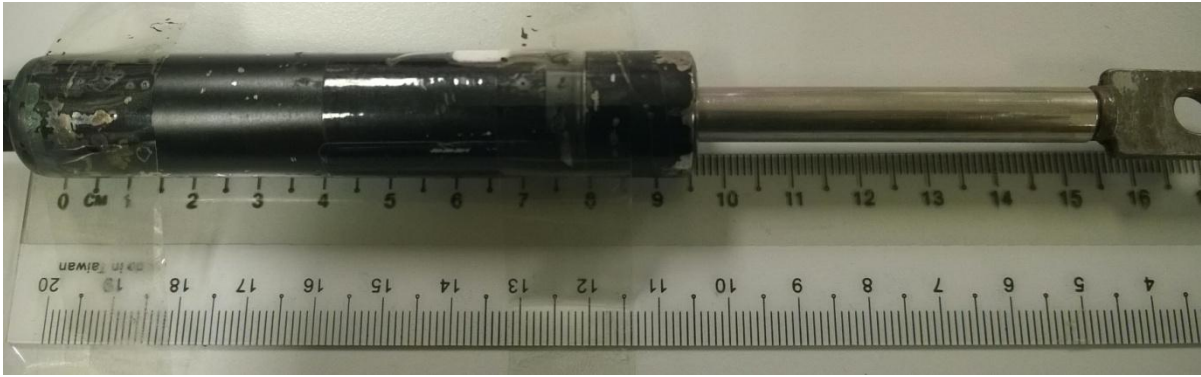
Figure 3.12: Experiment setup to record the time taken for the piston rod of gas spring to extend after being compressed

For the second experiment which is to obtain the length of the piston rod when load is added to the gas spring, the gas spring was fixed vertically between two plates. Then, load of mass 0.1kg is added one by one on top of the plate until the piston rod of the gas spring is fully compressed. Vernier caliper is used to measure the length of the piston rod each time a 0.1kg load added on it. Vernier caliper is chosen to measure the length of piston rod to make sure the high accuracy and precision of the data being collected. Figure3.13 shows the experiment setup for obtaining the length of the piston rod when load is added to the gas spring. The length of piston rod collected when load was added to the gas spring shows in Table A2 can be found in Appendix A.
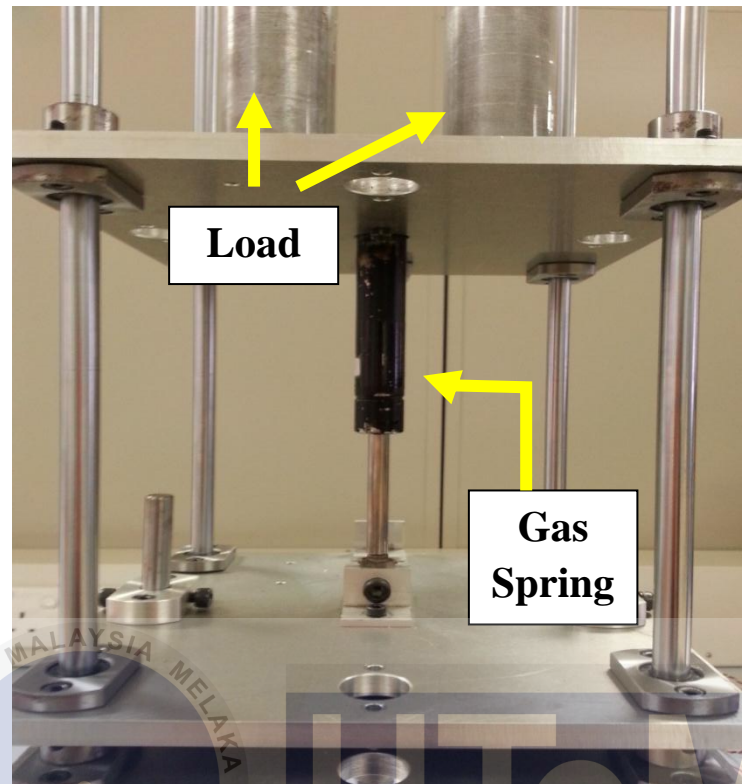
. Figure 3.13: Experiment setup for obtaining the length of the piston rod when load is added to the gas spring

After data shown in Table A2 has been collected, the data is then used to calculate the force and velocity as for force and velocity are needed for the calculation of the damping coefficient of the gas spring shown in Equation 3.3. Table A3 found in Appendix A shows the damping coefficient of a gas spring at different force and velocity.

3.1.1.7 Pneumatic Double Acting Cylinder

A pneumatic double acting cylinder (Impresstech Engineering (Melaka) Sdn. Bhd. and model: MAL 20X100-S) is used to provide pulse signal as the road bump of the experimental setup. This cylinder is named as Aluminium Mini Cylinder by manufacturer. The model MAL 20X100-S means that the bore of this cylinder is 20mm and the stroke of the cylinder is 100mm. Besides that, cylinder has valid pressure range from 0.15-0.80MPa. This shows that

the cylinder needs minimum pressure of 0.15MPa to extend the piston rod and 0.80MPa is the maximum pressure that can be apply to the cylinder. Basically, a double acting cylinder is an actuator that consists of two air ports which are pressure port and vent port for the air to flow in and out of the cylinder. Since this cylinder consists of two ports, therefore it can be powered in both directions. However, the pressure port and the vent port can be changed during the extension and retraction process of the cylinder. Figure 3.14 shows the photograph of the double acting cylinder.
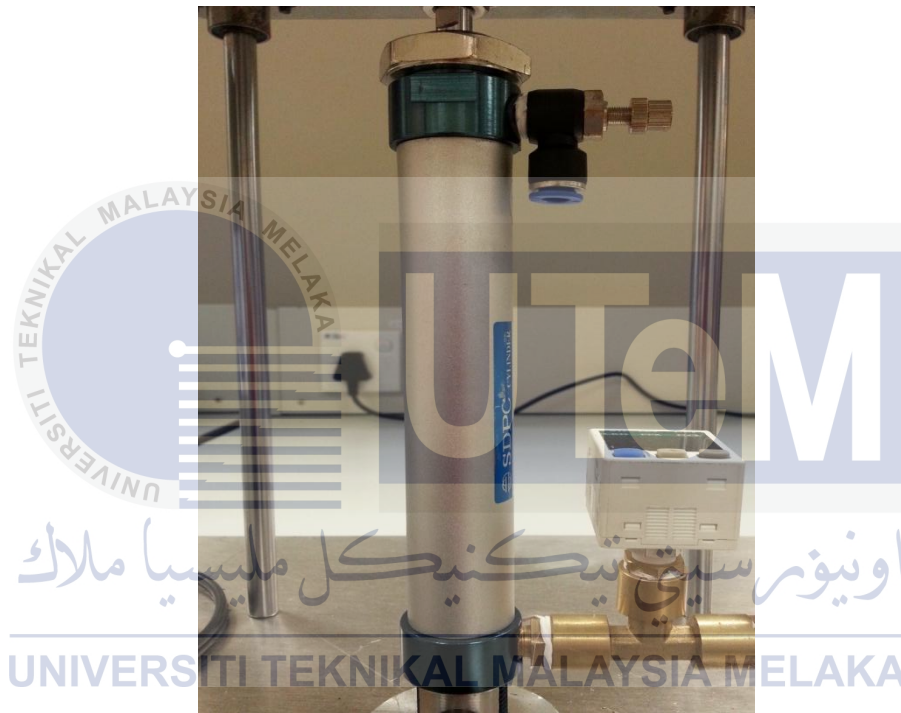
Figure 3.14: Double acting cylinder

3.1.1.8 Flow Control Valve

Two flow control valves (Impresstech Engineering (Melaka) Sdn. Bhd. and model: SC-220 OF-06-1/8) were used to control the flow rate of the air because the speed of the extension and retraction of the double acting cylinder was fast and intensively during experiment. These two control valves were placed at two air ports of the cylinder. The

extraction and retraction speed of piston rod of cylinder can be controlled manually by adjusting the screw (handle) of the flow control valve. Adjusting the screw will restrict the flow pipe and thus change the cross section of the pipe through which the air can flow. The knob can be adjusted from fully open to completely close to control the flow of the air. Figure 3.15 shows the photograph of the flow control valve.
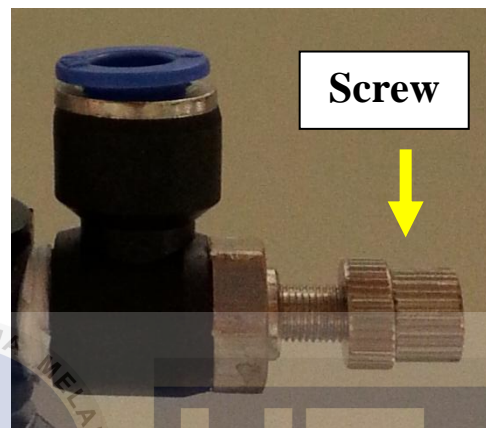
Figure 3.15: Flow control valve

3.1.1.9 Pressure Regulator

A pressure regulator (model: C1000-8) is used to regulate the compressed air flowing into the cylinder and maintain it at a constant value. This is a pressure regulator which consists of integrated filter, regulator and lubricator. The integrated filter is used to filter the compressed air flowing into the pressure regulator. Then regulator will regulate the compressed air flowing to the double acting cylinder to desired pressure by adjusting the knob of the pressure regulator. Lastly, lubricator will lubricate the compressed air flowing out the pressure regulator. The model C1000-8 means that the port size of the pressure regulator is 8mm. Besides that, this pressure regulator has valid pressure range from 0.00-1.00MPa where the maximum working pressure of the pressure regulator is 1MPa. Figure 3.16 shows the photograph of the pressure regulator.

Figure 3.16: Pressure regulator

3.1.1.10 Single Solenoid Valve 5/2 Way

A single solenoid valve 5/2 way (model: 4V210-08) is used to control the direction of the compressed air flowing in and out of the cylinder. 5/2 way valve consists of five ports and two air flowing positions to the cylinder. Figure 3.17 shows the photograph and schematic symbol of single solenoid valve 5/2 way respectively. Figure 3.18 shows the photograph of the single solenoid valve 5/2 way.
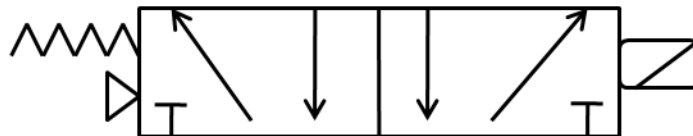
Figure 3.17: Schematic symbol of single solenoid valve 5/2 way
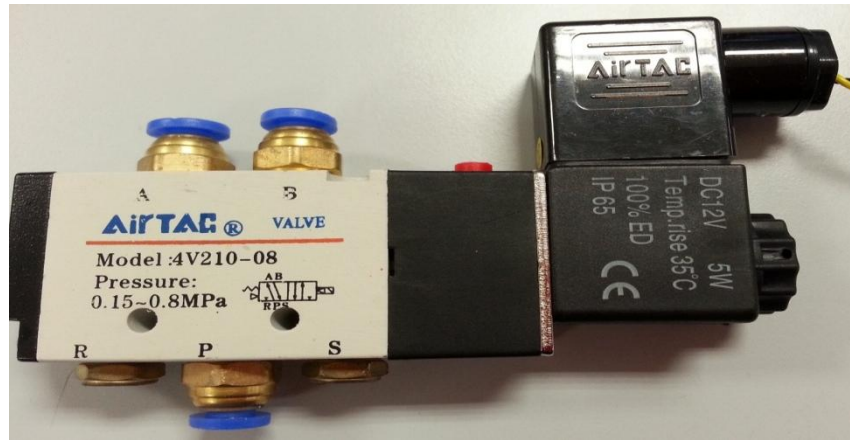
Figure 3.18: Single solenoid valve 5/2 way

3.1.1.11 Air Compressor

An air compressor (Kinki Mini Air Compressor and model: KAC-14 6L 1/4HP 100 PSI) was used to pump compressed air into double acting cylinder for the extension of the piston rod. The compressor converts air at atmospheric pressure into high pressure by changing its volume. The compressed air supply to the cylinder can be adjusted from 1 bar up to 10bar. Figure 3.19 shows the photograph of the air compressor.

Figure 3.19: Air compressor

3.2   Development of Quarter Car Model

Quarter car suspension model represents any one of the four wheels of the vehicle. It is used to model the vertical vibration of a vehicle. A schematic diagram and free body diagram of quarter car are developed in order to obtain the equation of the motion which can describe the dynamic behavior of quarter car. After that, the equation of motion is then converted to Simulink Model in MATLAB in order to apply pulse input as the road input for the system.

3.2.1   Derivation of Mathematical Model Quarter Car Passive Suspension System

Figure 3.20 shows the two-degree-of-freedom modeling of the quarter car passive suspension system. Figure 3.21 shows the free body diagram of this passive suspension system. This quarter car model consists of one sprung mass (vehicle body) and one unsprung mass (wheel and tire). There is a spring and a shock absorber connected in parallel between the sprung mass and unsprung mass which represents the suspension system. Furthermore, there is a spring connected below unsprung mass and this acts as the stiffness of the tire. In real world, there is no spring inside the tire. However, the air pressure inside the tire can be modeled as the spring.

There are two assumptions made in this mathematical model of quarter car passive suspension system. It is assumed that the vertical displacement of sprung mass, unsprung mass and road input upward direction as positive. In addition, the effect of friction is not taking into account. The modeling of Figure 3.20 is proposed by P.Alexandru et al. [10].
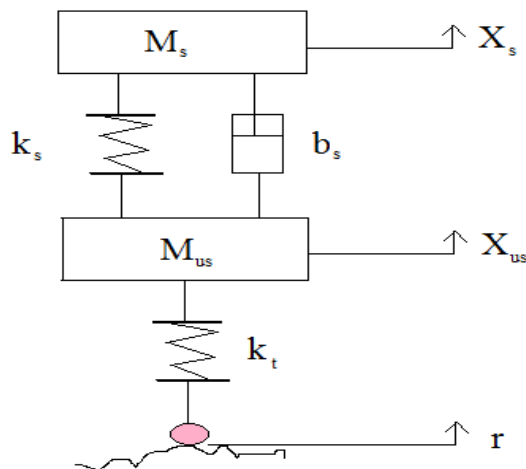
Figure 3.20: Schematic diagram of quarter car
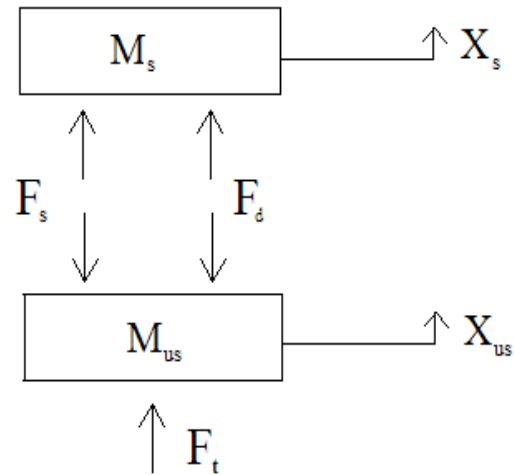
Figure 3.21: Free body diagram

Table 3.3: System Parameters for Passive Suspension System.

Parameter Name	Unit	Symbol
Mass of vehicle body (sprung mass)	[kg]	M_s
Mass of the wheel and tire (unsprung mass)	[kg]	M_{us}
Spring constant of the suspension system	[N/m]	k_s
Spring constant of the tire	[N/m]	k_t
Dashpot constant (shock absorber)	[Ns/m]	b_s
Vertical displacement of road input	M	R
Vertical displacement of sprung mass	M	X_s
Vertical displacement of unsprung mass	M	X_{us}

The mathematical model is derived by applying Newton's law to each mass and then identifying the forces acting on each mass. Since this is two-degree-of- freedom system, there will be two equations of motion which are one for the vehicle body mass and the other one is for the wheel mass. By referring to the free body diagram in Figure 3.21, it can be noticed that there are three different forces acting on vehicle body and wheel. The three forces are suspension spring force, suspension damper force and tire force respectively. The equation used to determine the three forces are shown below:

Suspension spring force:

$$F_s = k_s(X_{us} - X_s) \tag{3.5}$$

Suspension damper force:

$$F_d = b_s(\dot{X}_{us} - \dot{X}_s) \tag{3.6}$$

Tire force:

$$F_t = k_t(r - X_{us}) \tag{3.7}$$

For vehicle body mass, M_s, applying Newton's second law of motion by assuming upward direction as positive. From free body diagram in Figure 3.21, there are two forces which are suspension spring force and suspension damper force acting upward on the vehicle body. Therefore, the force exerted on the vehicle body mass is determined by substituting equation 3.5 and equation 3.6 into equation 3.8.

$$F_s + F_d = M_s\ddot{X}_s \tag{3.8}$$

$$k_s(X_{us} - X_s) + b_s(\dot{X}_{us} - \dot{X}_s) = M_s\ddot{X}_s \tag{3.9}$$

For wheel mass, M_{us}, applying Newton's second law of motion by assuming upward direction as positive. According to free body diagram in Figure 3.21, there are three forces which are suspension spring force, suspension damper force and tire force acting on the wheel and tire. Tire force is acting upward towards the wheel and tire whereas the suspension spring force and suspension damper force are acting downward towards the wheel and tire. Thus, the force exerted on the wheel mass is determined by substituting equation 3.5, equation 3.6 and equation 3.7 into equation 3.10.

$$F_t - (F_s + F_d) = M_{us}\ddot{X}_{us} \tag{3.10}$$

$$k_t(r - X_{us}) - [k_s(X_{us} - X_s) + b_s(\dot{X}_{us} - \dot{X}_s)] = M_{us}\ddot{X}_{us} \tag{3.11}$$

$$k_t(r - X_{us}) - k_s(X_{us} - X_s) - b_s(\dot{X}_{us} - \dot{X}_s) = M_{us}\ddot{X}_{us} \tag{3.12}$$

Equation 3.9 and 3.12 represent the equations of motion for the quarter car passive suspension system. These two equations are then converted to Simulink Model in MATLAB in order to determine the dynamics behavior of quarter car model.

3.2.2 Simulink Model in Matlab

Simulation studies based on the mathematical modeling of quarter car passive suspension system are conducted by using MATLAB. The dynamic behavior of quarter car model is stimulated by converting the equations of motion 3.9 and 3.12 into Simulink Model in MATLAB. Figure 3.22 shows the designed Simulink Model of the passive suspension system in MATLAB. This model consists of many basic blocks from the simulink library.

Figure 3.22: Designed Simulink model of the passive suspension system in MATLAB

CHAPTER 4

RESULTS ANALYSIS AND DISCUSSIONS

In this chapter, calibration results of the equipments used in experimental setup are shown in graphs. Then, repeatability test results which used to validate the consistency of the measurement results are covered in this chapter before proceed to experiments results. Next, experimental results with different mass and different pulse width are discussed. Lastly, the simulation and experimental results are analyzed

4.1 Calibration Results for Experimental Equipments

4.1.1 Infrared Sensor Calibration Result

Initially, the output value of the sensor is voltage. Hence, the infrared sensor is placed at 1cm away from the plate and increased by 1cm each time until it reached 30cm to determine the relationship between displacement and voltage. The infrared sensor is connected to the Arduino and the output reading has been observed through the scope in Matlab. Figure 4.1 shows the infrared sensor calibration result of output voltage (V) versus displacement (mm).

By referring to the Figure 4.1 shown below, it can be seen that the output voltage of the sensor increases at the displacement of 10mm up to 40mm. After that, the output voltage decreases gradually when measured from the displacement of 40mm until 300mm. The output voltage decreases at displacement of 40mm to 300mm because this is a distance sensor which has valid sensing range from 40mm to 300mm. The data collected in this calibration process are then used in the look up table of the experimental simulink block diagram.
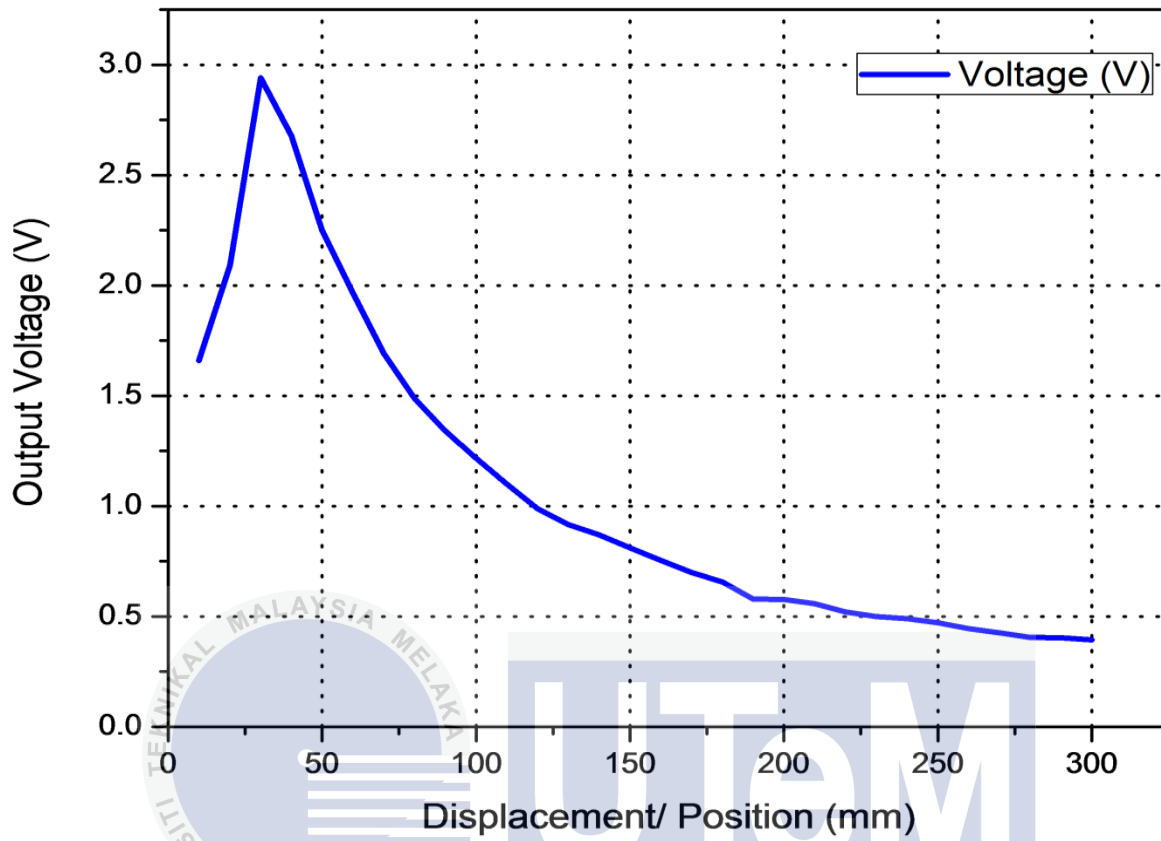
Figure 4.1: Infrared sensor calibration result of output voltage (V) versus displacement (mm)

In addition, the graph of output voltage versus inverse number of displacement had been plotted in order to get the equation which represents the characteristic of the infrared sensor. Linear plot has been plotted for getting the equation of the sensor. Figure 4.2 shows the infrared sensor calibration result of output voltage (V) versus inverse number of displacement (mm).

Voltage (V) = 111.19943*Displacement (mm) + 0.04301, is the linearized equation that describe the characteristic of the IR sensor.
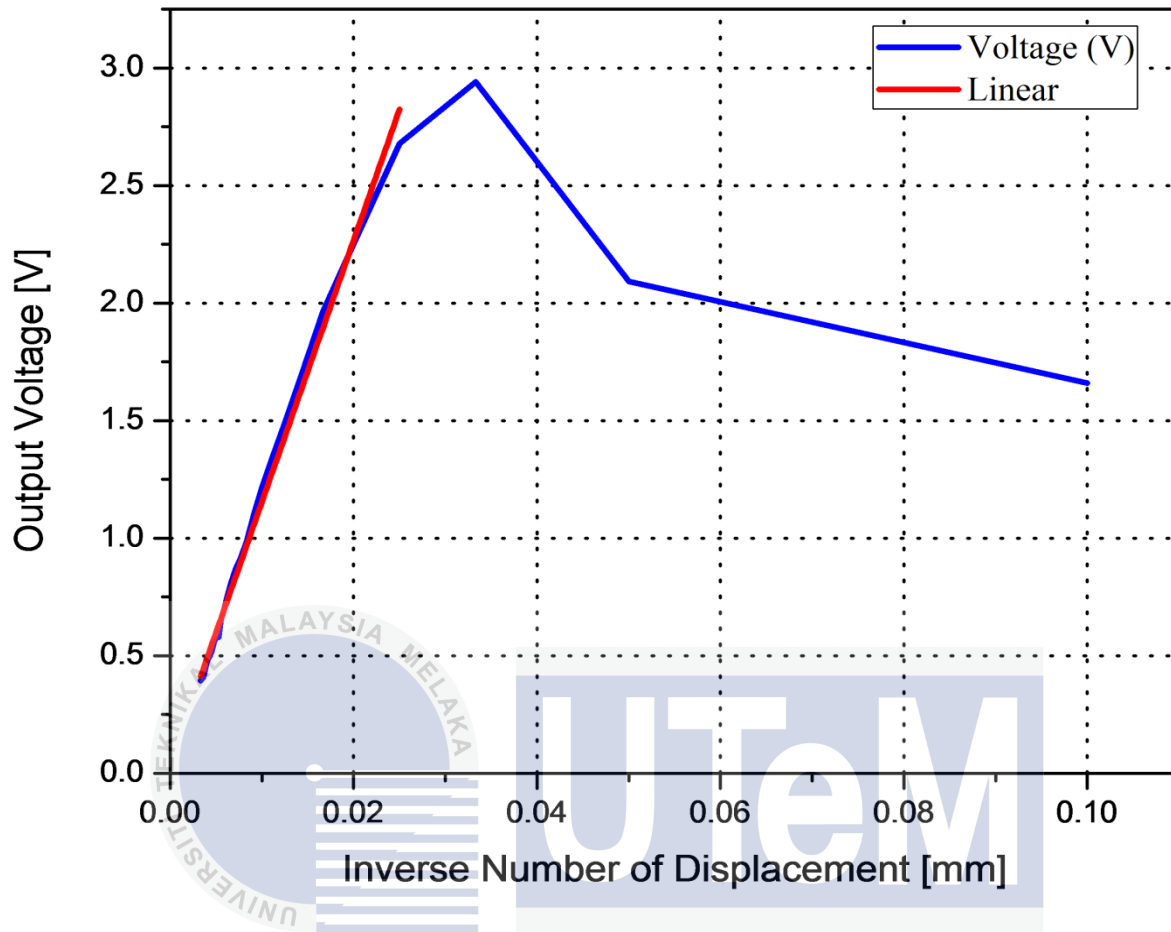
Figure 4.2: Infrared sensor calibration result of output voltage (V) versus inverse number of displacement (mm)

4.1.2   Gas Spring Calibration Result

The calibration result is obtained by giving different value of load to the gas spring. Load of mass 0.1kg is added one by one on the gas spring until the piston rod of the gas spring is fully compressed. Length of piston rod has been recorded each time a load is added on it. Vernier caliper is used to measure the length of the piston rod to ensure high accuracy of the data being obtained. Figure 4.3 shows the gas spring calibration result of force (N) versus velocity (m/s). Gradient of the graph is obtained by using the linear data being collected. Non linear data are not taking into consideration on finding the gradient of graph. Gradient obtained is representing the damping coefficient of gas spring.

Force (N) = -9.57296*Velocity (m/s) + 39.24, is the linearized equation that represents the characteristic of gas spring.
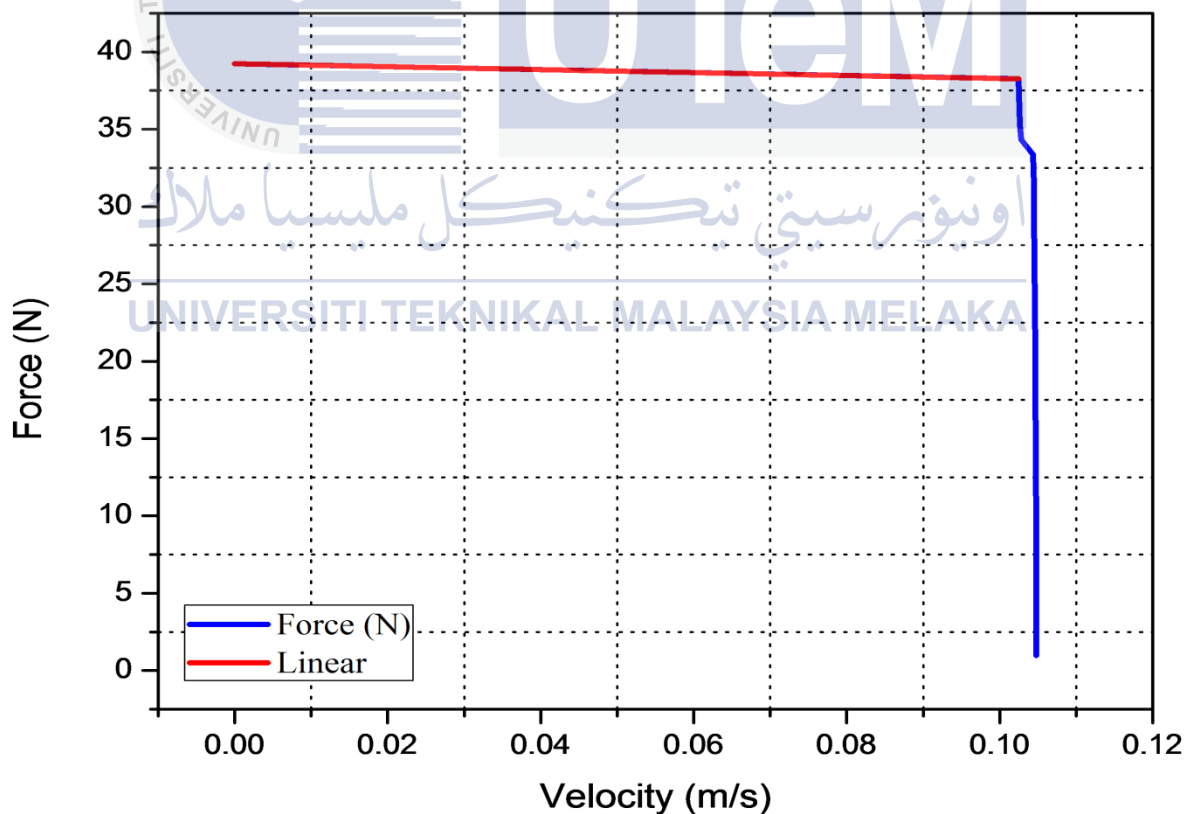
Figure 4.3: Gas spring calibration result of force (N) versus velocity (m/s)

4.1.3 Spring Calibration Result

4.1.3.1 Spring Places between Mass of Vehicle Body and Tire

The calibration process has been conducted by placing a load of mass 1kg on top of the spring in order to measure the length of the spring being compressed. The load is added one by one until the spring is fully compressed. Vernier caliper and ruler are used in this calibration process. Data collected are used to plot the graph in Figure 4.4. Figure 4.4 shows the calibration result of spring. Gradient of the graph which represents the spring constant of this spring is obtained. This spring constant is then used in Simulink Model in MATLAB for determining the dynamic behavior of quarter car.

Force (N) = 2411.41282*Length (m) + 6.73551, is the linearized equation that represents the characteristic of this spring.
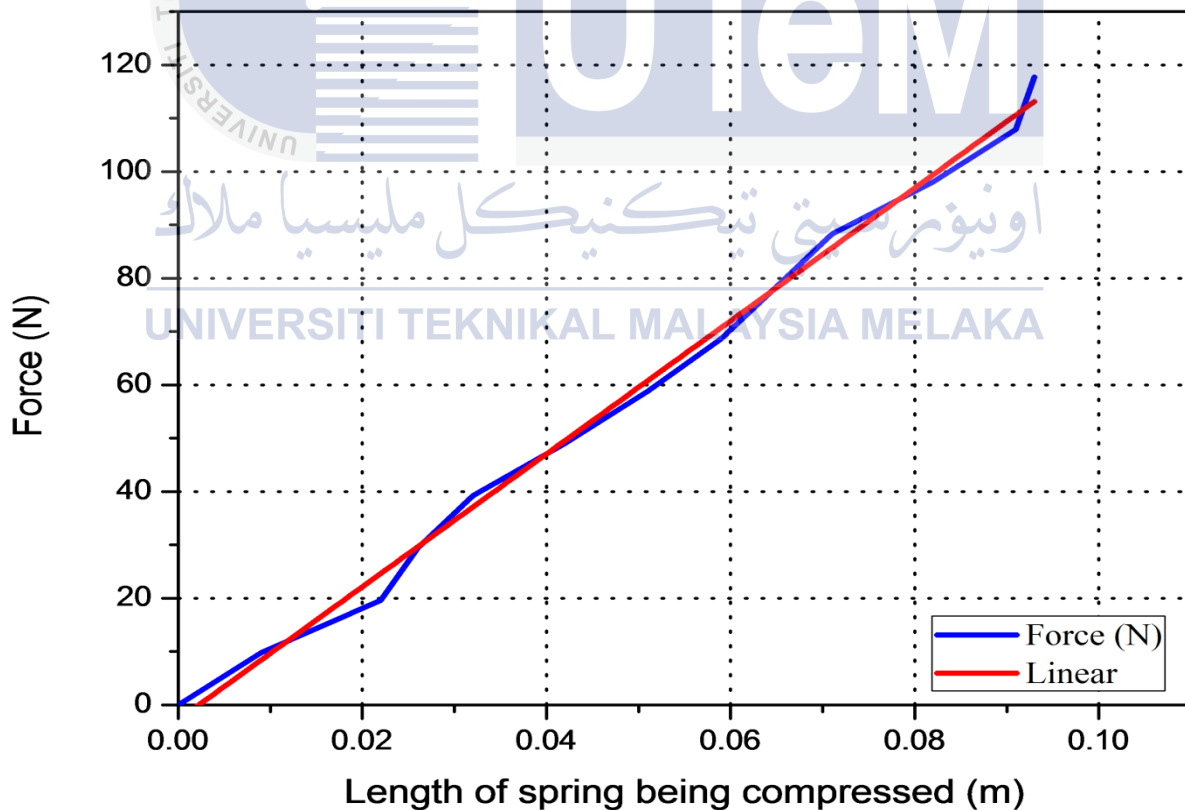
Figure 4.4: Spring places between mass of vehicle body and tire calibration result of force (N) versus length of spring being compressed (m)

4.1.3.2 Spring Represents the Air Pressure inside Tire

Steps used for the calibration result of spring in Section 4.1.3.1 are repeated here. After data being collected, graph in Figure 4.5 is plotted in order to get the equation which describes the characteristic of the spring. Figure 4.5 shows the calibration result of this spring. Gradient of the graph is representing the spring constant of this spring.

Force (N) = 1245.99381*Length (m) − 2.76877, is the linearized equation that represents the characteristic of this spring.
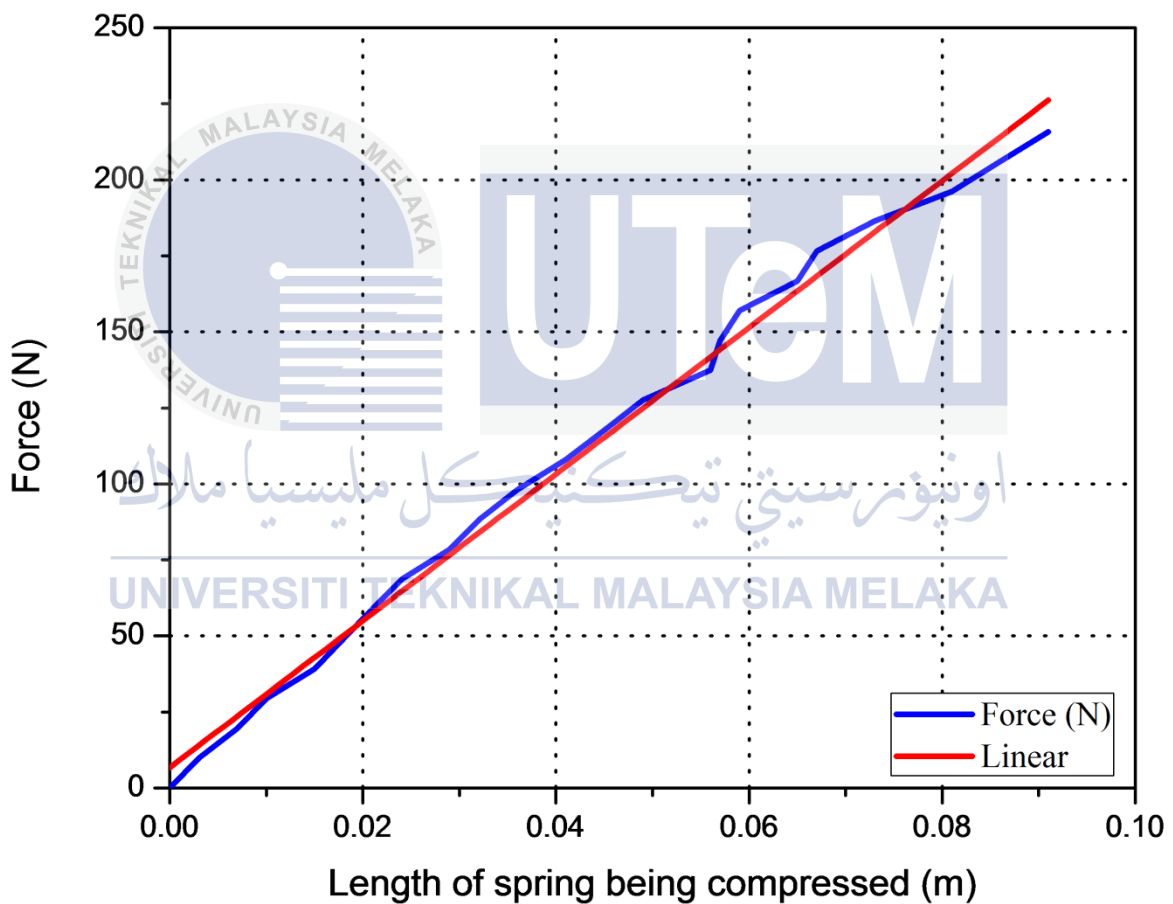
Figure 4.5: Spring represents the air pressure inside tire calibration result of force (N) versus length of spring being compressed (m)

4.2 Repeatability

Repeatability tests have been carried out to validate the measurement data for this passive suspension system prototype. This repeatability tests are divided into three experiments where the mass of vehicle body is changed for each different repeatability test. The mass of vehicle body carried out in this repeatability tests are 4.29kg, 4.59kg and 4.79kg. However, the mass of tire is fixed in 1.48kg during the whole experiments processes. Pulse input pressure with 0.4MPa, period of one cycle of 1s, pulse width is 50% and time taken for experiment which is 4s is set for all the experiments carried out here. Besides that, all the experiments have been repeated for 6 times and graphs are shown in Figure 4.6 to 4.23. In order to determine the consistency of the collected results, standard deviation is calculated for each experiment that has been conducted here. Standard deviation shows the tolerance error of the measurement results away from the mean. So, the smaller the standard deviation, the closer the measurement results with the mean and the better the consistency of the measurement results. Steps of calculating the standard deviation of each experiment are shown below. Table 4.1 below shows the data array of these experiments.

Table 4.1: Data array

Number of data, j=1,2, m-1, m	Number of measurement, i =1,2,n-1,n					
	1	2	3	4	5	n
1	-	-	-	-	-	-
↓	-	-	-	-	-	-
m	-	-	-	-	-	-

In this experiment, data is collected for 4seconds. Equation 4.1 shows the formula used to calculate the number of data per measurement.

$$m = \frac{T}{\Delta T} \tag{4.1}$$

Where

m = number of data per measurement

T = experiment duration (s)

ΔT = sampling time (s)

In order to calculate the standard deviation of the row of data, the mean of the data is calculated, Equation 4.2 shows the equation of mean.

$$\text{Mean, } \bar{x} = \frac{\sum_{i=1}^{n} x_i}{n} \tag{4.2}$$

Where

xi = ith measurement

n = number of repeatability

Next, Equation (4.3) shows the formula of the standard deviation of the row of data.

$$\text{Standard Deviation, } \sigma j = \sqrt{\frac{\sum_{i=1}^{6}(x_i - \bar{x})^2}{n-1}} \tag{4.3}$$

In this case, there will be m number of standard deviation, σj, so in order to obtain the overall mean and standard deviation, the following equations are needed. Equation 4.4 shows the formula of overall mean while equation 4.5 shows the formula of overall standard deviation.

$$\text{Overall mean, } \overline{x}(overall) = \frac{\sum_{j=1}^{m} \sigma j}{m} \tag{4.4}$$

$$\text{Overall Standard Deviation, } \sigma j(overall) = \sqrt{\frac{\sum_{j=1}^{m}(\sigma j - \overline{x(overall)})^2}{m-1}} \tag{4.5}$$

4.2.1 Repeatability Test with Mass of Vehicle Body = 4.29kg
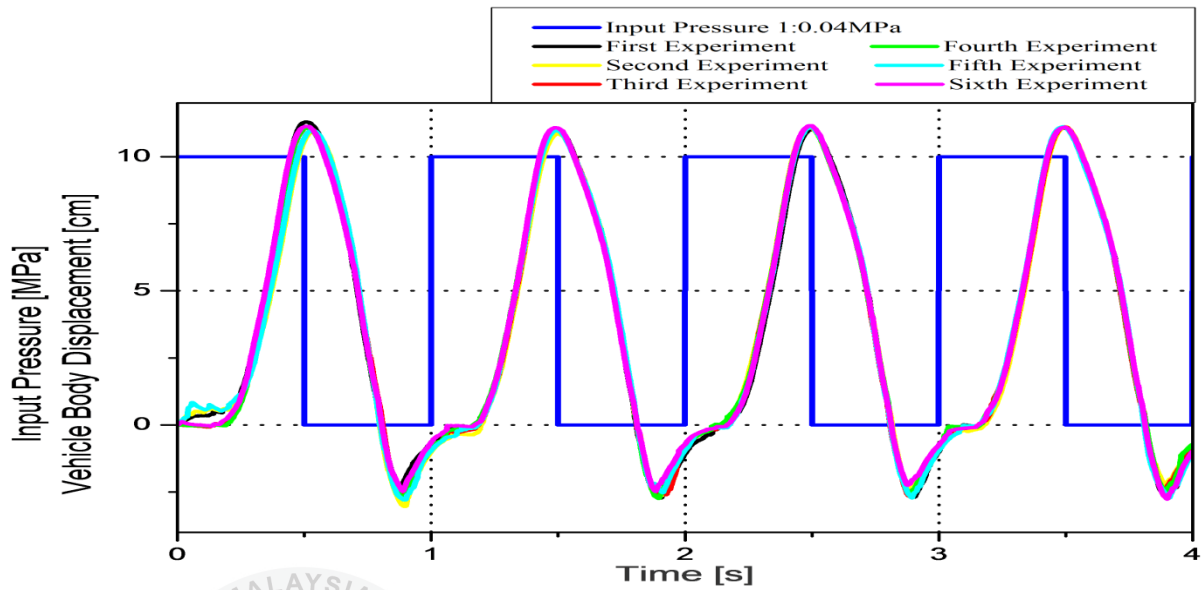
Figure 4.6: Repeatability test result of vehicle body displacement with mass = 4.29kg

Mean = 0.154147

Standard Deviation = 0.109544
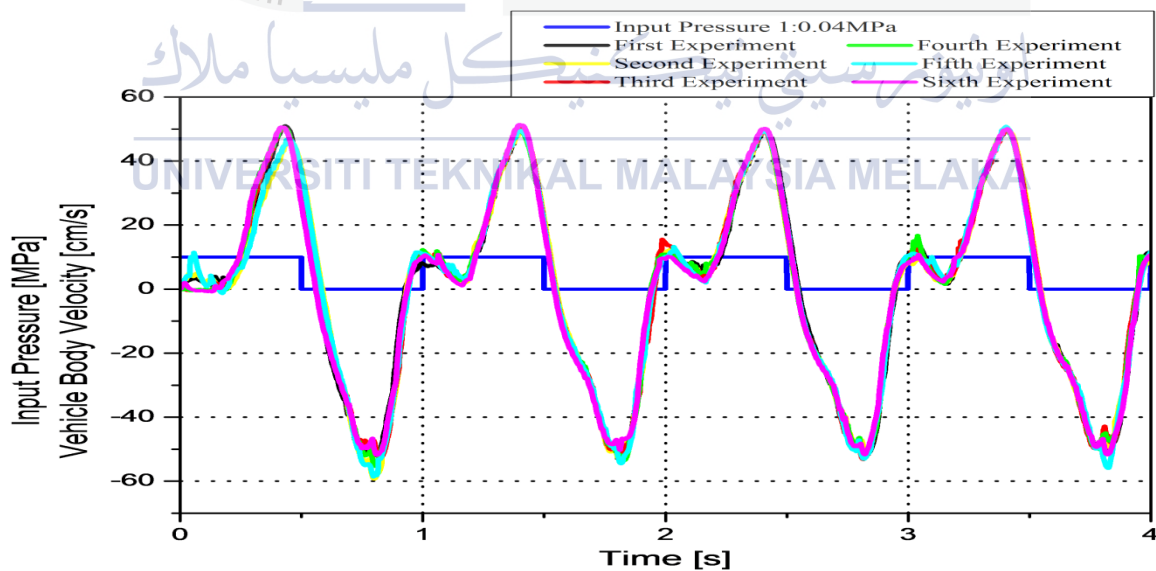
Figure 4.7: Repeatability test result of vehicle body velocity with mass = 4.29kg

Mean = 1.558425

Standard Deviation = 1.088125
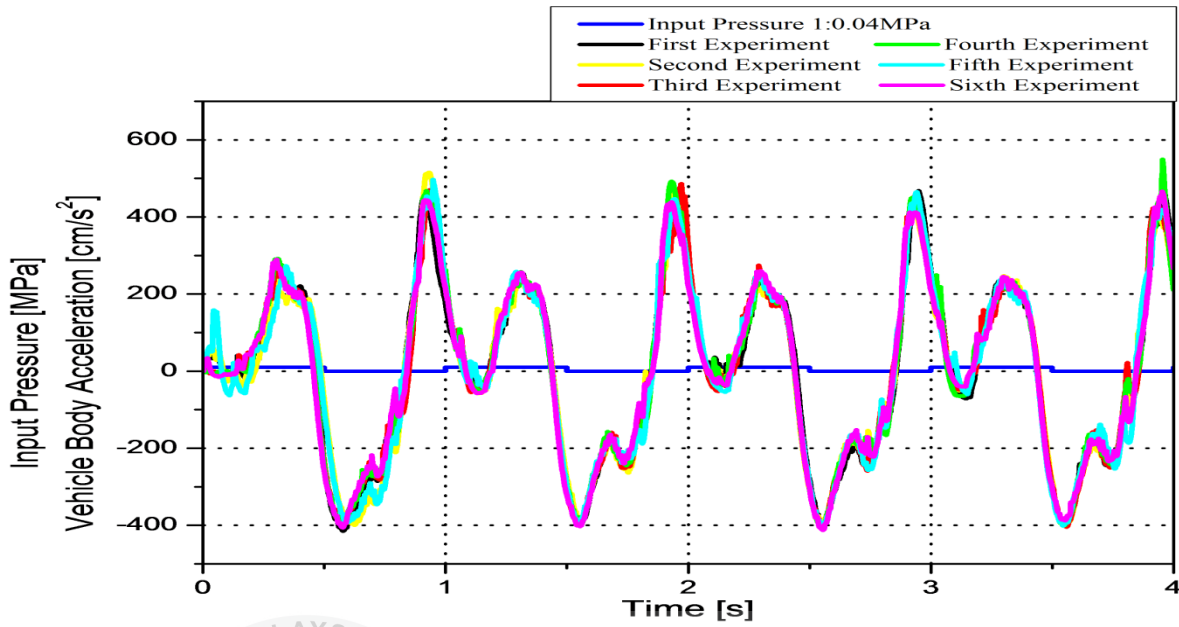
Figure 4.8: Repeatability test result of vehicle body acceleration with mass = 4.29kg
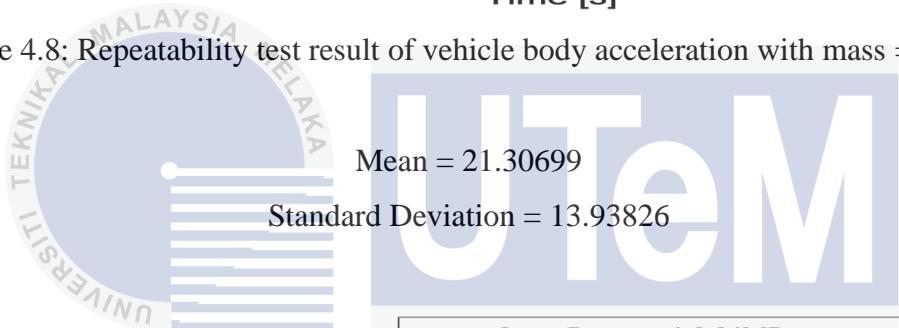
Mean = 21.30699

Standard Deviation = 13.93826
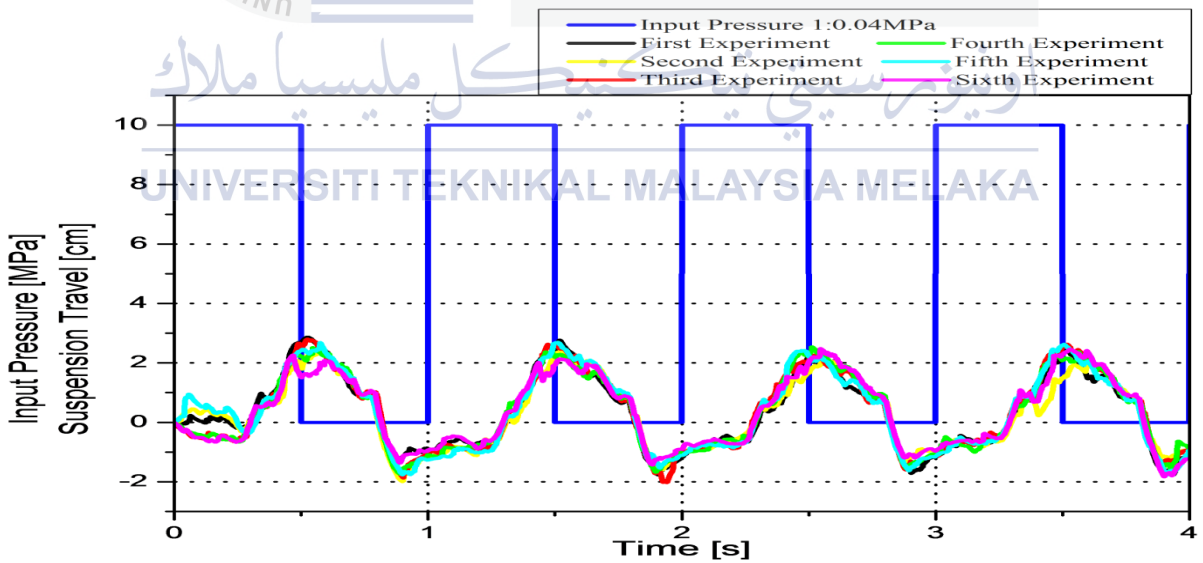
Figure 4.9: Repeatability test result of suspension travel with mass = 4.29kg

Mean = 0.189603

Standard Deviation = 0.110446
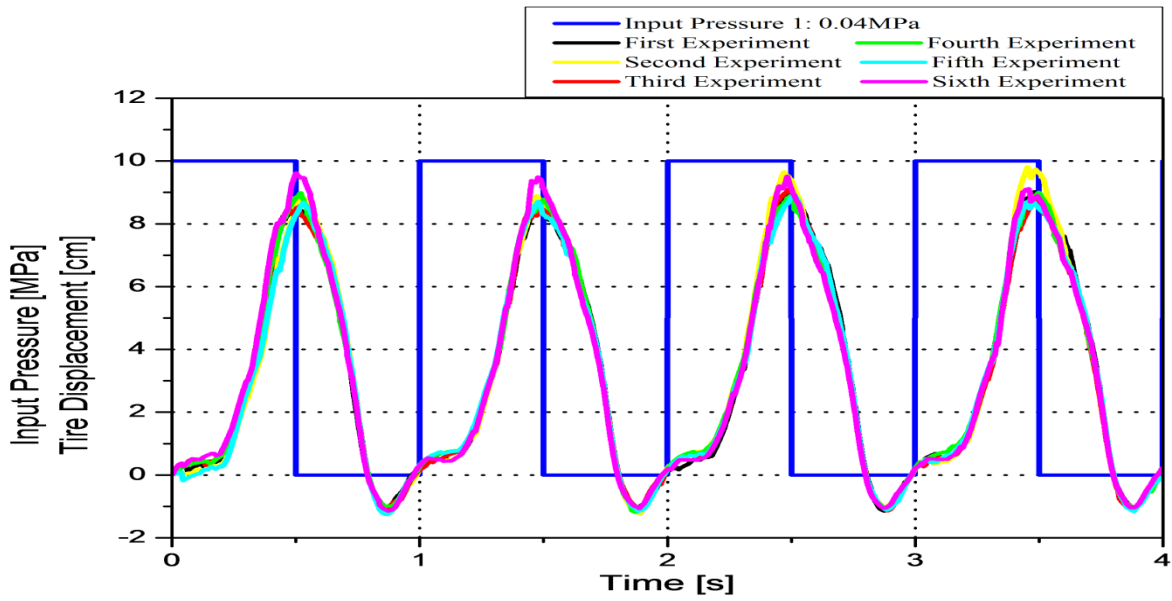
Figure 4.10: Repeatability test result of tire displacement with mass = 4.29kg

Mean = 0.161294

Standard Deviation = 0.121578
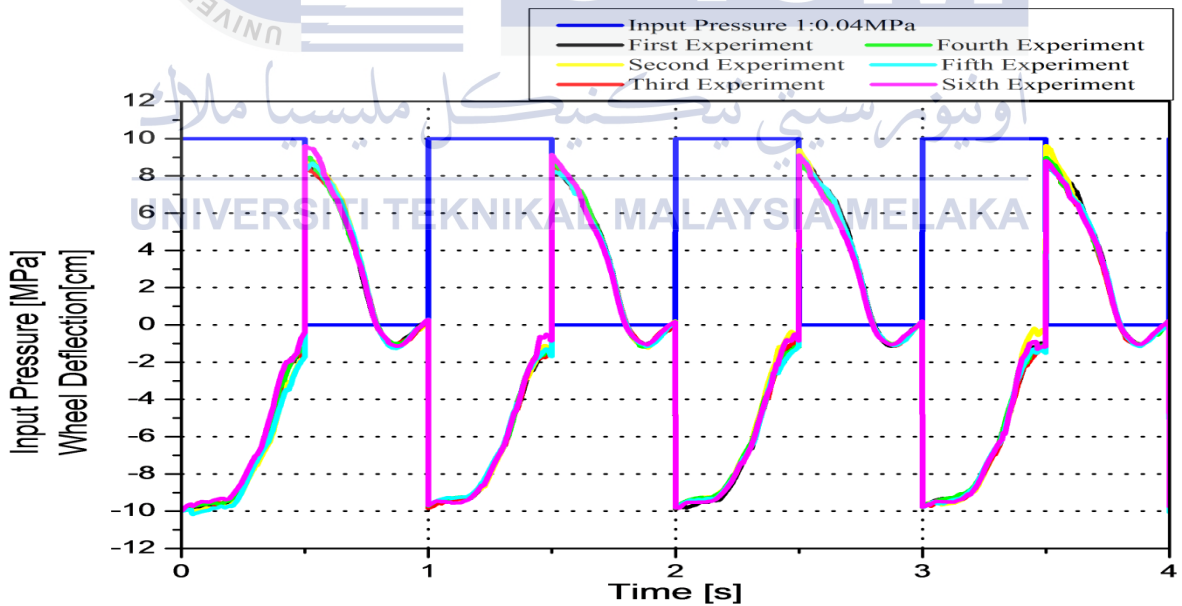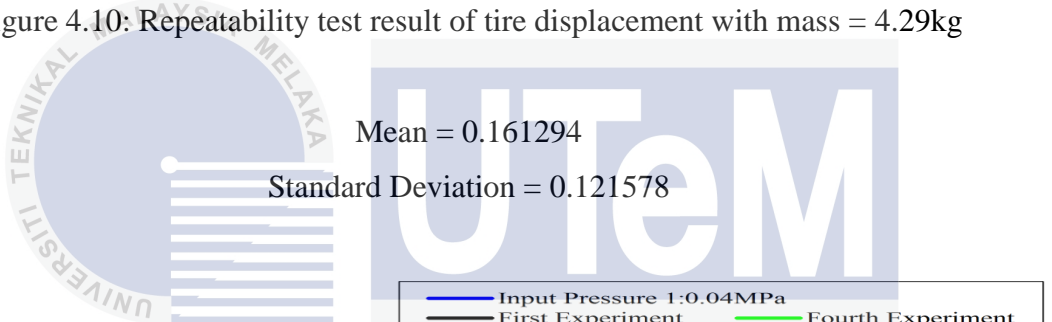
Figure 4.11: Repeatability test result of wheel deflection with mass = 4.29kg

Mean = 0.161294

Standard Deviation = 0.121578

4.2.2 Repeatability Test with Mass of Vehicle Body = 4.59kg
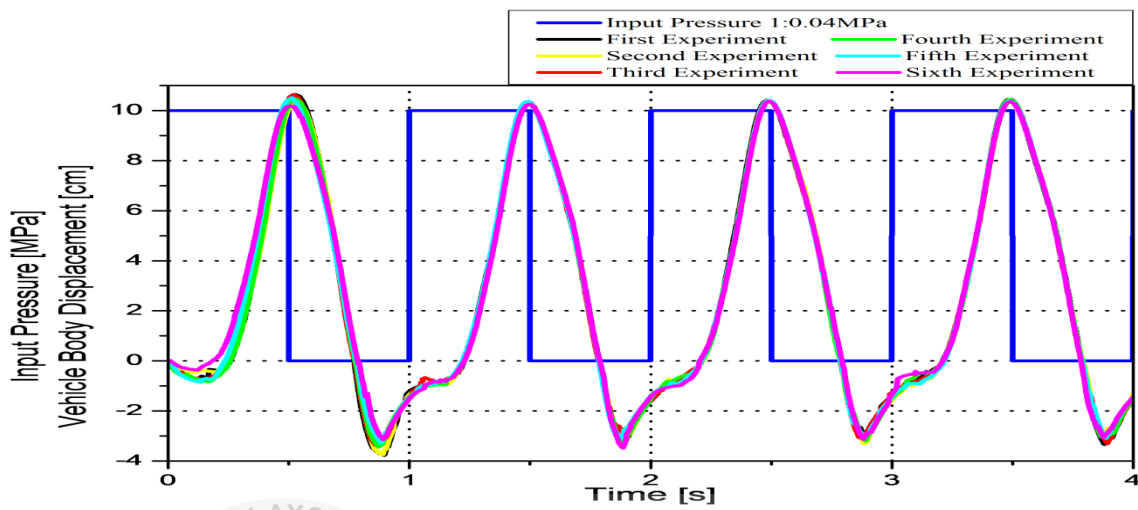
Figure 4.12: Repeatability test result of vehicle body displacement with mass = 4.59kg

Mean = 0.148254

Standard Deviation = 0.132075
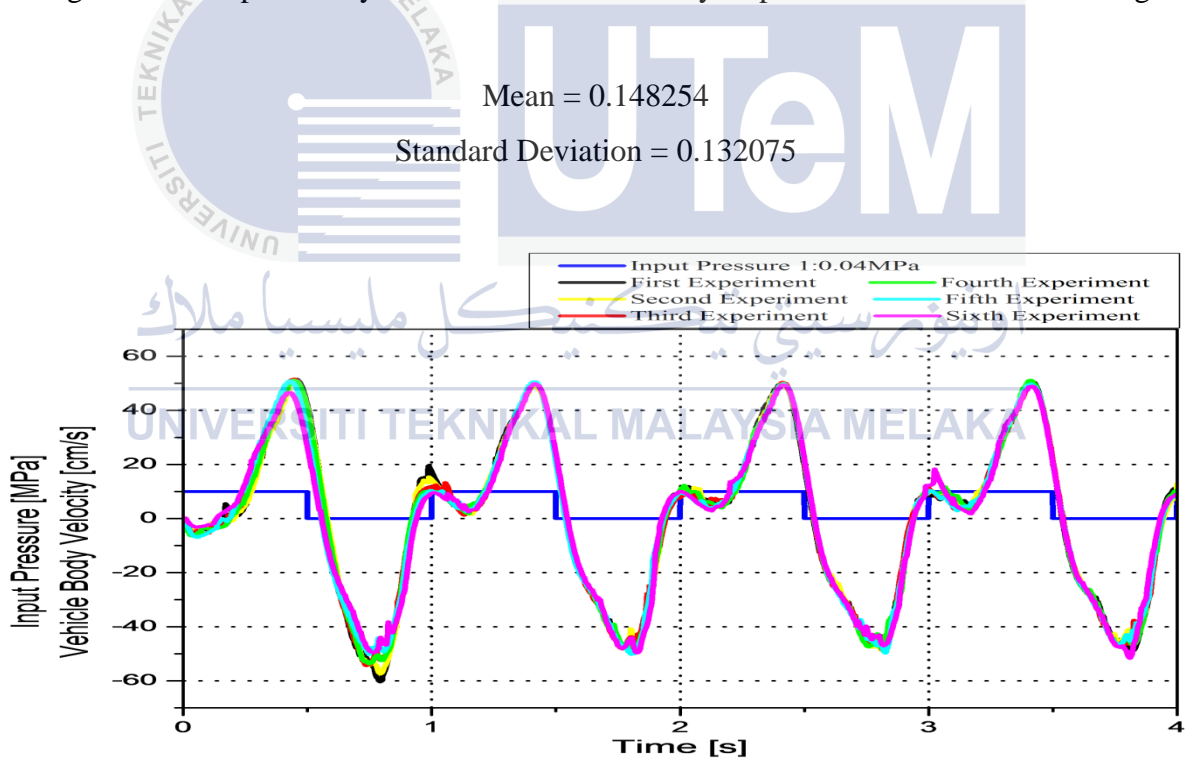
Figure 4.13: Repeatability test result of vehicle body velocity with mass = 4.59kg

Mean = 1.652356

Standard Deviation = 1.194043
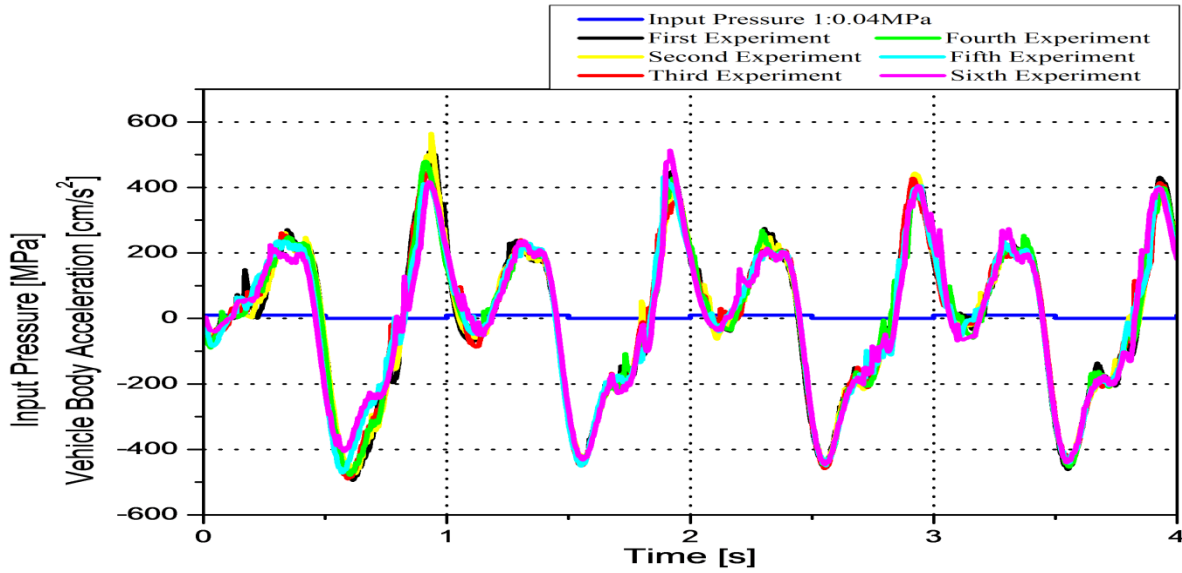
Figure 4.14: Repeatability test result of vehicle body acceleration with mass = 4.59kg

Mean = 23.48326

Standard Deviation = 15.26317
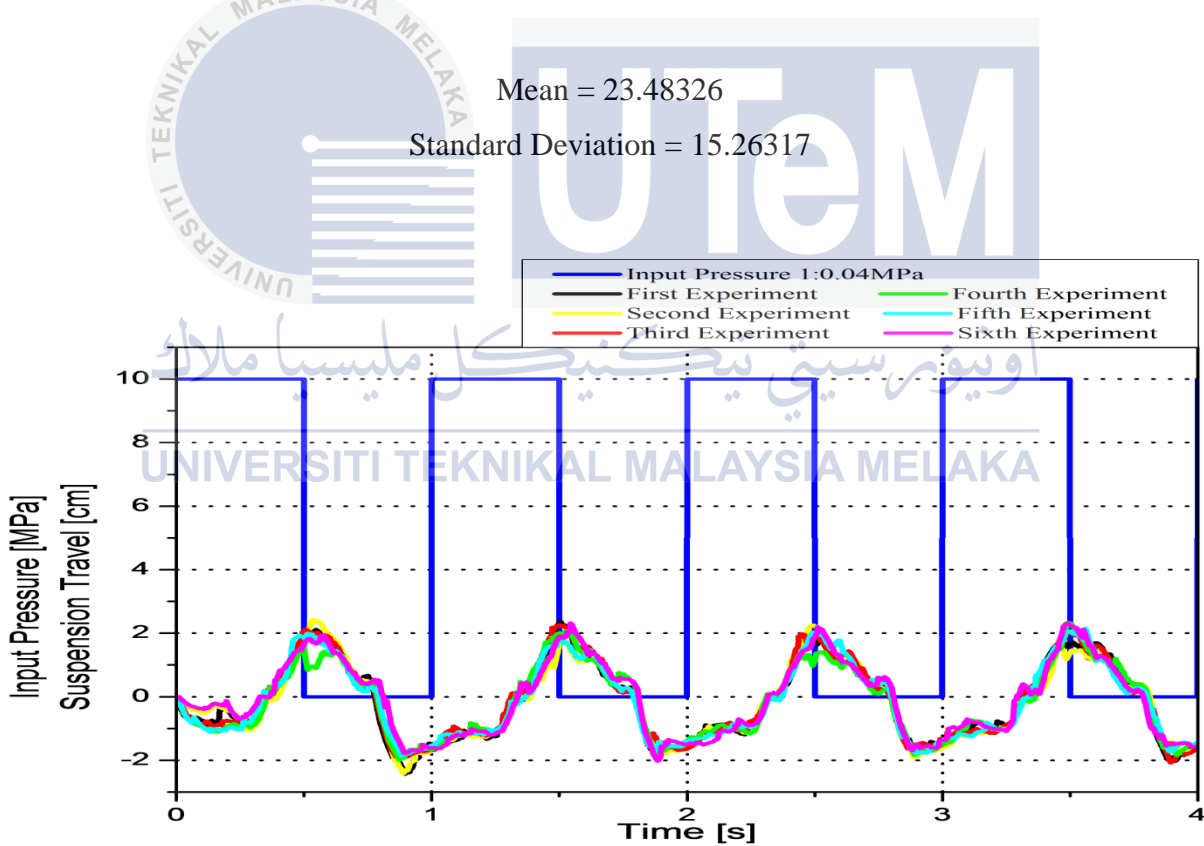
Figure 4.15: Repeatability test result of suspension travel with mass = 4.59kg

Mean = 0.175426

Standard Deviation = 0.088081
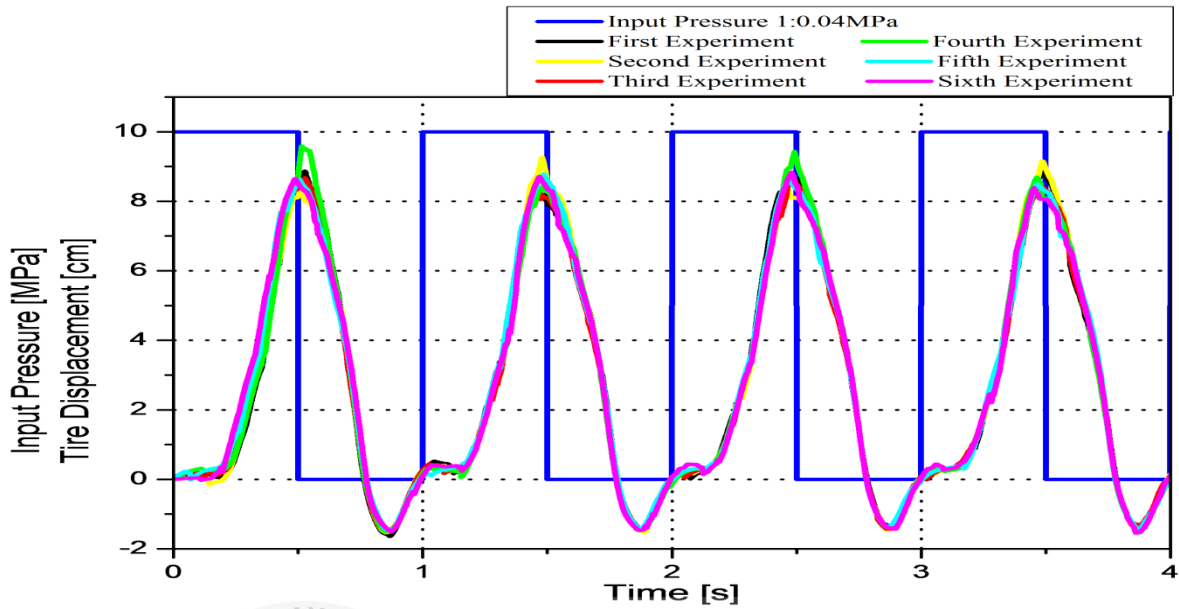
Figure 4.16: Repeatability test result of tire displacement with mass = 4.59kg

Mean = 0.150699

Standard Deviation = 0.11985
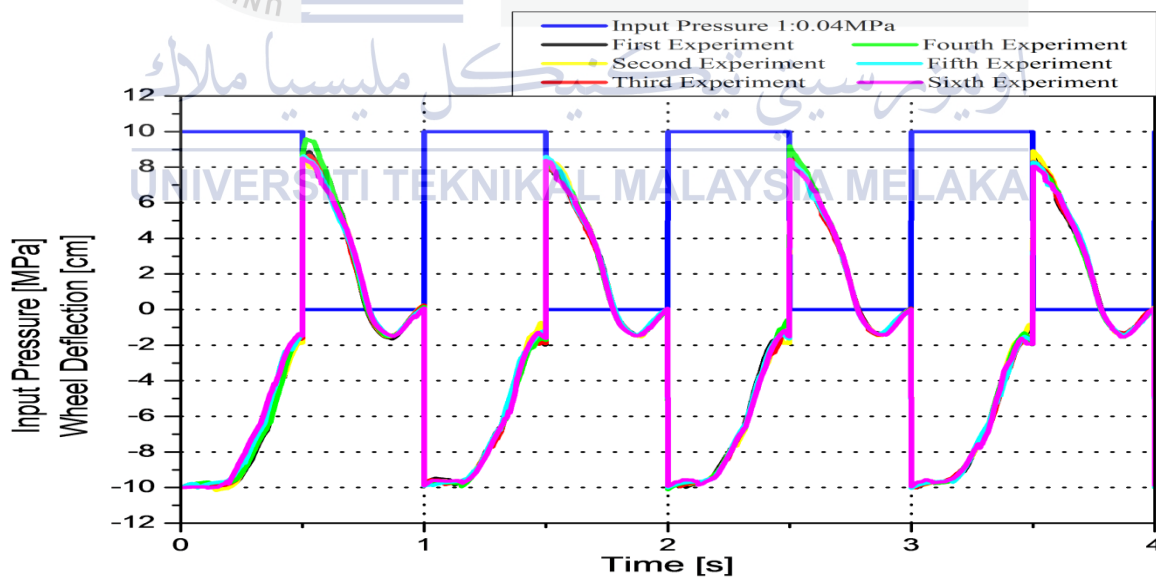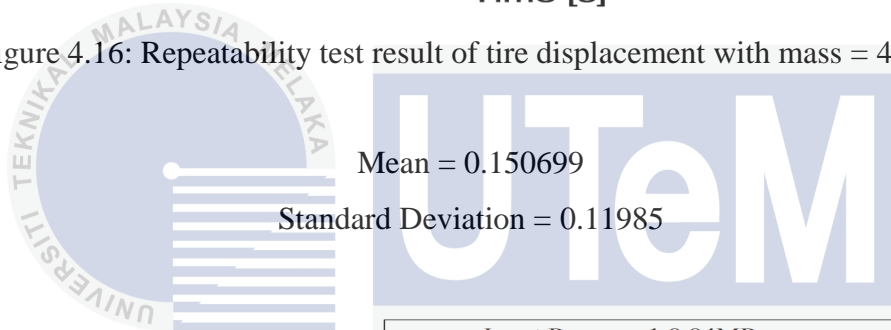
Figure 4.17: Repeatability test result of wheel deflection with mass = 4.59kg

Mean = 0.150699

Standard Deviation = 0.11985

4.2.3 Repeatability Test with Mass of Vehicle Body = 4.79kg
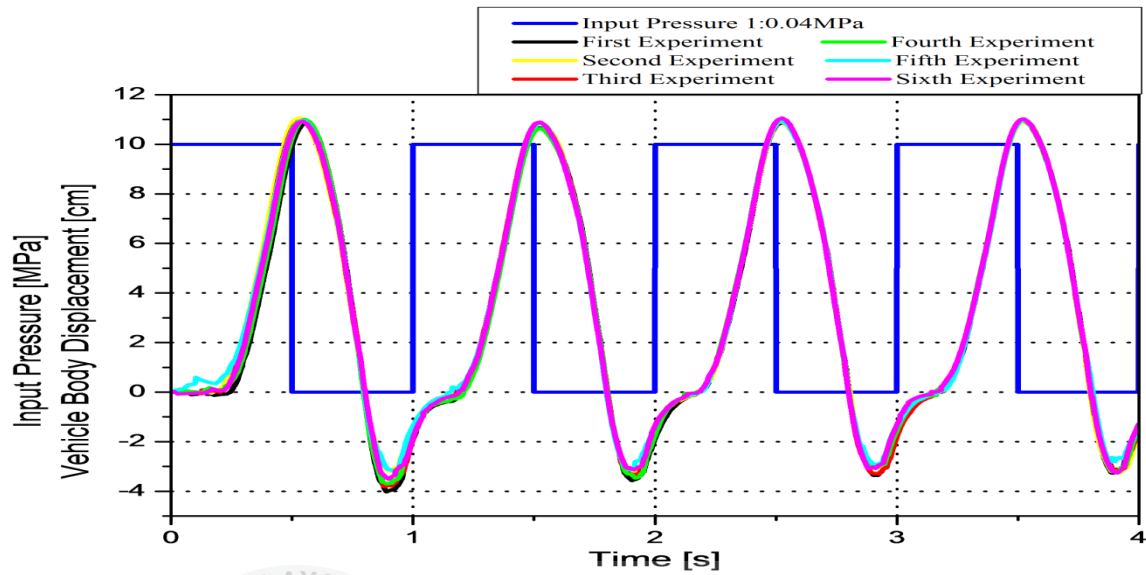
Figure 4.18: Repeatability test result of vehicle body displacement with mass = 4.79kg

Mean = 0.147323

Standard Deviation = 0.114662
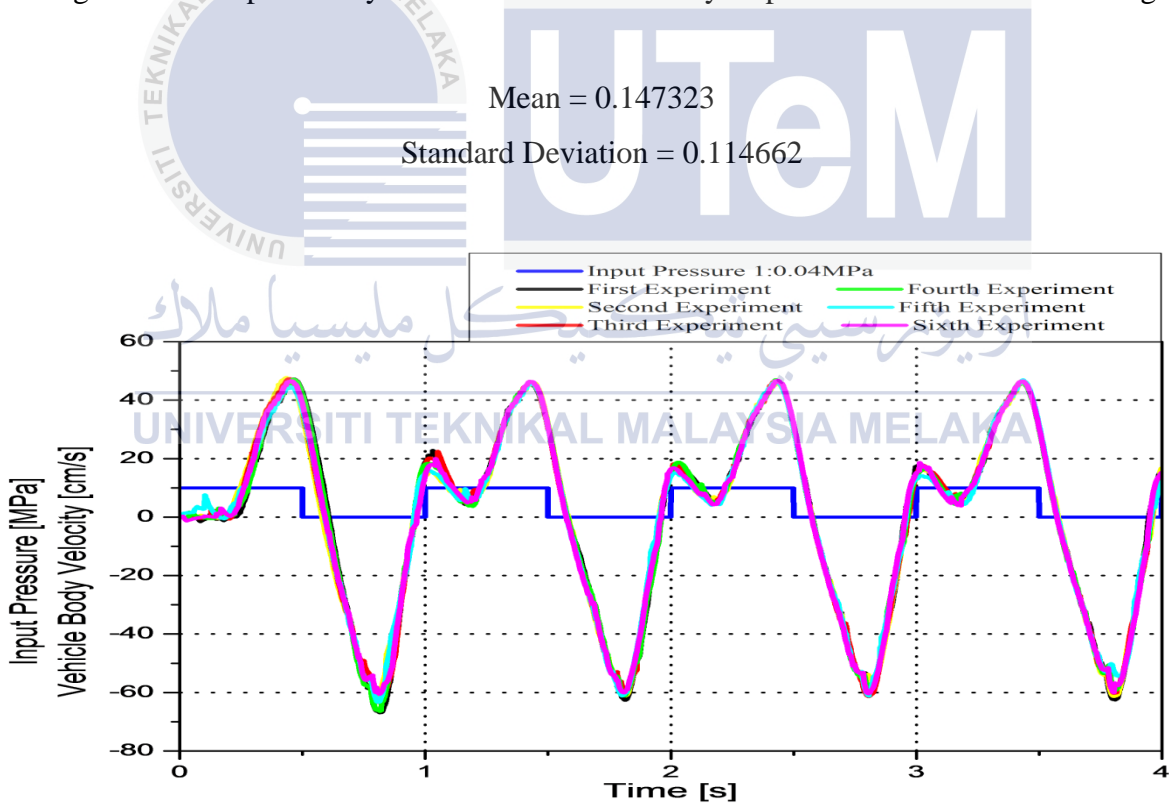
Figure 4.19: Repeatability test result of vehicle body velocity with mass = 4.79kg

Mean = 1.398659

Standard Deviation = 0.997398
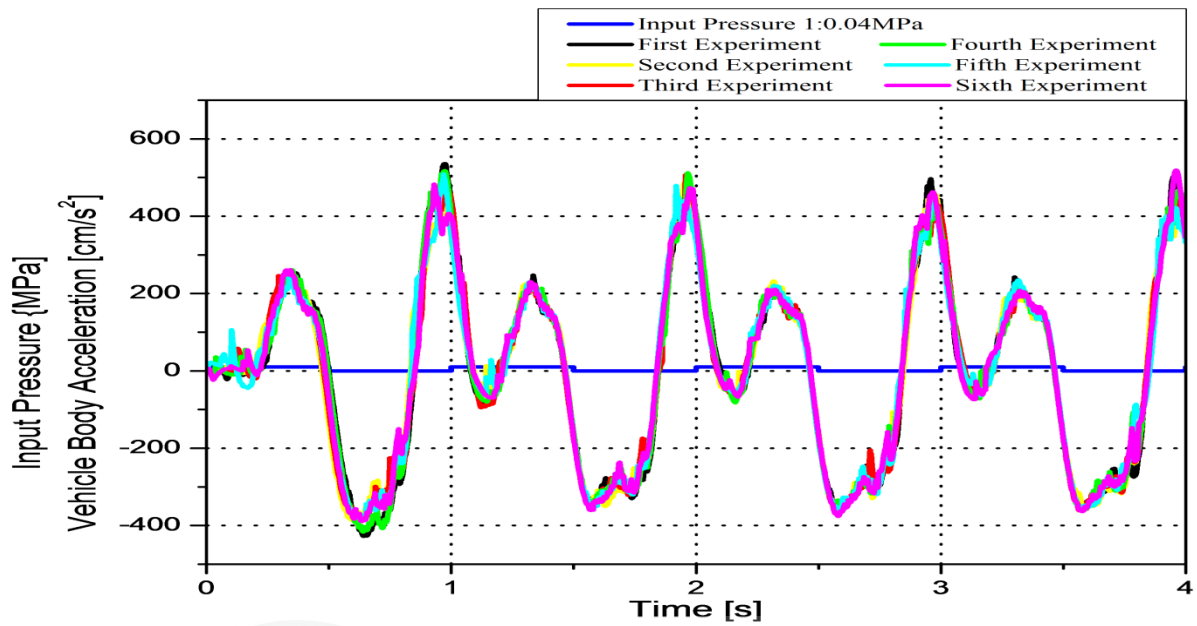
Figure 4.20: Repeatability test result of vehicle body acceleration with mass = 4.79kg

Mean = 19.90344

Standard Deviation = 12.99442
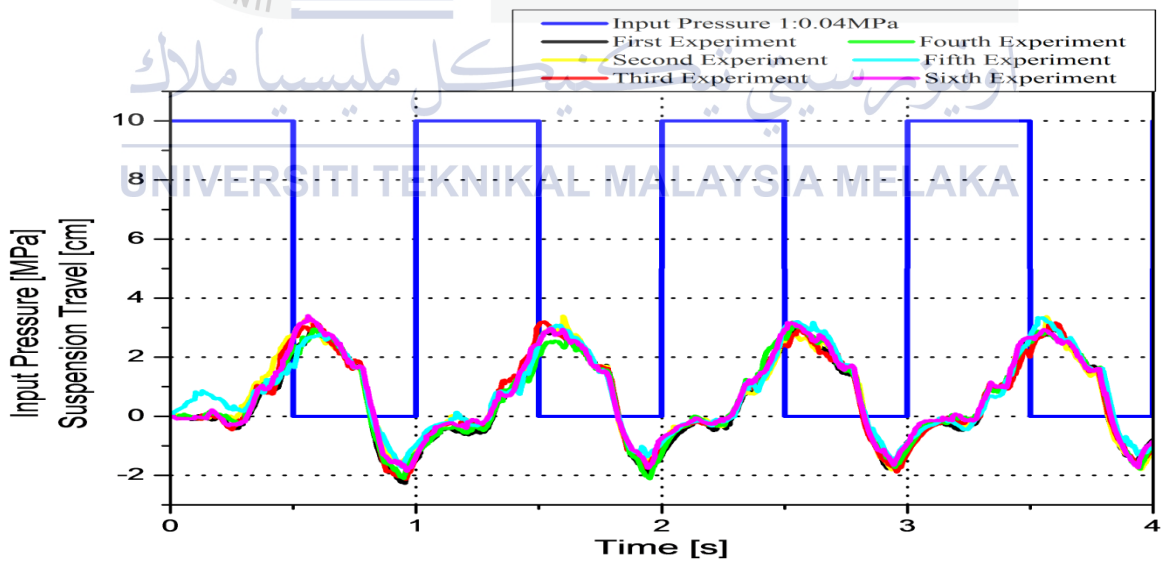
Figure 4.21: Repeatability test result of suspension travel with mass = 4.79kg

Mean = 0.174902

Standard Deviation = 0.083539
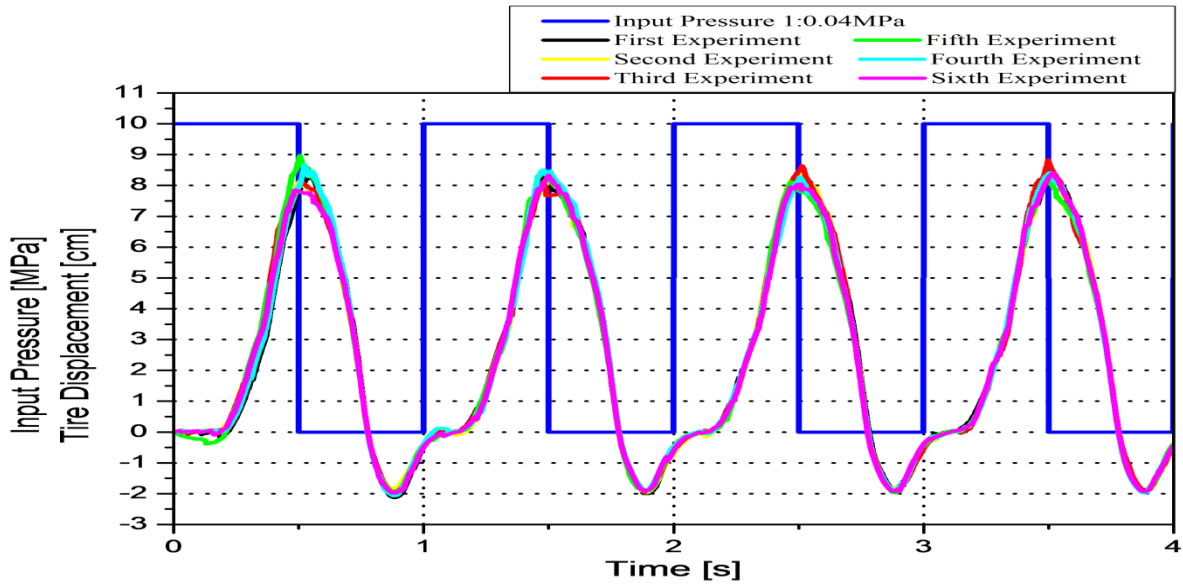
Figure 4.22: Repeatability test result of tire displacement with mass = 4.79kg

Mean = 0.124039

Standard Deviation = 0.090254
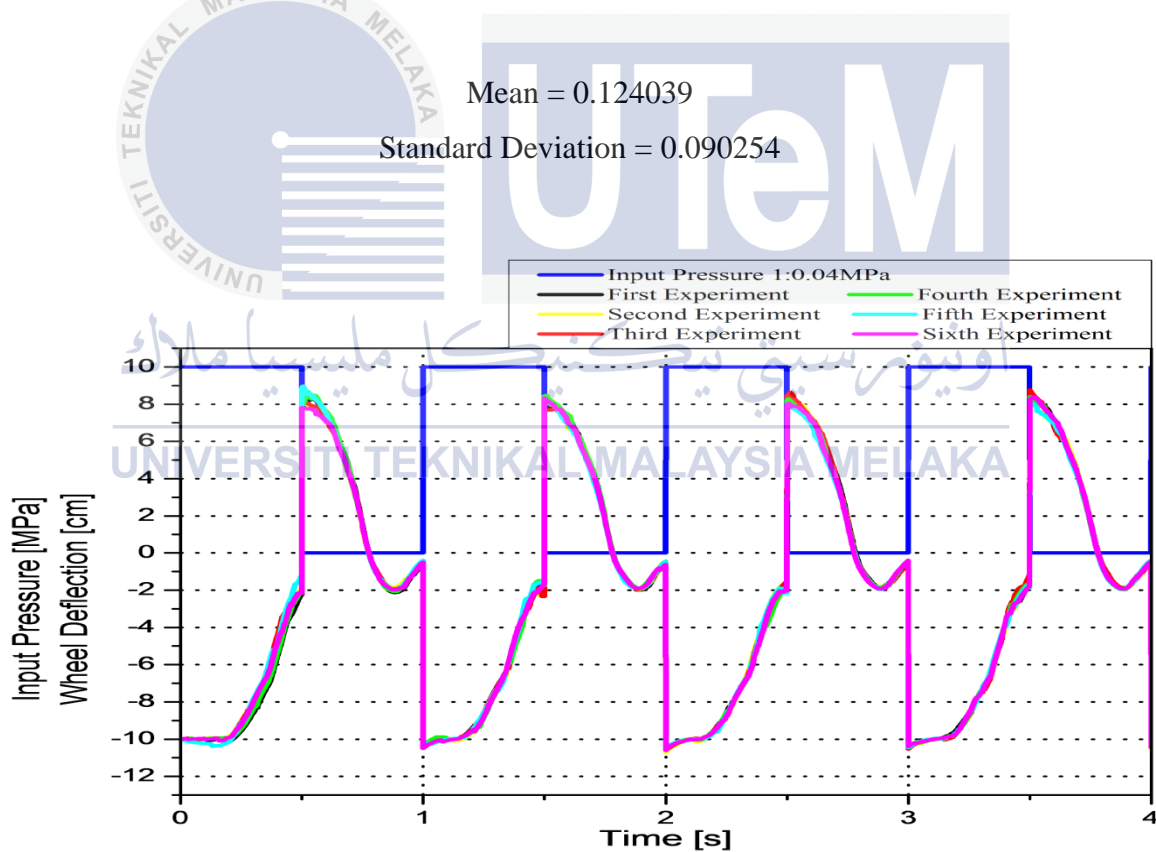
Figure 4.23: Repeatability test result of wheel deflection with mass = 4.79kg

Mean = 0.124039

Standard Deviation = 0.090254

4.3 Experiments with Different Mass and Different Input

Experiments with different mass have been carried out in order to determine the dynamic and characteristics of this passive suspension system prototype. First of all, the mass of vehicle body carried out here are 4.29kg, 4.59kg and 4.79kg while the mass of tire is remained constant at 1.48kg during all experiments processes. Secondly, pulse input pressure with 0.4MPa and time taken for the experiments are set at 4s for all experiments. However, the period of one cycle and pulse width are set differently during the experiments processes. Table 4.2 shows the types of experiments that have been conducted. All the plotted graphs of each experiment can be found in Appendix C.

Table 4.2: Types of experiments

Experiment	Pulse Input Pressure (MPa)	Pulse Width (%)	Period of one cycle (s)	Time taken for whole experiment (s)
A	0.4	50	1	4
B	0.4	75	1	4
C	0.4	50	2	4
D	0.4	25	2	4

Next, the graphs of vehicle body displacement from different types of experiments are compared. Figure 4.24 to 4.27 below show the vehicle body displacement of Experiment A to Experiment D respectively where vehicle body displacement is representing the ride quality of a vehicle. By referring to the four different graphs below, it can be seen that this passive suspension system prototype performs different characteristic when different type of pulse width is supplied to the prototype.
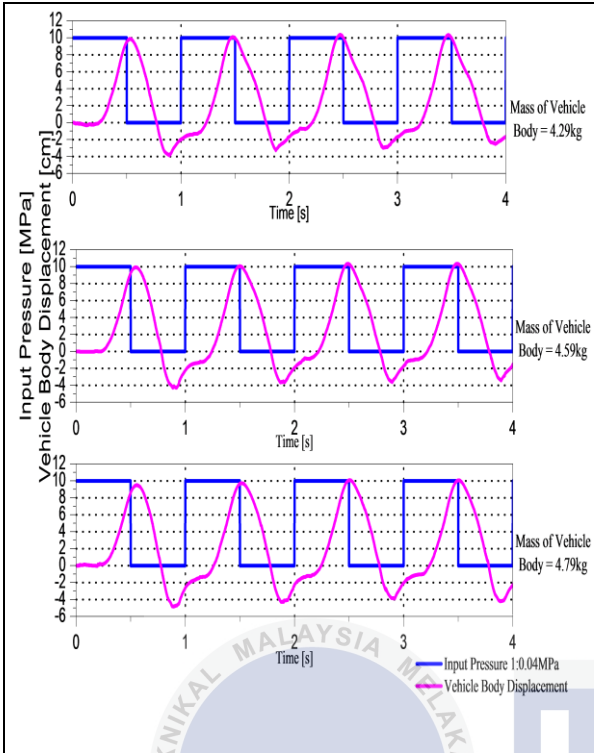
Figure 4.24: Vehicle body displacement of Experiment A
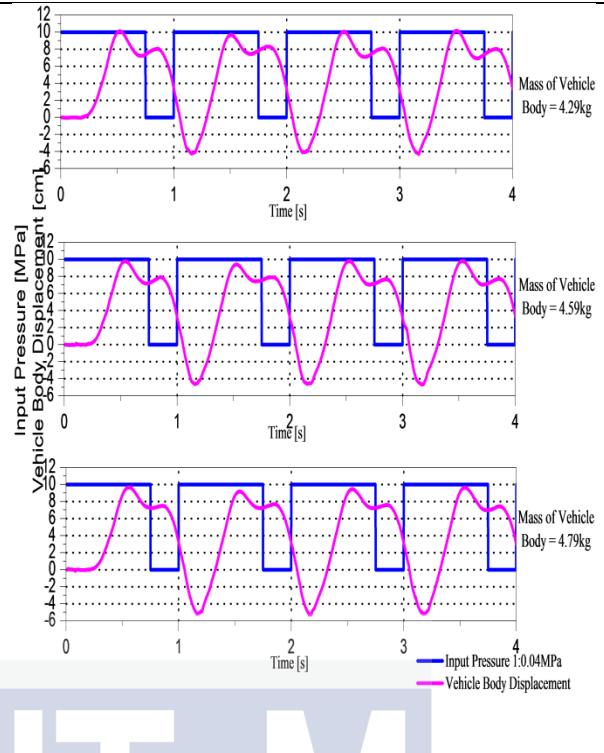
Figure 4.25: Vehicle body displacement of Experiment B
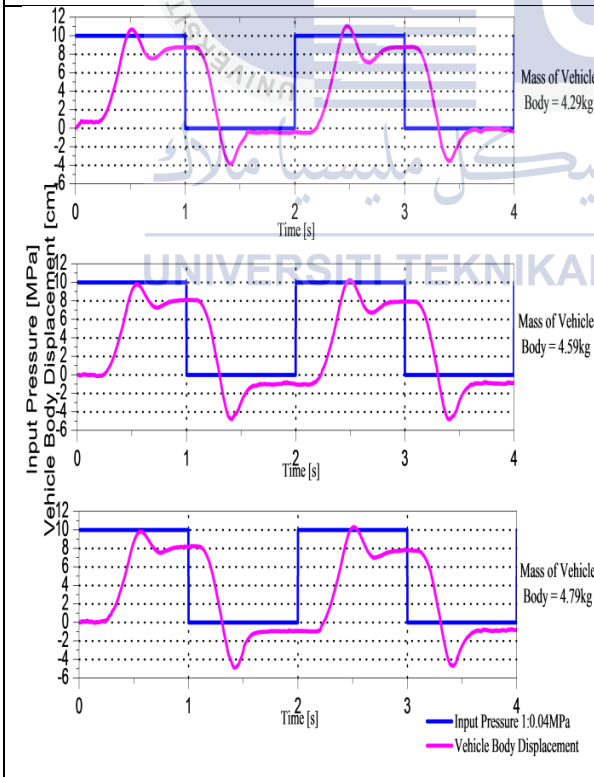
Figure 4.26: Vehicle body displacement of Experiment C.
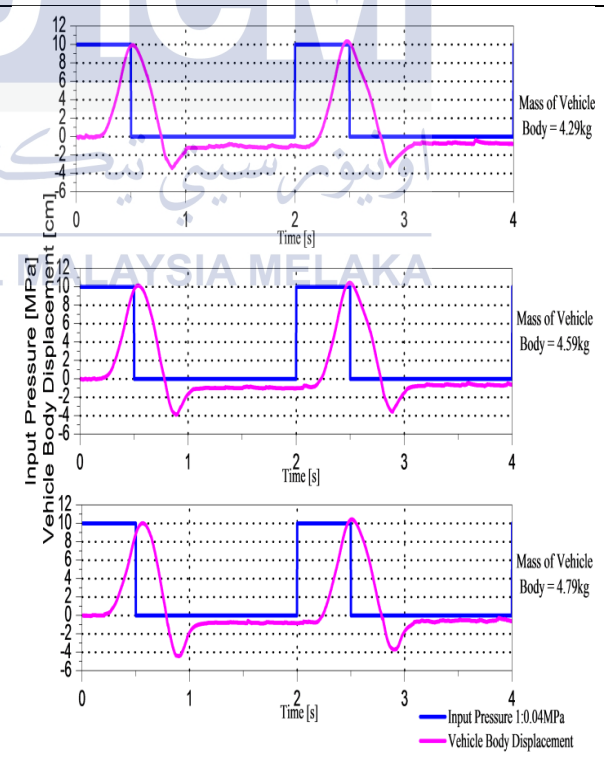
Figure 4.27: Vehicle body displacement of Experiment D.
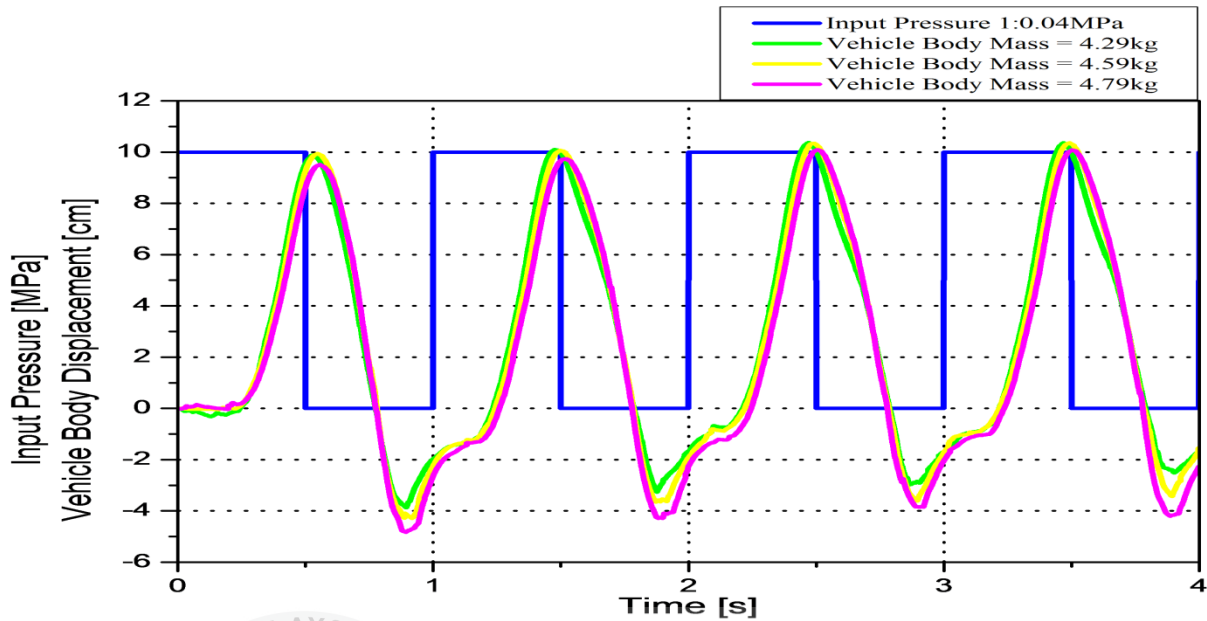
Figure 4.28: Vehicle body displacement of Experiment A using different vehicle body mass

Table 4.3: Dynamic response of Experiment A

Mass (kg)	Peak Magnitude (cm)	Undershoot (cm)	Response Time (s)
4.29	9.881	-3.842	0.526
4.59	9.942	-4.282	0.548
4.79	9.510	-4.826	0.557

For Figure 4.28, the period of one cycle is 1s and the pulse width is 50% of the period. This means that the piston rod of double acting cylinder is fully extended until 0.5s then only the piston rod will retract back to the origin position. This process is repeated for 4s (4 cycles) then only the double acting cylinder stop functioning. By looking at Figure 4.28, it can be observed that there is time delay in experiment because piston rod of the cylinder takes time to be fully extended (due to existence of pressurized air) which leads towards time delay. Besides that, there is no oscillation when the piston rod is extended but there is undershoot on the graph when the piston rod is retracted back to the origin position. This is happening in view of the vehicle body mass does not have sufficient time to settle down when the piston rod has been retracted back. When the piston rod is retracted back, the vehicle body mass is pulled down by the piston rod as well as the gravitational force and thus produces undershoot. After

that, the piston rod extended again when the vehicle body mass oscillates half way and therefore produces the shape of undershoots shown in graph. The shape of the graphs with different vehicle body mass is more or less the same. However, by referring to Table 4.3, undershoot of the graph is increased as the vehicle body mass increases. This is because the mass of an object is directly proportional to the gravitational force. Hence, the greater the vehicle body mass, the greater the gravitational pull exert on the vehicle body mass. In spite of that, the peak magnitude is supposedly to decrease as the mass of vehicle body increases because large gravitational force will hold down the oscillation of the system. Yet the peak magnitude with vehicle body mass of 4.59kg is the highest among the others. This is due to the unbalanced condition of the placement of vehicle body mass. Since the load is not placed equally on the plate, thus the force does not distributed equivalently. In addition, the response time for the heavier vehicle body mass to be pulled down by the cylinder is longer as compared with lighter mass. This is because an object with larger mass contains larger momentum. Larger momentum causes the vehicle body mass to move against the movement of the piston rod. As a result, the vehicle body mass takes longer time and larger force to move accordingly to the movement of the piston rod.
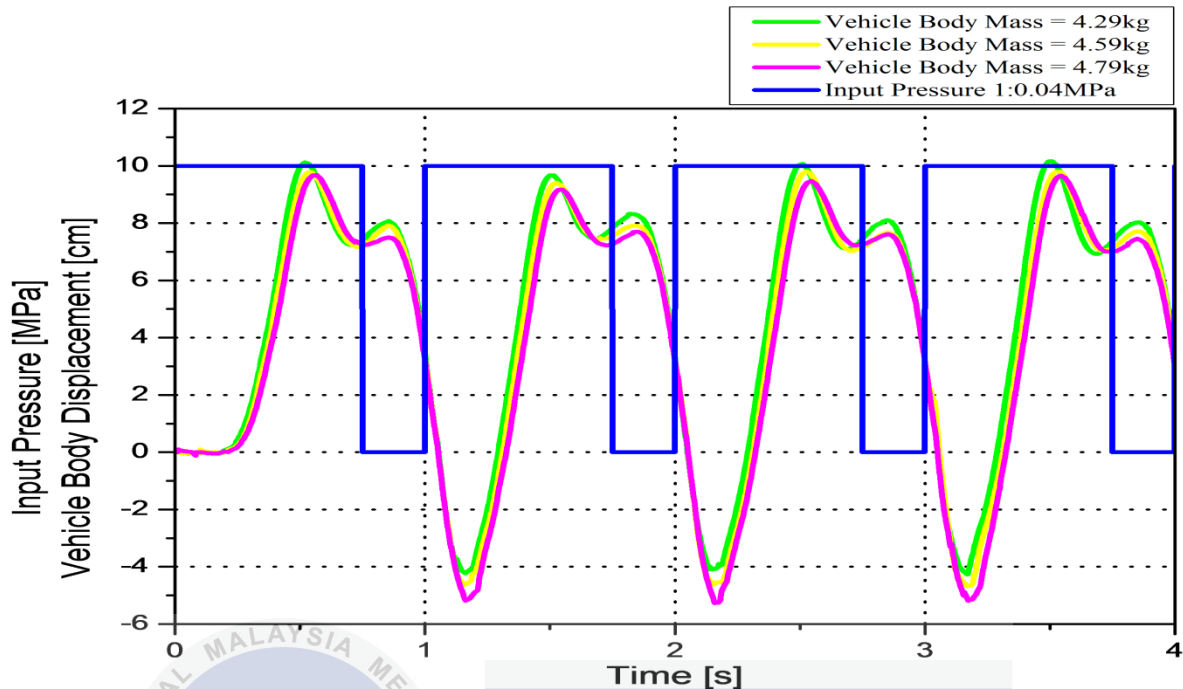
Figure 4.29: Vehicle body displacement of Experiment B using different vehicle body mass

Table 4.4: Dynamic response of Experiment B

Mass (kg)	Peak Magnitude (cm)	Undershoot (cm)	Response Time (s)
4.29	10.121	-4.225	0.519
4.59	9.785	-4.630	0.546
4.79	9.684	-5.181	0.563

Figure 4.29 shows experiment with period of one cycle is 1s and the pulse width is 75% of the period. The piston rod of double acting cylinder is fully extended until 0.75s then only the piston rod will retract back to the origin position. This process is repeated for 4s (4 cycles) then only the double acting cylinder stop functioning. First of all, time delay problem is happening in this experiment as well and it will happen in all experiments due to the time taken for the piston rod to be fully extended. Next, it can be seen that there is oscillation in Experiment B when the piston is extended as compared to Experiment A. This is because the piston rod is fully extended within 0.5s and remains stationary until 0.75s then only it retracted back to original position. Thus vehicle body mass has time to settle down when the piston rod remains stationary during extending process. After 0.75s, the piston retracted back to original

position and extended again at 1s. The vehicle body mass does not have time to oscillate since the retracted time is very fast. So the vehicle body mass will oscillate based on the retracting and extending speed of the piston rod. Anyhow, the vehicle body mass is still pulled by the gravitational force which causes it to move below the origin position. By referring to Table 4.4, same case happens here where the amplitude of undershoot is larger as the mass increases. However, the overshoot is decreases as the vehicle body mass increases. This is because greater mass contains greater gravitational force and hence restricting the oscillation of the vehicle body mass.
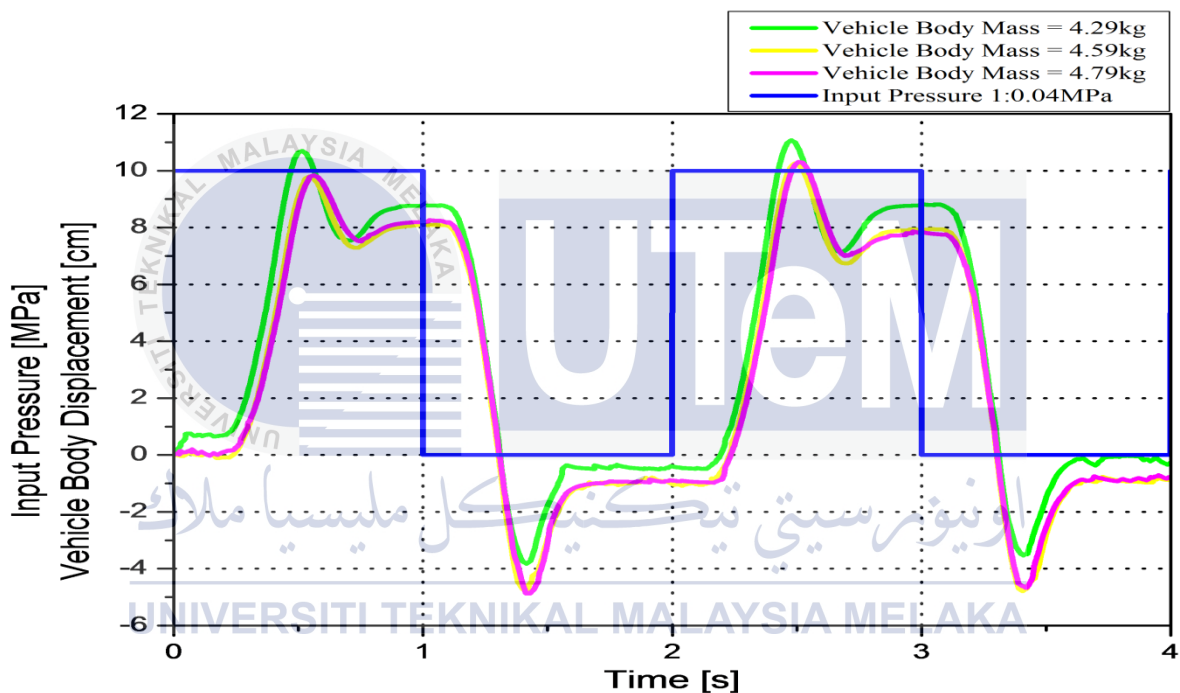
Figure 4.30: Vehicle body displacement of Experiment C using different vehicle body mass

Table 4.5: Dynamic response of Experiment C

Mass (kg)	Peak magnitude (cm)	Undershoot (cm)	Response Time (s)
4.29	10.694	-3.82	0.516
4.59	9.79	-4.75	0.545
4.79	9.83	-4.87	0.563

Now, let's proceed to Figure 4.30 where the period of one cycle is 2s and the pulse width is 50% of the period. This shows that the piston rod of double acting cylinder is fully extended and remains stationary until 1s then only the piston rod will retract back to the origin position. This process is repeated for 4s (2 cycles). Firstly, it can be noticed that the vehicle body mass is oscillating when the piston rod is extended and remain stationary until 1s. The steady state for this experiment is longer as compared to Experiment B since the pulse width and period of one cycle for this experiment are larger than Experiment B. Longer period of one cycle and larger pulse width allow the vehicle body mass to have longer time to settle down before the piston rod retracted back. After 1s, piston rod retracted back and high force from cylinder makes the plate to move negative direction and therefore produced undershoots. Again, the piston rod kept constant until 2s then extended to start a new cycle. Before a new cycle begins, it can be observed that the vehicle body mass does not fully return back to the original position. This is caused by the damper which does not fully extended back during the experiment. Furthermore, Table 4.5 shows undershoot of this experiment increases with the increase of vehicle body mass due to gravitational force. However, nonlinear characteristic in this prototype causes the peak magnitude of vehicle body mass of 4.79kg larger than vehicle body mass of 4.59kg.
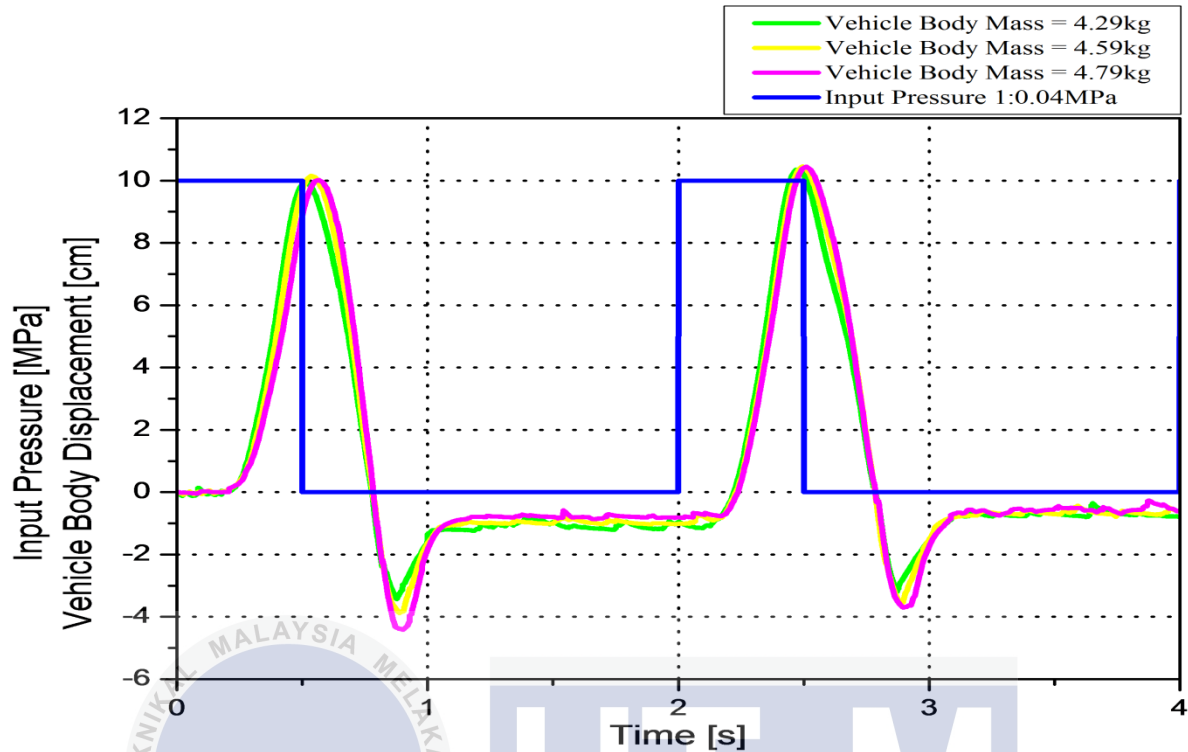
Figure 4.31: Vehicle body displacement of Experiment D using different vehicle body mass

Table 4.6: Dynamic response of Experiment D

Mass (kg)	Peak Magnitude (cm)	Undershoot (cm)	Response Time (s)
4.29	9.928	-3.428	0.507
4.59	10.152	-3.880	0.535
4.79	10.017	-4.415	0.566

Lastly, let's have a look at Figure 4.31 where the period of one cycle is 2s and the pulse width is 25% of the period. The piston rod of double acting cylinder is fully extended and remains stationary until 0.25s then only the piston rod will retract back to the origin position. This process is repeated for 4s (2 cycles). By observing Figure 4.31, there is no oscillation due to the fast extension and retracted time of the piston rod in this experiment. Vehicle body mass does not have enough time to reach steady state since the piston rod retracted back at 0.25s. Then, undershoot is produced when the high force from cylinder pulled down the vehicle body to negative direction. Table 4.6 shows the undershoot increases with the increase of the vehicle body mass. After the piston rod is retracted back, it remains

stationary until 2s then only extended back to start a new cycle. Long period of resting time of piston rod allows vehicle body to settle down and reach steady state. But again, the limitation of the damper causes the vehicle body not to oscillate back to the original position. Instead of that, the response time for the vehicle body to be move in negative direction is longer with the increase of the mass of vehicle body. Larger mass with larger momentum causes the vehicle body mass takes longer time to move in the direction of the piston rod.

Next, comparison of the graph of tire displacement obtained from different types of experiments is shown below. Figure 4.32 to 4.35 below shows the tire displacement of Experiment A to Experiment D where tire displacement is representing the car handling of a vehicle. By referring to the four different graphs below, it can be seen that this passive suspension system prototype performs different characteristic when different type of pulse width is supplied to the prototype.
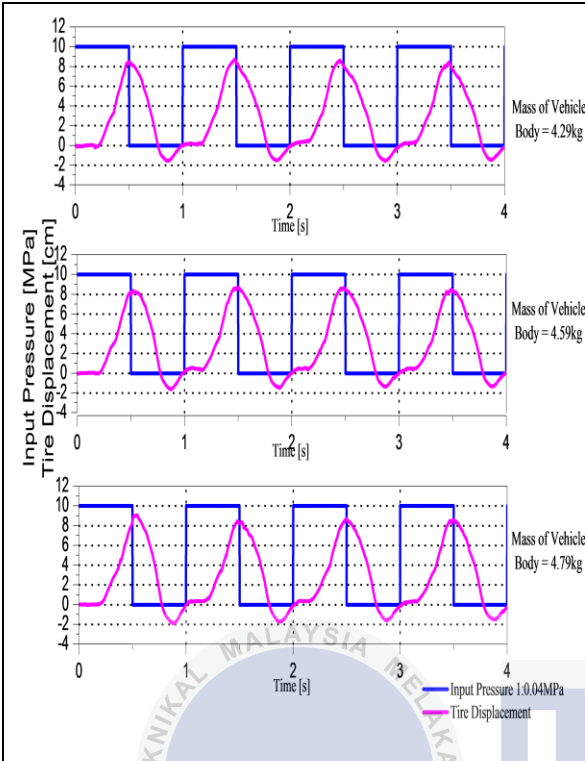
Figure 4.32: Tire displacement of Experiment A
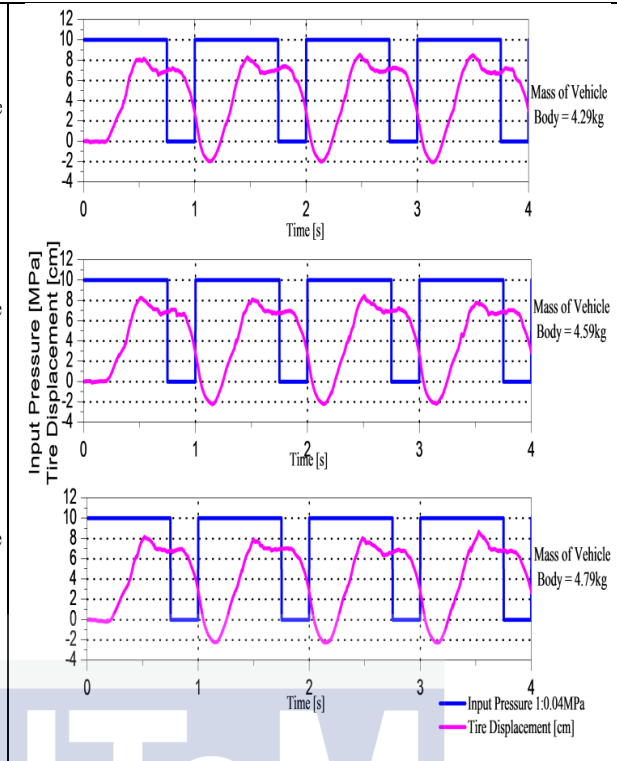
Figure 4.33: Tire displacement of Experiment B
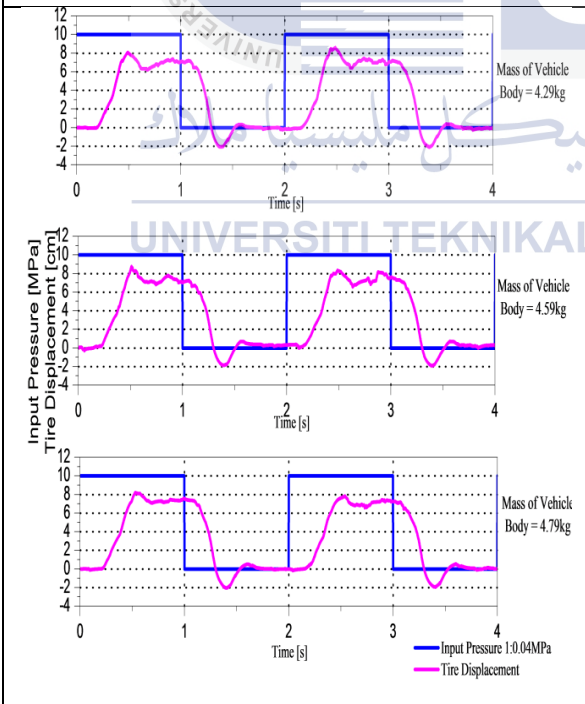
Figure 4.34: Tire displacement of Experiment C
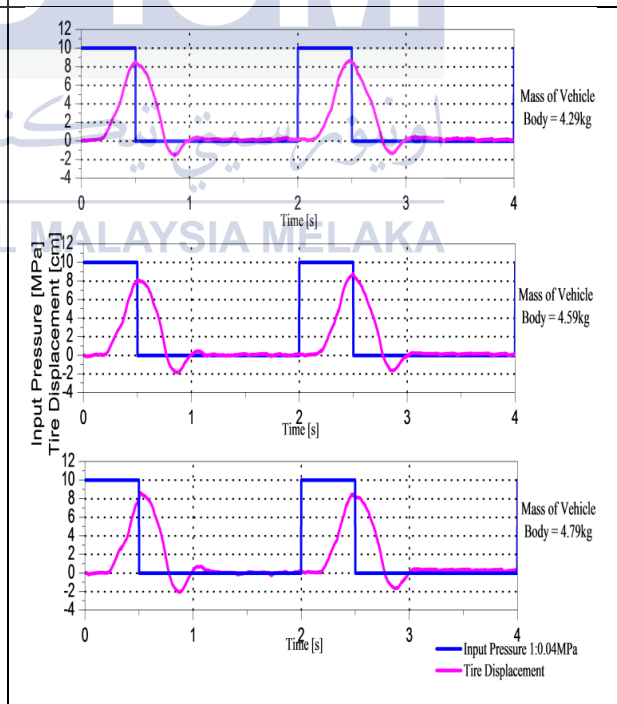
Figure 4.35: Tire displacement of Experiment D

Figure 4.36 to 4.39 show the combined graph of tire displacement using different vehicle body mass for Experiment A, B, C and D respectively. By looking at Figure 4.36 to 4.39, it can be noticed that the shape of the graphs of tire displacement are more or less the same with the graphs of vehicle body displacement shown in Figure 4.28 to 4.31 for the same experiments that have been conducted. However, the graphs of the tire displacement contain more oscillations as compared to the graphs of vehicle body displacement. This is because there is a damper and a spring connected between the vehicle body and the tire which act as the vehicle suspension system whereas there is no damper and only a spring which represents the air pressure of the tire is connected between the tire and the road disturbance. The damper is used to absorb the shock from the road and therefore regulate the oscillation of the vehicle body. Since there is no damper connected between tire and road disturbance, the oscillation of the tire is therefore cannot be regulated. Other than that, the tire is always oscillating back to the original position as compared to vehicle body due to the absence of damper in the tire.
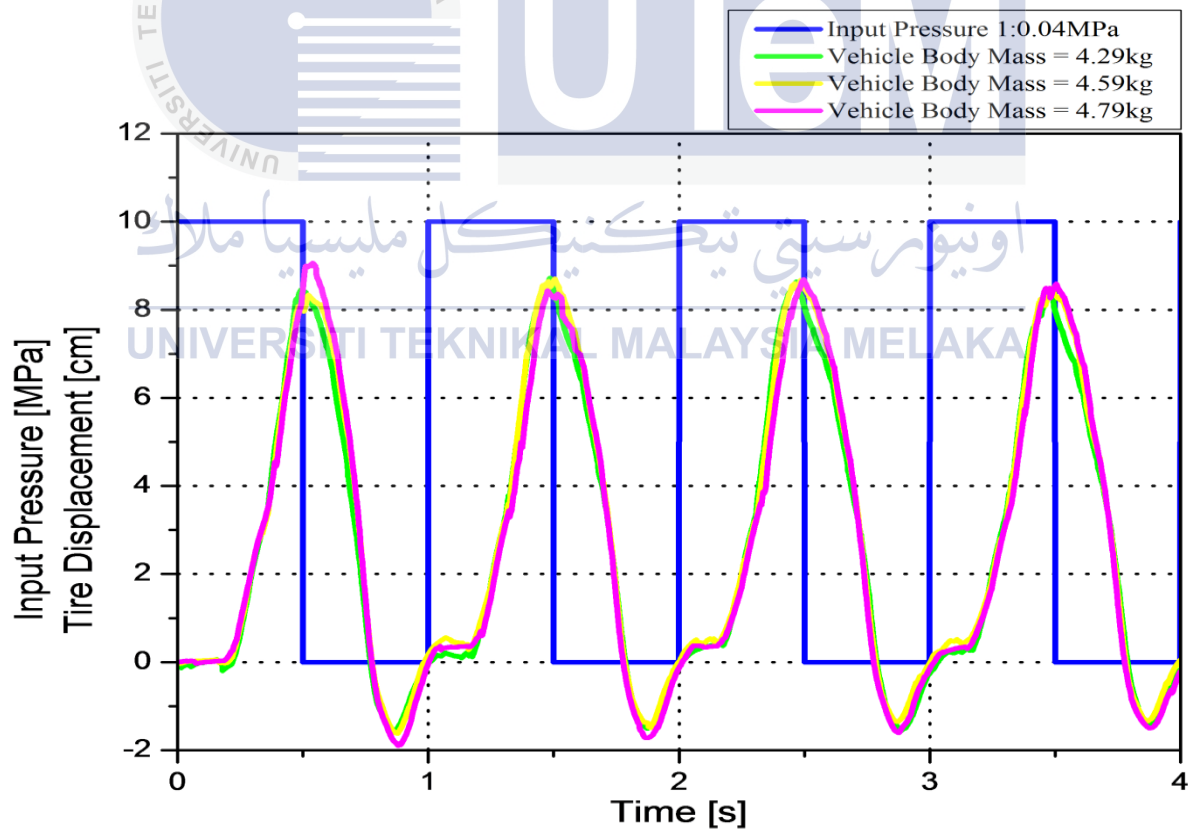
Figure 4.36: Tire displacement of Experiment A using different vehicle body mass
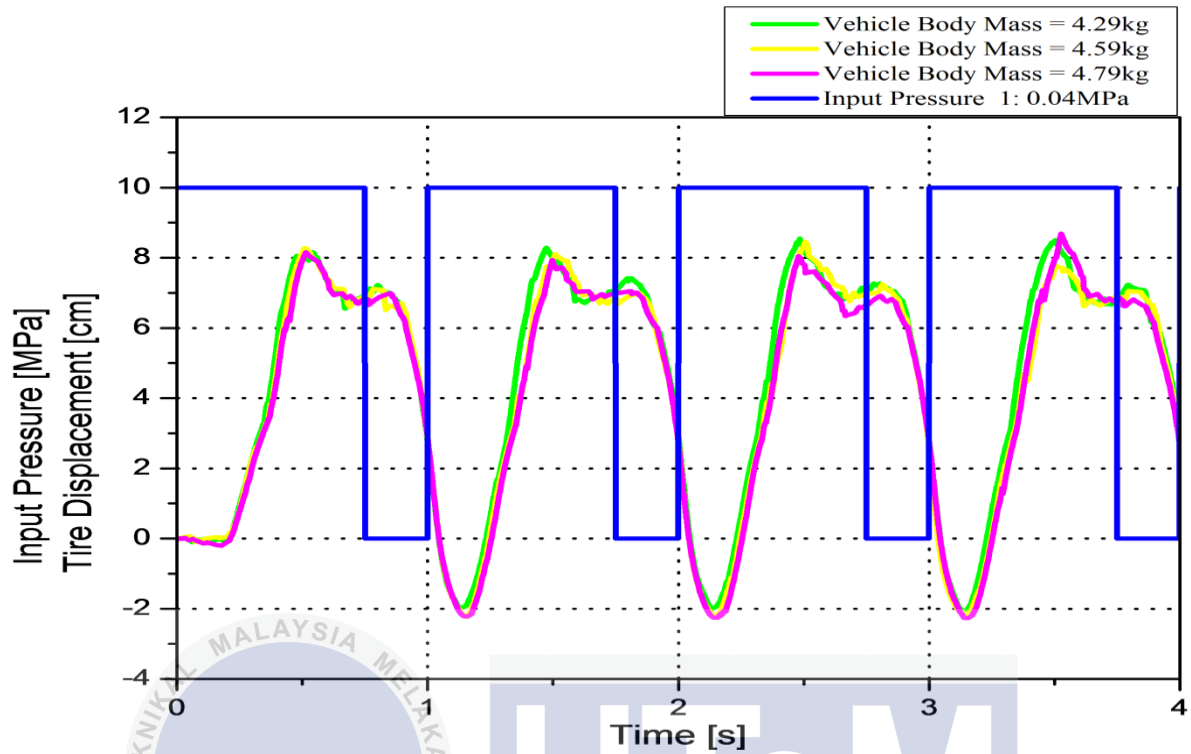
Figure 4.37: Tire displacement of Experiment B using different vehicle body mass
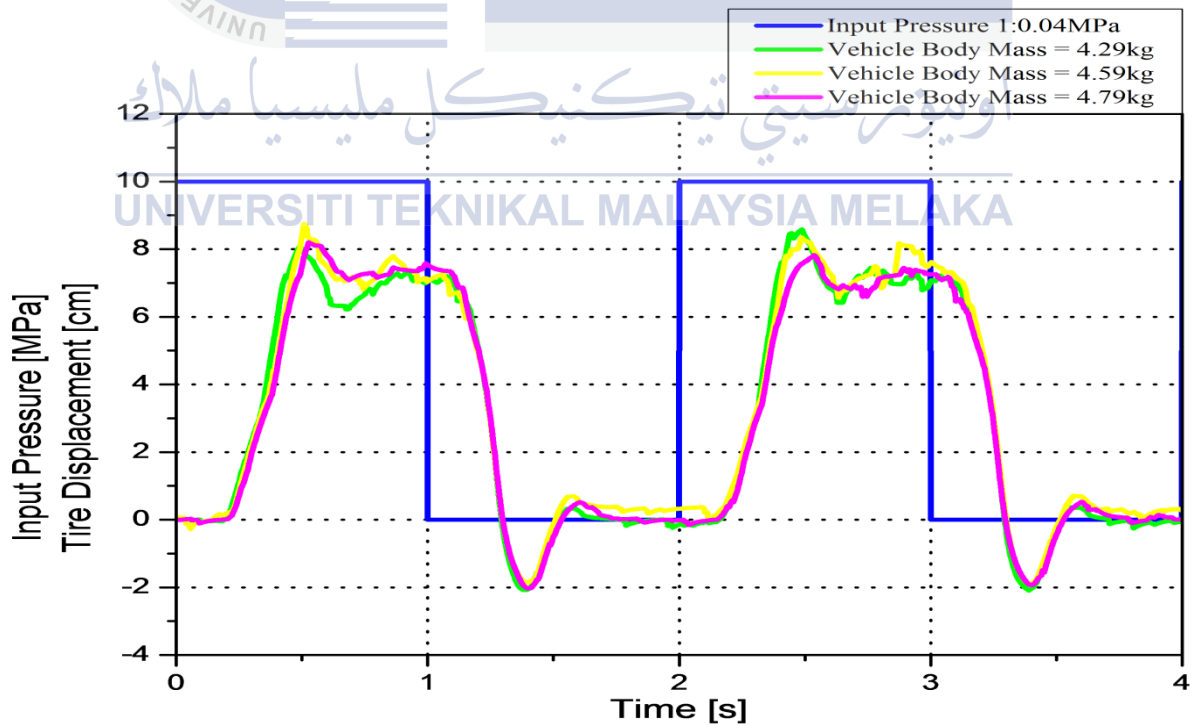
Figure 4.38: Tire displacement of Experiment C using different vehicle body mass
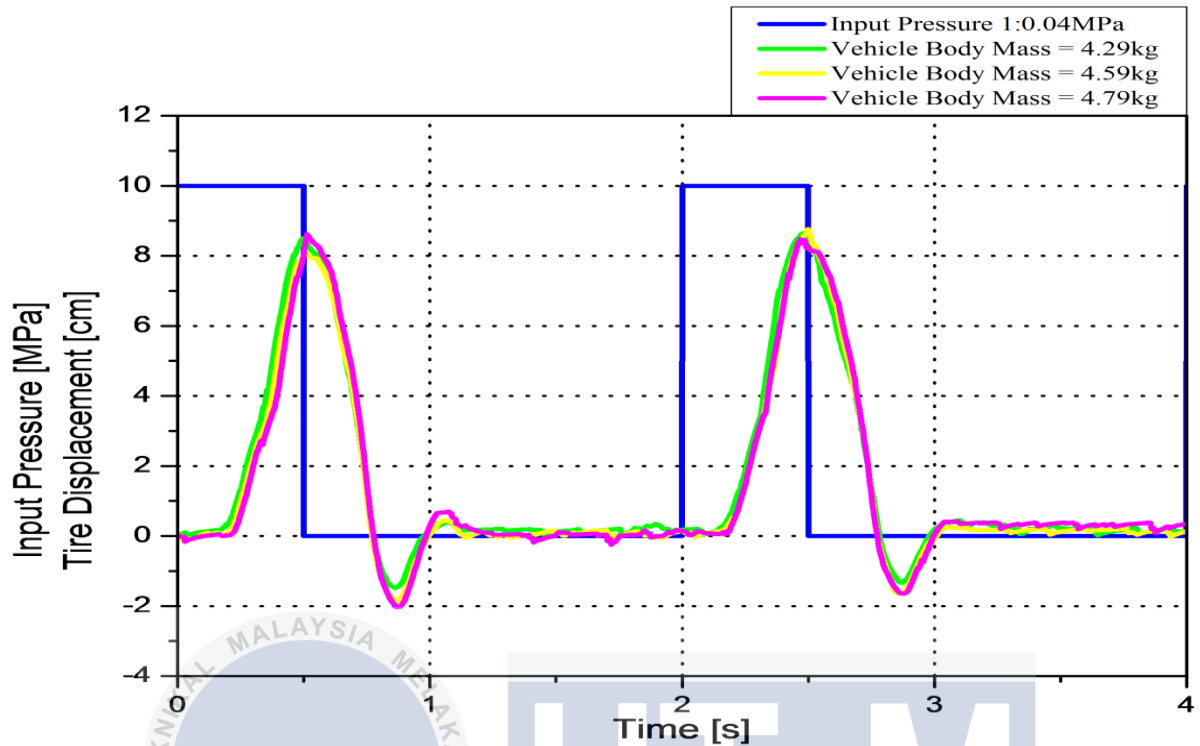
Figure 4.39: Tire displacement of Experiment D using different vehicle body mass

After conducted experiments with different mass and different pulse width of the input pressure, it can be concluded that this passive suspension system prototype shows different characteristic with respect to the pulse width of the input pressure. Furthermore, this prototype can only support up to 4.79kg on the top plate which represents the vehicle body. If the load added on the plate is more than 4.79kg, the plate represents the vehicle body will then hit with the plate which represents the tire during experiments. This is due to the limitation of the spring and damper that have been used in this prototype.

4.4   Simulation and Experimental Results Analysis and Discussion

This part shows the comparison and analysis of the experimental and simulation results. The experiments have been carried out using the experiment setup shown in Figure 3.2 whereas the simulation has been conducted using the simulink block diagram shown in Figure 3.22. The simulink block diagram of the simulation is connected based on the equation of motion which obtained from the free body diagram exhibited in Figure 3.21. For both simulation and experimental process, pulse input signal has been used as the road disturbances that passing by a vehicle. Besides that, compressed air of 0.4MPa has been supplied to the double acting cylinder during the whole experimental process. Table 4.6 shows the parameters being used in experimental and simulation process. The values of damping constant and spring constant are obtained from the calibration result in Section 4.1.

Table 4.7: Parameters used in experimental and simulation process

Parameter Name	Unit	Value
Mass of vehicle body (sprung mass)	[kg]	4.29
Mass of the wheel and tire (unsprung mass)	[kg]	1.48
Spring constant of the suspension system	[N/m]	1245.99381
Spring constant of the tire	[N/m]	2411.41282
Dashpot constant (shock absorber)	[Ns/m]	9.57296

Figure 4.42 to 4.47 show the experimental and simulation result for the pulse input signal used during simulation and experimental process, pulse input signal with filter during experimental process, vehicle body displacement, vehicle body velocity, vehicle body acceleration, tire displacement, suspension travel, and wheel deflection of the system respectively. Figures mentioned above are comparing both simulation and experimental results.

During experimental process, a sensor has been placed below the plate which represents the road disturbance that applies to the system. The placement of the sensor is used to verify the accuracy of the experimental input signal with the simulation input signal. Since the stroke of double acting cylinder is 100mm, this means that the stroke will extend fully

until 100mm which represents the road disturbance. Hence, the pulse input for the simulation is set as 100mm. By referring to Figure 4.40, it can be observed that there is a difference between the input signal of the simulation and experimental results. The input signal for the experiment contains a lot of noises and disturbances when the sensor is recorded the data. Since this is an open loop system, the system is very sensitive to noises and disturbances surrounding and does not consist controller to compensate the disturbances occur in the system. Hence, a low-pass filter is added to eliminate the noise and disturbances occur in the experimental result. The distance measuring range for the sensor is 38.3ms with tolerance of $\pm$9.6ms. Therefore the maximum boundary measurement is 20.87Hz and this value is taken as the cut-off frequency of the sensor. Equation 4.1 shows the formula of the low pass filter.

$$\text{Low pass filter} = \frac{Wc}{s+Wc} \tag{4.1}$$

Where

Wc = cut-off frequency (Hz)
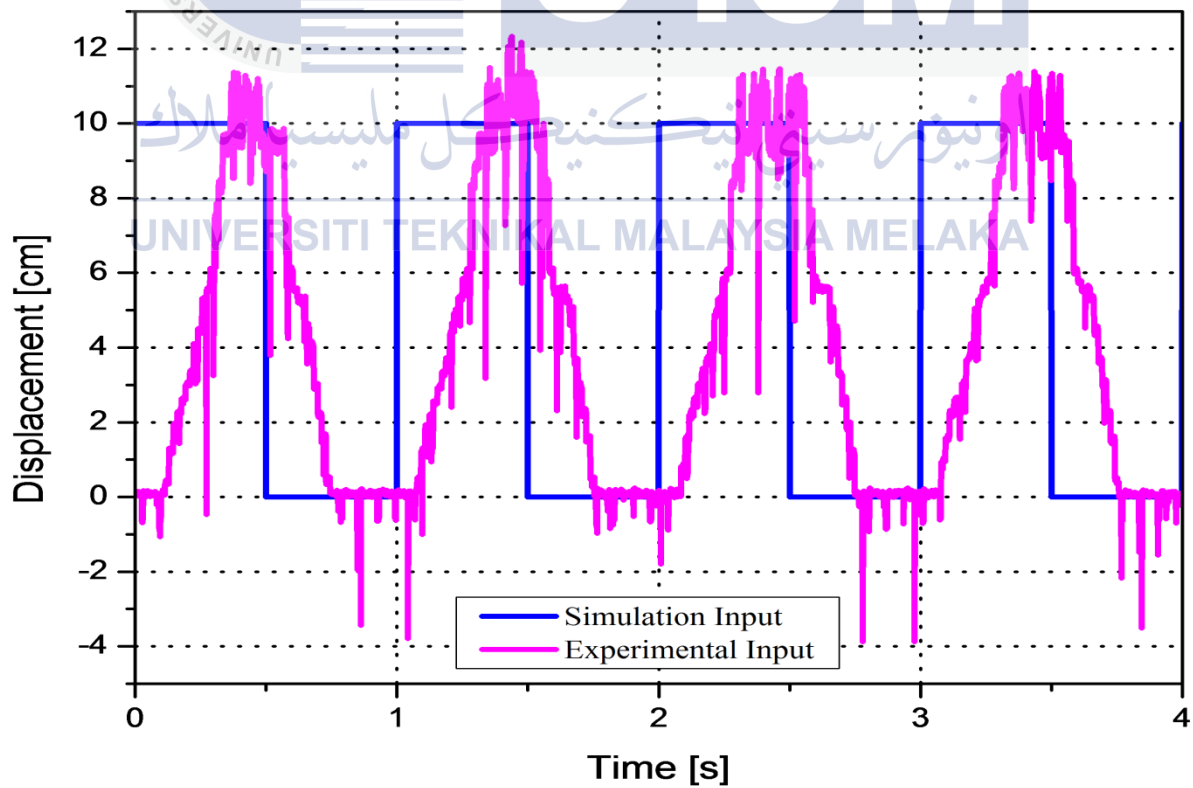
Figure 4.40: Pulse input signal used during simulation and experimental process.

Now, let's have a look on Figure 4.41. It can be observed that the noises and disturbances of the input signal with filter of the experimental result has been greatly reduced as compared to the input signal of the experimental result without filter which shown in Figure 4.40. The graph is now smoother than the previous graph presented in Figure 4.40. Usually, noises only occur at high frequency. Therefore, if the cut-off frequency is lower, noises that are above the cut-off frequency will not be captured. Hence, system will only capture the data and the noises captured in the system will be reduced. As filter has smoother the graph of the experimental results, filter is then added in all experiments that have been carried out in real time. However, the input signal from experimental result is lagging behind the input signal of the simulation result. There is a time delay of 0.258s in real time because double acting cylinder takes time to extend its piston rod to the desired displacement. Hence, all the experiment output responses will lag behind the simulation output response. Even though the time delay is 0.258s, it is still consider as fast response in real time.

Besides that, the amplitude of the experimental result is smaller than the simulation result. This is happening because the infrared sensor is easily affected by environmental factors such as brightness, humidity, temperature, weather and so on. All these environmental factors will directly affect the sensing value in the sensing area. Consequently, the experimental results collected using infrared sensor is not 100% representing the exact displacement of the moving plate and the reading will be in tolerance of ±4cm differ from the exact reading.
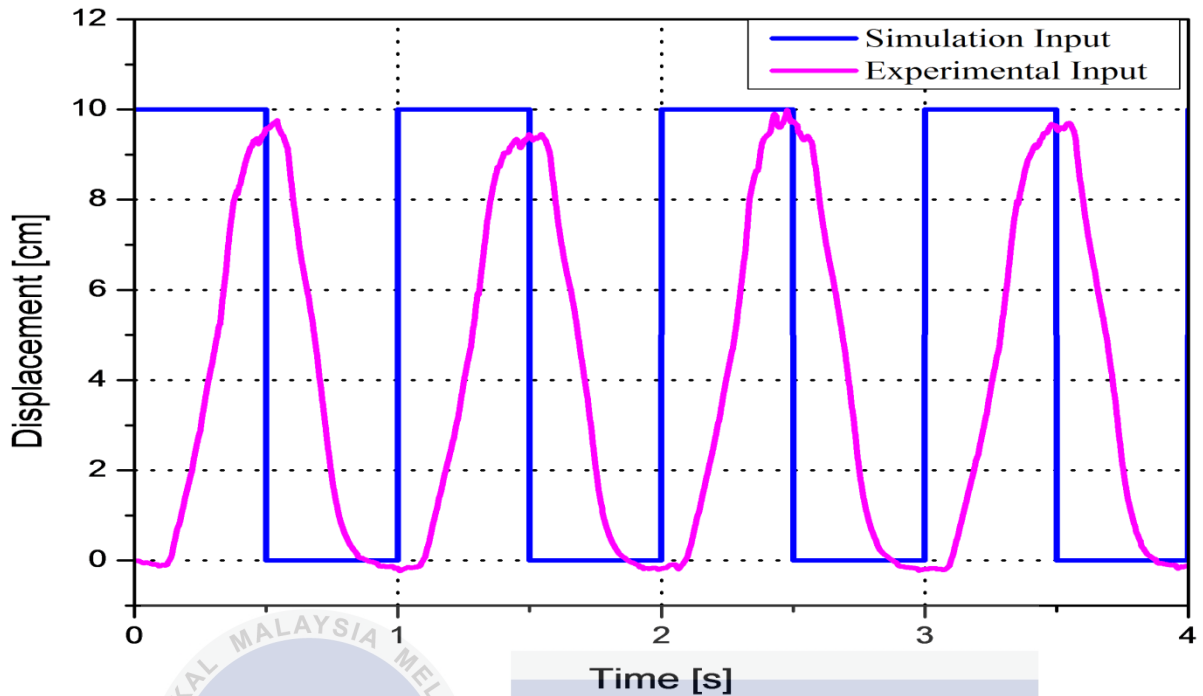
Figure 4.41: Pulse input signal with filter during experimental process

Next, dynamic behaviors of suspension system are discussed. Figure 4.42, 4.43 and 4.44 show the vehicle body displacement, vehicle body velocity and vehicle body acceleration. The vehicle body displacement is representing the ride quality of a vehicle. Therefore, the lower the oscillation of the vehicle body, the better the ride quality of the vehicle.

By referring to Figure 4.42, 4.43 and 4.44, it can be observed that the oscillations of the simulation result are higher and larger than the experimental result. This is because simulation is linearized system as friction is not taking into consideration. However, experimental setup in real time is nonlinear system because friction exists when the experiment is carrying out. Basically, friction in the real plant is non linear parameter. Therefore, the friction in the plant will change its value based on the surrounding conditions. Types of friction and causes that influence the simulation and experimental results are discussed later. Although the amplitude of the simulation and experimental results are different, the shape of the results for both simulation and experiment is more or less the same. Simulation output response shows a decreasing waveform whereas the experimental output response shows an almost constant waveform.
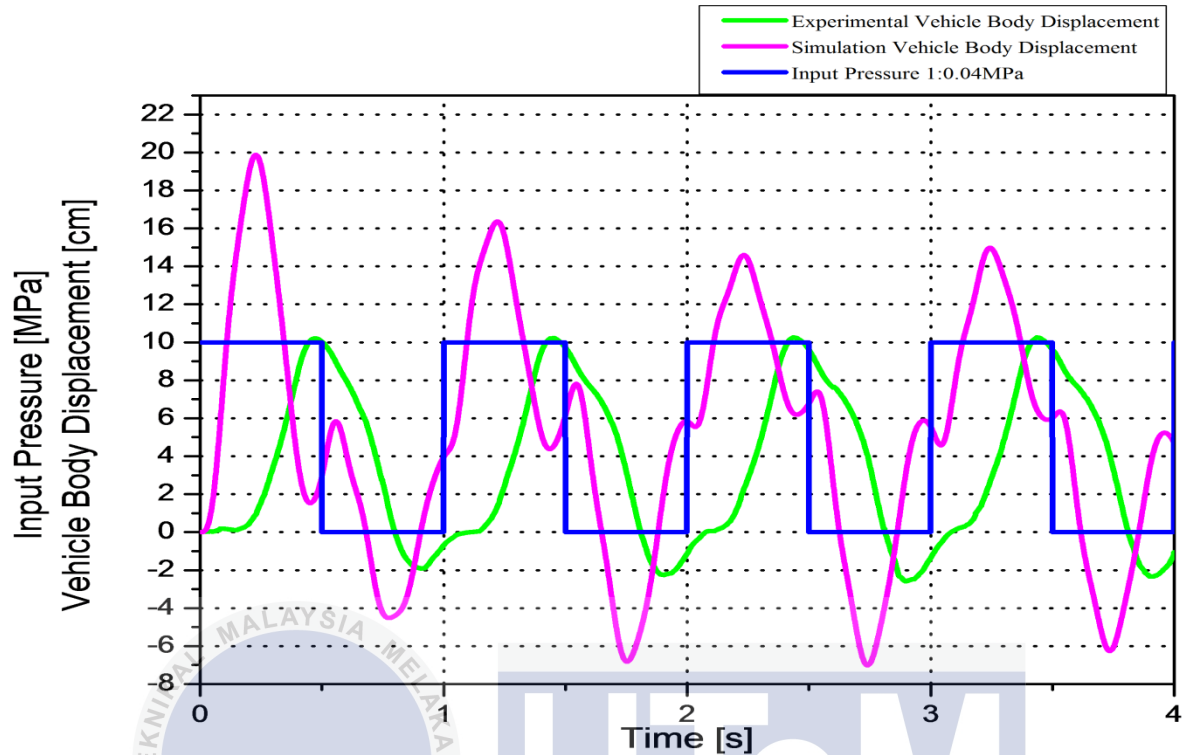
Figure 4.42: Vehicle body displacement of simulation and experimental result
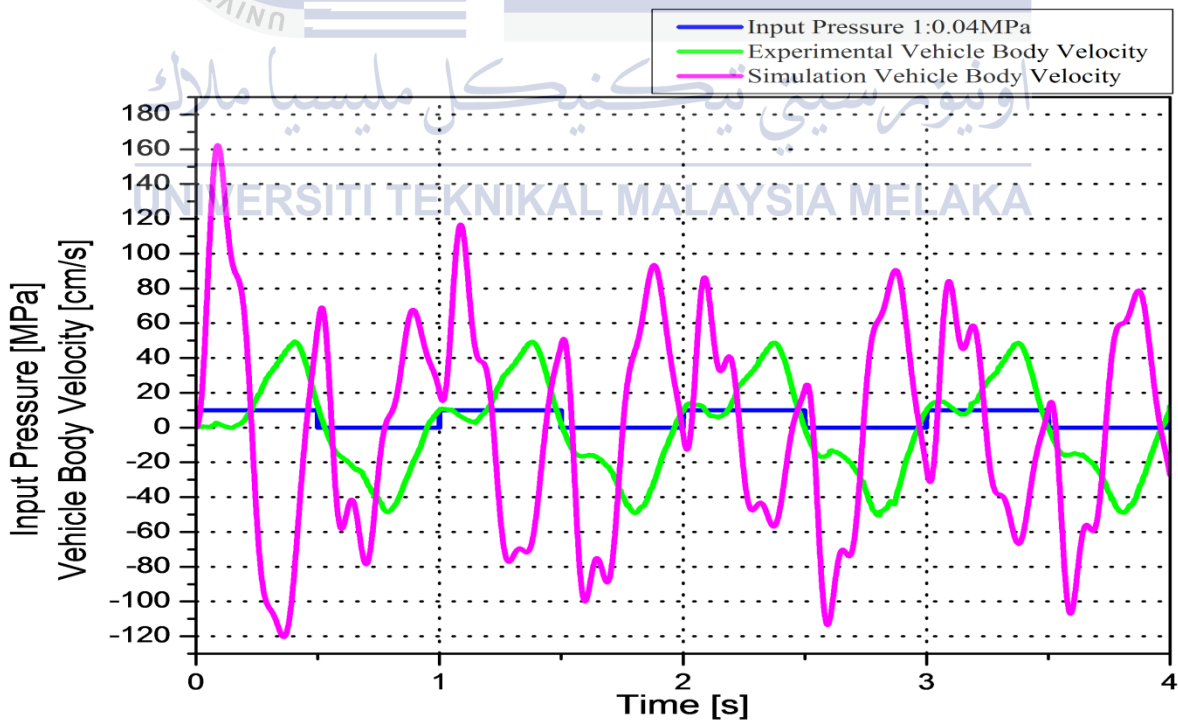
Figure 4.43: Vehicle body velocity of simulation and experimental result
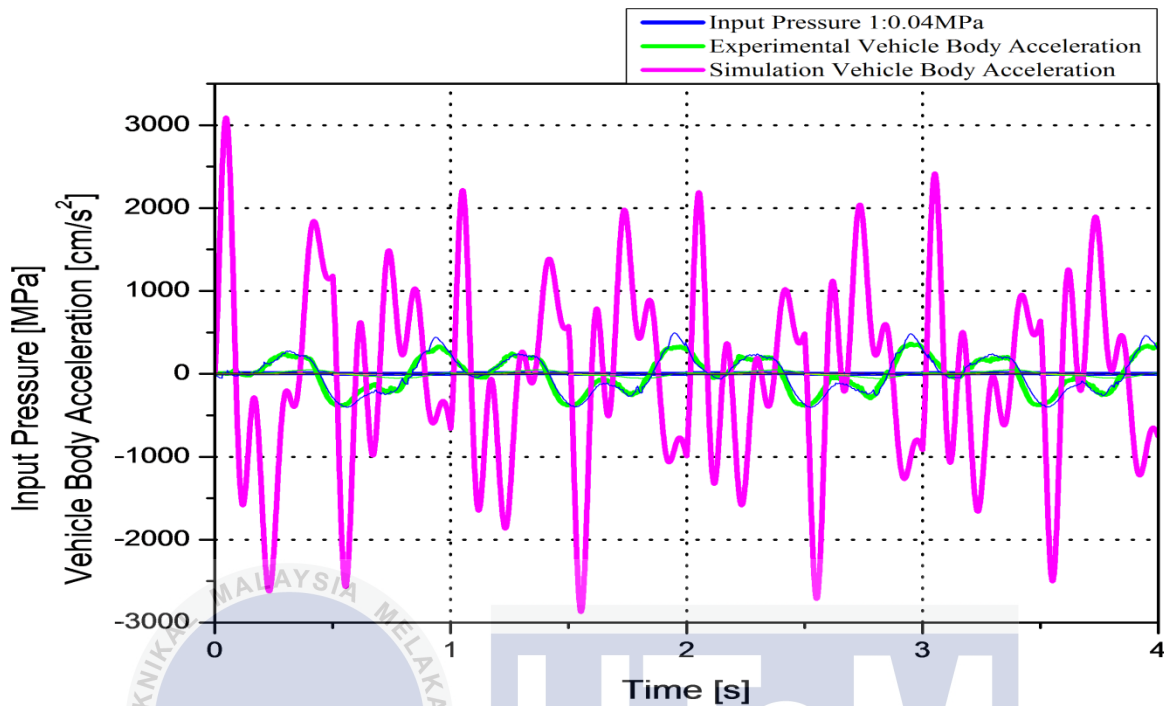
Figure 4.44: Vehicle body acceleration of simulation and experimental result

Figure 4.45, 4.46 and 4.47 show the tire displacement, suspension travel and wheel deflection of the system which represents the performance of car holding and ride stability. In order to have a good ride stability and good road holding, the tire displacement of a vehicle must be low so that it will not loss contact with the road. Friction is increased if tire is keeping contact with the road so it enables driver to control the vehicle better.

By looking at Figure 4.45, 4.46 and 4.47, it is clearly seen that simulation output response has higher oscillations. Even though the oscillation of simulationoutput response is higher than experimental output response, the difference of amplitude is now smaller as comparing to previous graphs. The shape of both simulation and experimental results are actually more or less the same if there is no time delay in real time.
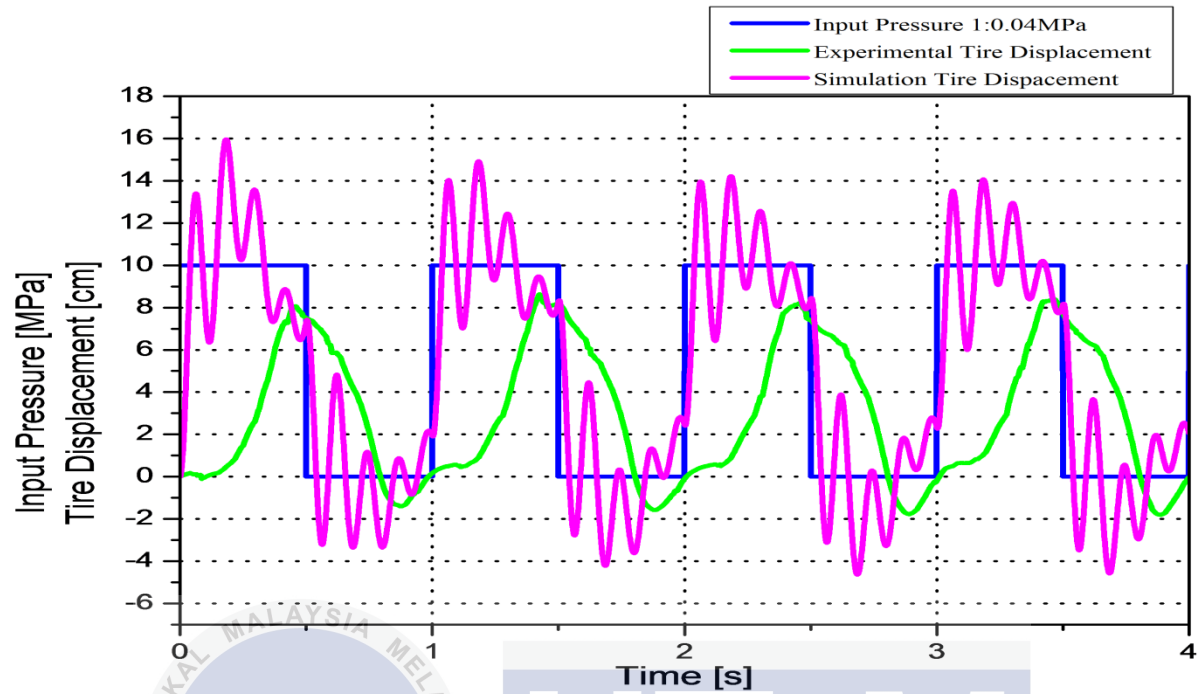
Figure 4.45: Tire displacement of simulation and experimental result
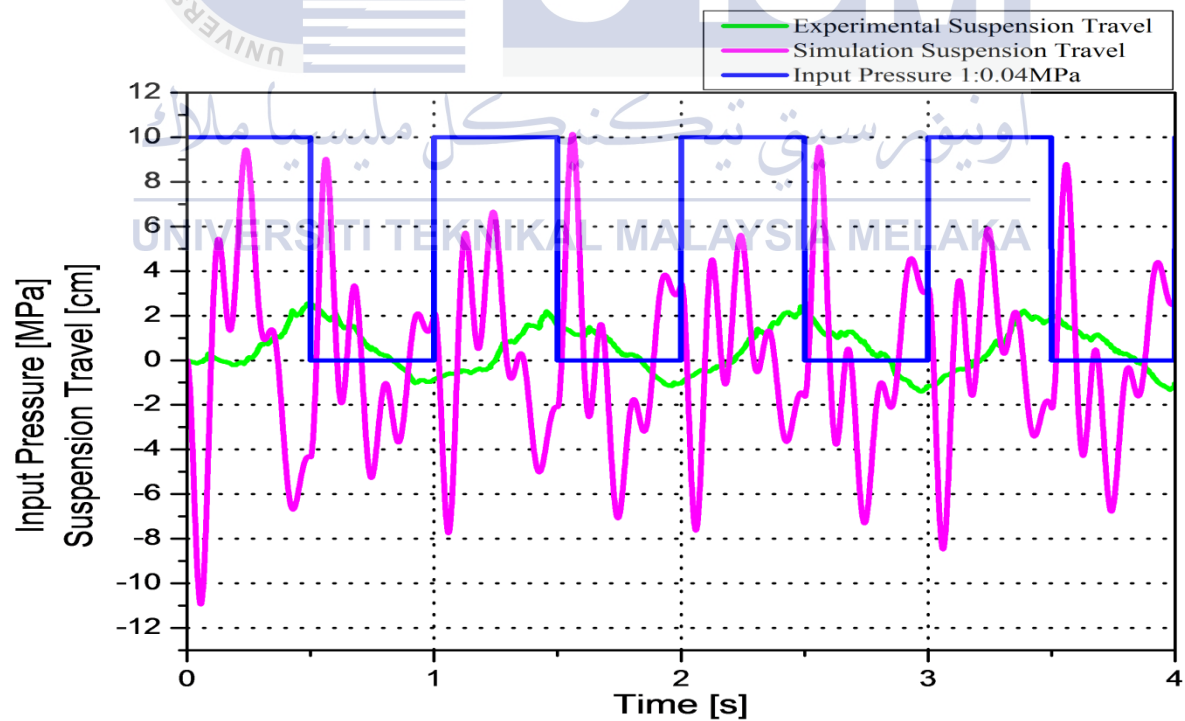
Figure 4.46: Suspension travel of simulation and experimental result
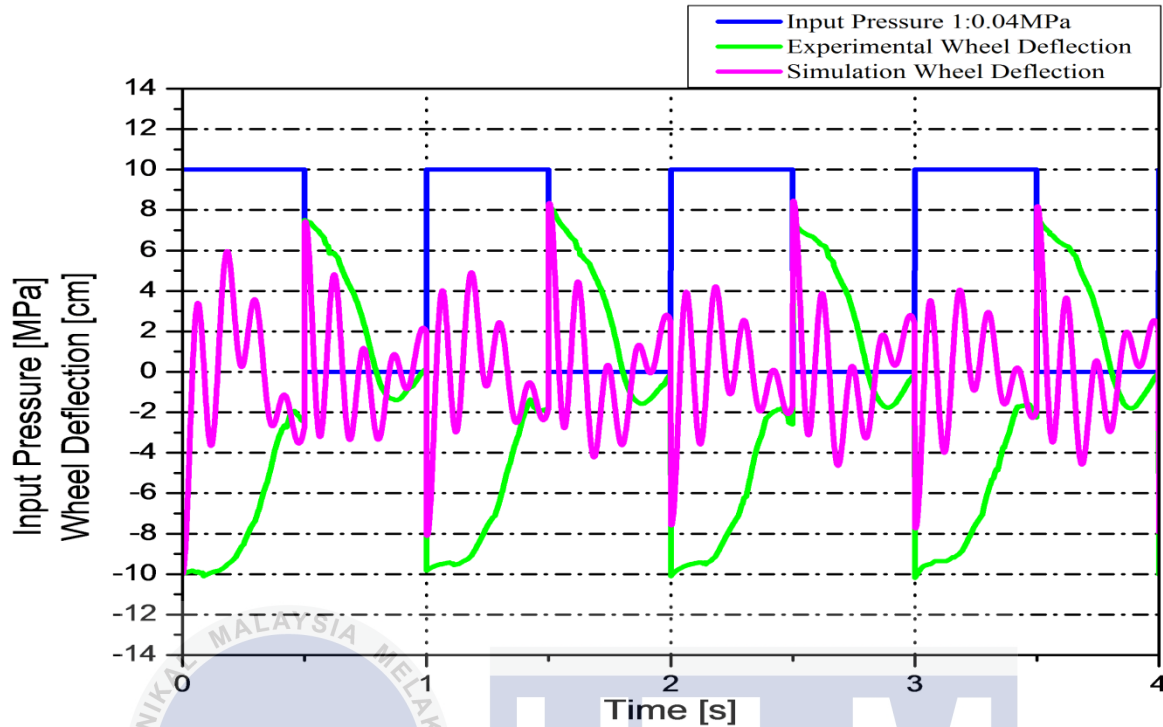
Figure 4.47: Wheel deflection of simulation and experimental result

Now, let's see what type of frictions and causes that exactly affect the results of the experiment. Gas spring is used as the damper in this experimental setup to regulate the oscillation of the plate which represents the vehicle body. This gas spring is a nonlinear device as the calibration result of gas spring in Figure 4.3 shows a nonlinear graph. The value of the damping constant of the gas spring used in simulation is taken based on the linear data and the nonlinear data are neglected. Experimentally the damping constant of gas spring is larger than simulation since nonlinear data is taking into account in experimental setup. As a result, the value of the damping constant used in simulation and experimental is actually inconsistent with each other. Larger damping constant causes the vehicle body to oscillate less as it will regulate more the movement of the vehicle body. This is why the overshoot and oscillation of the experimental results are lesser than simulation results. Besides that, theoretically the calibration method for the gas spring is correct however experimentally the calibration method might not be the exact method to calibrate this gas spring. Thus, this is another reason that causes the value of damping constant is varied with each other in simulation and experiment.

In addition, sensor distortion is another factor that causes the experimental and simulation results to be conflict with each other. As mentioned previously, infrared sensor is easily affected by environmental factors such as brightness, humidity, temperature, weather and so on. Hence, the accuracy of the infrared sensor is strongly depending on the environment surrounding the experimental setup. Although calibration of sensor for verifying the accuracy of the sensor has been done before conducting the experiment, the humidity and the temperature inside the laboratory will still influence the reading of the sensor. Furthermore, the brightness inside the laboratory will cause offset value to the reading of the sensor. Running experiment in brighter environment will get different sensor reading as compared to running experiment in darker environment. As a result, sensor causes great impact on recording the exact and accurate reading on the movement of plates in real time.

On top of that, fabrication process of the experimental setup is one of the factors that affect the experimental results. Measurements and dimensions of the holes on the plates must be fabricated accurately and precisely to increase the compatibility of the experimental setup. Fabrication error of the experimental setup in the factory causes large friction to exist when conducting experiment. If the fabrication of the holes on 2 plates are differ 0.5cm with each other where one of the plate has a hole 2cm away from the edge of plate whereas the other plate has a hole 1.5cm away from the edge of the plate, then a huge friction occurs when shafts are placed between that two plates. Huge friction occurs because holes of two plates are not identical hence the plates are not able to move linearly. Instead of that, air resistance is another type of friction that affects the experimental output response. When the plates of the experimental setup are moving up and down, the plates are actually acting in the opposite direction of the air resistance. So, air resistance in opposite direction will therefore slow down the velocity of the moving plate and prevent it to oscillate much.

Last but not least, pneumatic double acting cylinder is actually a nonlinear device. Friction actually exists when the cylinder is functioning. Friction is keep changing with the velocity of the piston rod where different velocity of the piston rod will produce different levels of friction. In addition, lubrication condition of the pressure regulator will affect the air pressure flowing into the pneumatic double acting cylinder. Lubrication in the pressure

regulator is used to smoother out the flow of the air pressure. If the lubricant has been wear and tear then air pressure will not be smoothed out and frictions will then increases. On top of that, nonlinearity of bearing will also increase the friction in the experimental setup. Even though bearing is used to reduce the friction of the linear movement between the shafts and the plates, however the ball bearing itself does contains small friction that resist the oscillation of the plates. Usually, lubricant is used to lubricate the balls inside the bearing so that the balls will roll over each other to reduce the friction. However, the balls will hardly roll over each other once the lubricant has been wear and tear. This is why ball bearing is listed as one of the nonlinear device.

In a nutshell, simulation output response is always ideal and the results are all have been linearized. Hence, this is the reason why experimental and simulation results will never be the same since the friction in real plant keeps changing continuously but there is no friction in the simulation.
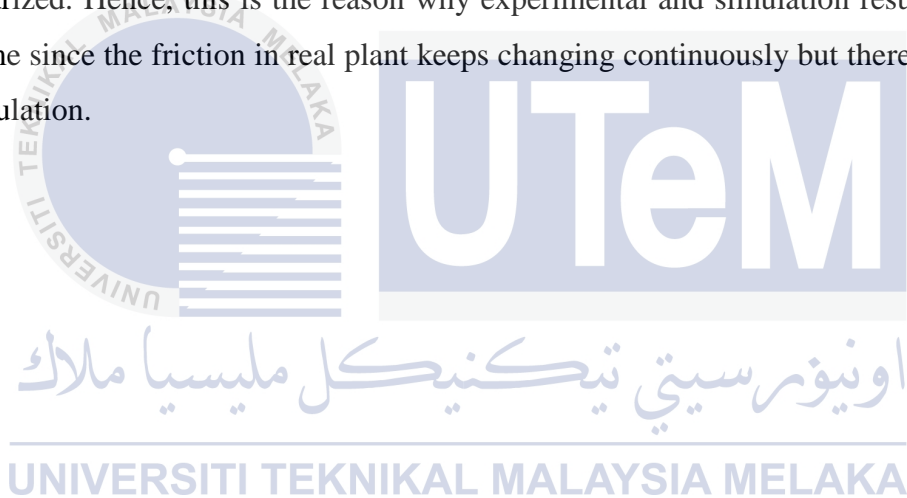
CHAPTER 5

CONCLUSION AND FUTURE WORKS

During this report, experimental setup represents passive suspension system based on modeling of quarter-car suspension system has been successfully constructed and experiments have been conducted in order to determine this experimental setup characterization. Different mass and different pulse width of input pressure directly affected the characteristic of this passive suspension system experimental setup. Since the characteristic of this experimental setup has been analyzed through experiments, the performances of this passive suspension system prototype can then be improved using different types of controller such as PID Controller, Fuzzy Logic Controller, Neural Network Controller and so on. Besides that, simple simulation has been done in order to compare the simulation and experiments results. However, the amplitude of the simulation and experimental results are different but the shape of the results for both simulation and experiment is more or less the same. This is because simulation is linearized system whereas experimental setup is a nonlinear system. Friction is not taken into consideration in simulation however the friction in experiments exists and keeps changing continuously.

Even though this experimental setup has been successfully constructed, there are several limitations that affect the performances of the experimental setup. Firstly, it is recommended to change the current infrared sensor to a better displacement sensor as the reading value of infrared sensor is affected by environmental effects especially light intensity, temperature and humidity of surrounding area. Next, the gas spring and the spring being used in this experimental setup need to be changed in order to run experiments for heavier load. Lastly, this research is only deal with two-degree-of-freedom modeling of the quarter car

passive suspension system experimental setup. Hence, it is recommended to construct a full vehicle suspension system experimental setup to represent the real vehicle suspension system.

REFERENCES

[1]   L. Kong, X. Zhao, and B. Qi, "*Study on Semi-Active Suspension System of Tracked Vehicle Based on Variable Universe Fuzzy Control*", IEEE International Conference on Mechatronics and Automation, pp. 2276-2280, 2011.

[2]   A. Agharkakli, G. S. Sabet, and A. Barouz, "*Simulation and Analysis of Passive and Active Suspension System Using Quarter Car Model for Different Road Profile*", International Journal of Engineering Trends and Technology, Volume31Issue5, pp. 636-644, 2012.

[3]   L. J. Yue, C. Y. Tang, and H. Li, "*Research on Vehicle Suspension Systems based on Fuzzy Logic Control*", IEEE International Conference on Automation and Logistics, pp. 1817-1821, 2008.

[4]   Y. Zheng, "*Research on Fuzzy Logic Control of Vehicle Suspension System*", International Conference on Mechenic Automation & Control Engineering (MACE), pp. 307-310, 2010.

[5]   T. R. M. Rao, G. V. Rao, K. S. Rao, and A. Purushottam, "*Analysis Of Passive And Semi Active Controlled Suspension Systems For Ride Comfort In An Omnibus Passing Over A Speed Bump*", IJRRAS 5(1), pp. 7-17, 2010.

[6]   J. Sun, and Y. Sun, "*Comparative Study on Control Strategy of Active Suspension System*", Third International Conference on Measuring Technology and Mechatronics Automation, pp. 729-732, 2011.

[7]   F. Kou and Z. Fang, "*An Experimental Investigation into the Design of Vehicle Fuzzy Active Suspension*", IEEE International Conference on Automation and Logistics, pp. 959-963, 2007.

[8]   D. S. Joo, N. Al-Holou, J. M. Weaver, T. Lahdhiri, and F. Al-Abbas, "*Nonlinear Modeling of Vehicle Suspension System*", American Control Conference, pp. 115-118, 2000.

[9]   Y. Li and S. Liu, "*Preview Control of an Active Vehicle Suspension System Based on a Four-Degree-of-Freedom Half-Car Model*", Second International Conference on Intelligent Computation Technology and Automation, pp. 826-830, 2009.

[10]   C. Alexandru and P. Alexandru, "*A comparative analysis between the vehicles' passive and active suspensions*", International Journal of Mechanics, Issue 4, Volume 5, pp. 371-378, 2011.

[11]   A. Malekshahi and M. Mirzaei, "*Designing A Non-Linear Tracking Controller for Vehicle Active Suspension Systems Using An Optimization process*", International Journal of Automotive Technology, Volume 13, No. 2, pp. 263-271, 2012.

[12]   Y. Ai, F. Zhang, and Z. Wang, "*Study on Techniques for Active Control of An Engine-Vehicle Suspension System*", Chinese Control and Decision Conference, pp. 2967-2970, 2008.

[13]   L. H. Nguyen, K. S. Hong, and S. Park, "*Road-Frequency Adaptive Control for Semi-Active Suspension Systems*", International Journal of Control, Automation, and Systems, pp. 1029-1038, 2010.

[14]   M. A. Eltantawie, "*Decentralized Neuro-Fuzzy Control for Half-Car with Semi-Active Suspension System*", International Journal of Automotive Technology, Volume 13, No. 3, pp. 423-431, 2012.

[15]   D. Hanafi, "*PID Controller Design for Semi-Active Car Suspension Based on Model from Intelligent System Identification*", Second International Conference on Computer Engineering and Applications, pp. 60-63, 2010.

[16]   Reza N. Jazar, "*Vehicle Dynamics: Theory and Applications*", Spring. pp. 455, 2008.

[17]   Y. P. Kuo, N. S. Pai, J. S. Lin, and C. Y. Yang, "*Passive Vehicle Suspension System Design Using Evolutionary Algorithm*", Knowledge Acquisition and Modeling Workshop, pp. 292-295, 2008.

[18]   X. Y. Yee. (2011, December 13). *Potholes on major roads and highways causing hardship to motorists* [Online]. Available: http://www.thestar.com.my/story.aspx?file=%2f2011%2f12%2f13%2fsouthneast%2f10078665&sec=southneast

[19]   K. L. Phuah. (2011, November 12). *Potholes continue to endanger motorists* [Online]. Available: http://www.nst.com.my/streets/northern/potholes-continue-to-endanger-motorists-1.4558

[20]   Zaheer. (2010, August 9). *How to Replace Conventional Shock Absorbers in Your Automobile* [Online]. Available: http://www.motorward.com/2010/08/how-to-replace-conventional-shock-absorbers-in-your-automobile/

[21]   Admin.   (2011).   *Suspension   overview*   [Online].   Available: http://wallpaperstobackground.blogspot.com/2011/07/suspension-overview.html

[22]   Sunny Ray, "*Quanser Mechatronic Controls Laboratory*", Quanser Innovate Educate, pp. 1-33, 2010.

[23]   S.J. Huang, H.Y. Chen, "*Adaptive Sliding Controller with Self-Tuning Compensation for Vehicle Suspension Control*", Mechatronics. Volume 16, pp. 607-622, 2006.

[24]   R.Rosli, M.Mailah, G.Priyandoko, "*Active Suspension System for Passenger Vehicle using Active Force Control with Iterative Learning Algorithm*", WSEAS TRANSACTIONS on SYSTEMS and CONTROL, Volume 9, pp. 120-129, 2014.

[25]   S.Patil, Dr. Shridhar G. Joshi, "*Development and Control of a Prototype Hydraulic Active Suspension System for Road Vehicles*", International Journal of Emerging Technology and Advanced Engineering, Volume 2, pp.438-443, 2012.

APPENDIX A

Experimental Setup Equipments Calibration Results

Table A1: Infrared sensor calibrated result

Displacement (mm)	Infrared Sensor Output Voltage (V)
10	1.6590
20	2.0920
30	2.9400
40	2.6790
50	2.2510
60	1.9630
70	1.6920
80	1.4890
90	1.3410
100	1.2160
110	1.1000
120	0.9888
130	0.9175
140	0.8701
150	0.8113
160	0.7545
170	0.6992
180	0.6571
190	0.5787
200	0.5764
210	0.5575
220	0.5206
230	0.5006
240	0.4902
250	0.4710
260	0.4443
270	0.4268
280	0.4056
290	0.4038
300	0.3937

Table A2: Gas spring calibration result of length of piston rod collected when load is
added to the gas spring

Mass of load (kg)	Length of piston rod (m)
0.1	0.05500
0.2	0.05500
0.3	0.05500
0.4	0.05500
0.5	0.05500
0.6	0.05500
0.7	0.05500
0.8	0.05500
0.9	0.05500
1.0	0.05500
1.1	0.05500
1.2	0.05499
1.3	0.05499
1.4	0.05498
1.5	0.05497
1.6	0.05497
1.7	0.05496
1.8	0.05496
1.9	0.05495
2.0	0.05494
2.1	0.05494
2.2	0.05493
2.3	0.05492
2.4	0.05490
2.5	0.05490
2.6	0.05488
2.7	0.05487
2.8	0.05487
2.9	0.05486
3.0	0.05486
3.1	0.05485
3.2	0.05485
3.3	0.05481
3.4	0.05480
3.5	0.05399
3.6	0.05388
3.7	0.05384
3.8	0.05383
3.9	0.05380
4.0	0

Table A3: Damping coefficient of gas spring at different force and velocity

Force (N)	Velocity (ms^{-1})	Damping coefficient (Ns/m)
0.981	0.104761905	9.364091
1.962	0.104761905	18.72818
2.943	0.104761905	28.09227
3.924	0.104761905	37.45636
4.905	0.104761905	46.82045
5.886	0.104761905	56.18455
6.867	0.104761905	65.54864
7.848	0.104761905	74.91273
8.829	0.104761905	84.27682
9.810	0.104761905	93.64091
10.791	0.104761905	103.0050
11.772	0.104742857	112.3895
12.753	0.104742857	121.7553
13.734	0.104723810	131.1450
14.715	0.104704762	140.5380
15.696	0.104704762	149.9072
16.677	0.104685714	159.3054
17.658	0.104685714	168.6763
18.639	0.104666667	178.0796
19.620	0.104647619	187.4863
20.601	0.104647619	196.8607
21.582	0.104628571	206.2725
22.563	0.104609524	215.6878
23.544	0.104571429	225.1475
24.525	0.104571429	234.5287
25.506	0.104533333	243.9987
26.487	0.104514286	253.4295
27.468	0.104514286	262.8157
28.449	0.104495238	272.2516
29.430	0.104495238	281.6396
30.411	0.104476190	291.0807
31.392	0.104476190	300.4704
32.373	0.104400000	310.0862
33.354	0.104380952	319.5411
34.335	0.102838095	333.8743
35.316	0.102628571	344.1147
36.297	0.102552381	353.9362
37.278	0.102533333	363.5696
38.259	0.10247619	373.3453
39.24	0	0

Table A4: Calibration result of spring places between mass of vehicle body and tire

Mass of load (kg)	Length of Spring (m)	Length of spring being compressed (m)	Force (N)
0	0.14	0.00	0.00
1	0.131	0.009	9.81
2	0.118	0.022	19.62
3	0.114	0.026	29.43
4	0.108	0.032	39.24
5	0.098	0.042	49.05
6	0.089	0.051	58.86
7	0.081	0.059	68.67
8	0.075	0.065	78.48
9	0.069	0.071	88.29
10	0.058	0.082	98.10
11	0.049	0.091	107.91
12	0.047	0.093	117.72

Table A5: Calibration result of spring represents the air pressure inside tire

Mass of load (kg)	Length of Spring (m)	Length of spring being compressed (m)	Force (N)
0	0.150	0.000	0.00
1	0.147	0.003	9.81
2	0.143	0.007	19.62
3	0.140	0.010	29.43
4	0.135	0.015	39.24
5	0.132	0.018	49.05
6	0.129	0.021	58.86
7	0.126	0.024	68.67
8	0.121	0.029	78.48
9	0.118	0.032	88.29
10	0.114	0.036	98.10
11	0.109	0.041	107.91
12	0.105	0.045	117.72
13	0.101	0.049	127.53
14	0.094	0.056	137.34
15	0.093	0.057	147.15
16	0.091	0.059	156.96
17	0.085	0.065	166.77
18	0.083	0.067	176.58
19	0.077	0.073	186.39
20	0.069	0.081	196.20
21	0.064	0.086	206.01
22	0.059	0.091	215.82

APPENDIX B

Draft of Experimental Setup
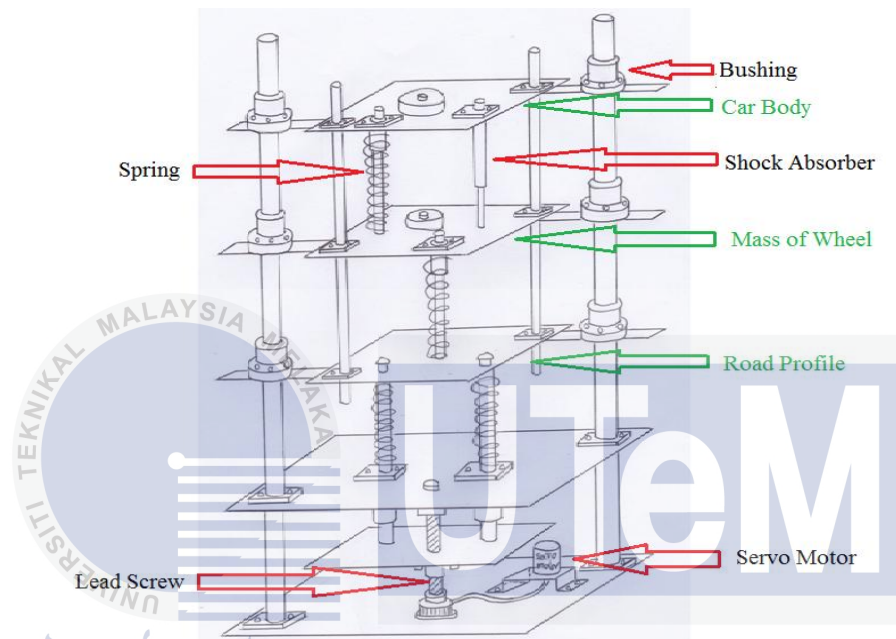
Figure B1: First draft for the prototype of the passive suspension system
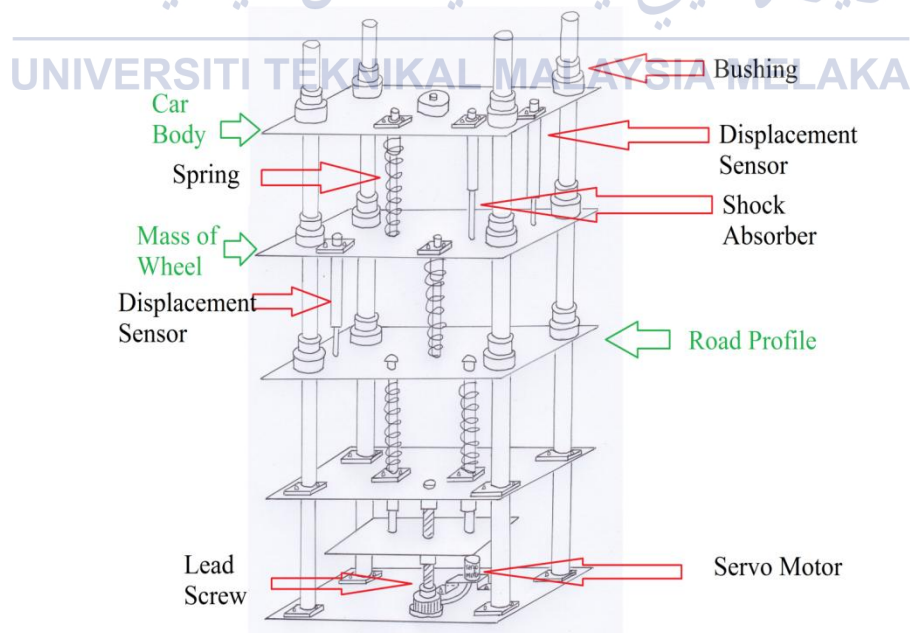
Figure B2: Second draft for the prototype of the passive suspension system
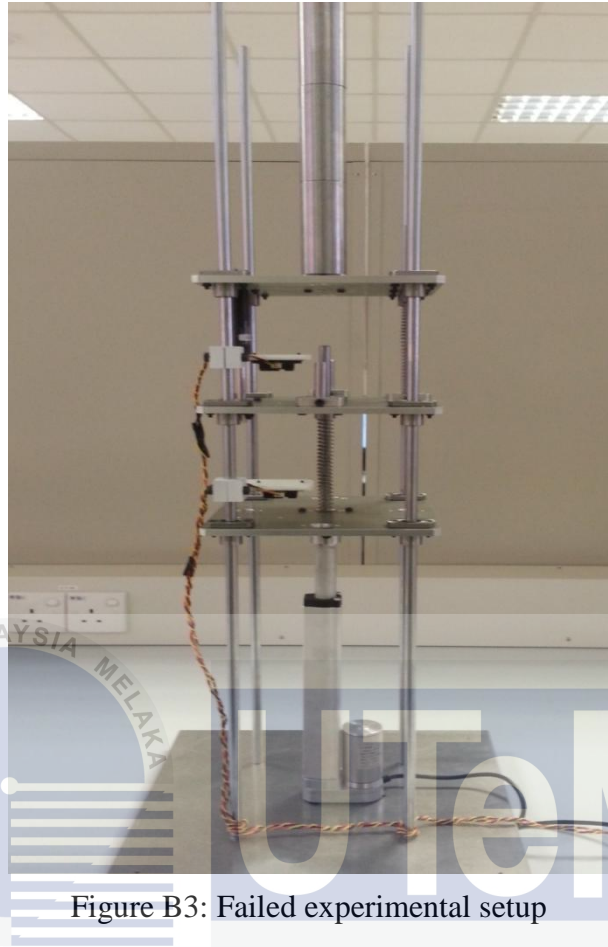
Figure B3: Failed experimental setup

Appendix C

Graphs of Experiments

<u>**Experiment A**</u>
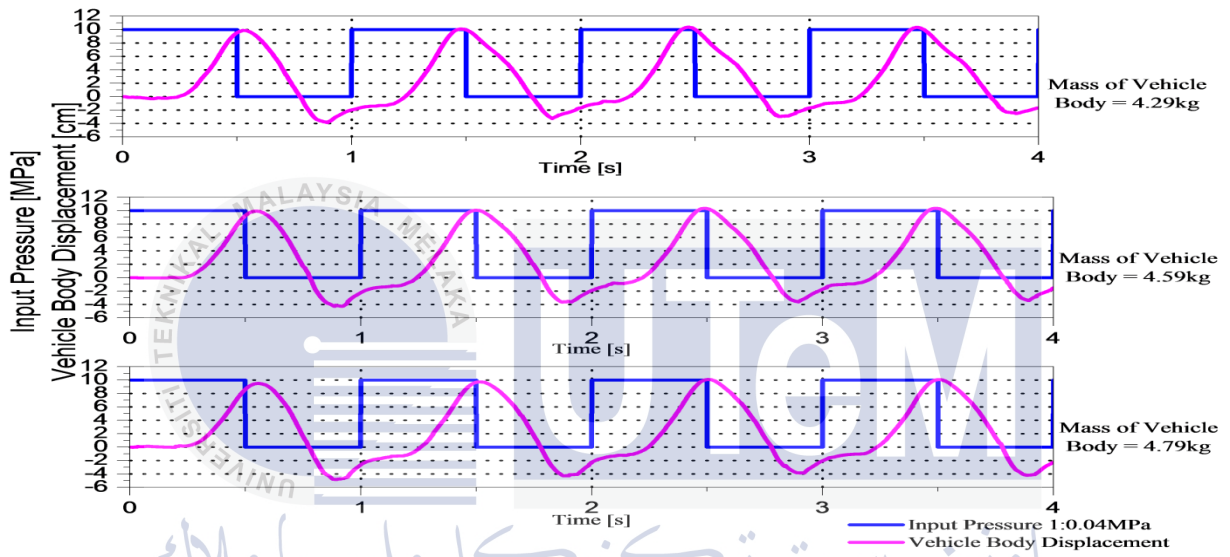
Figure C1: Vehicle body displacement of Experiment A
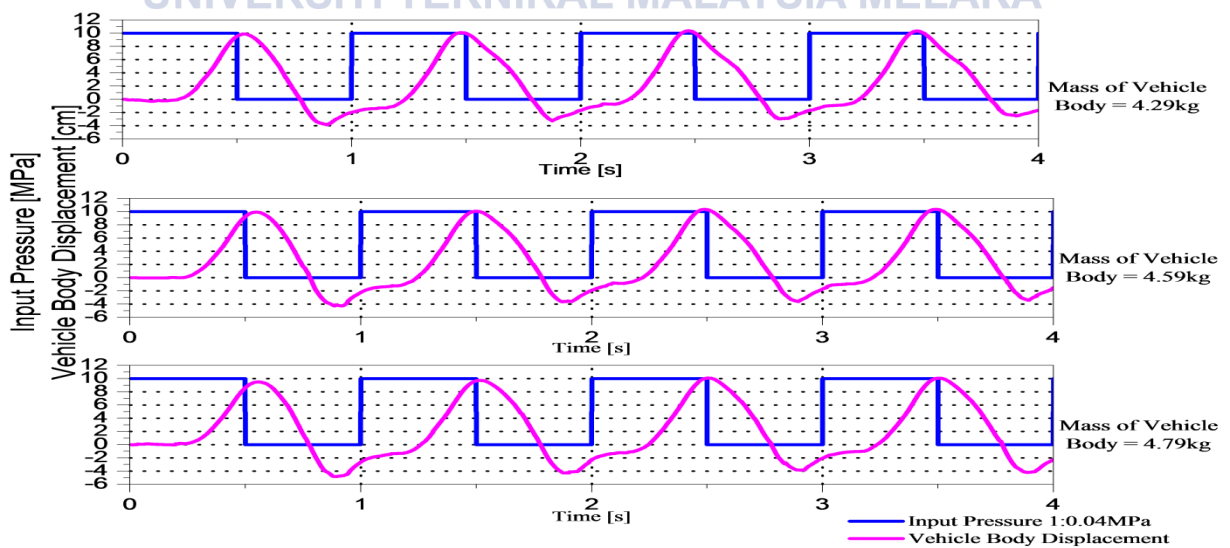
Figure C2: Vehicle body velocity of Experiment A
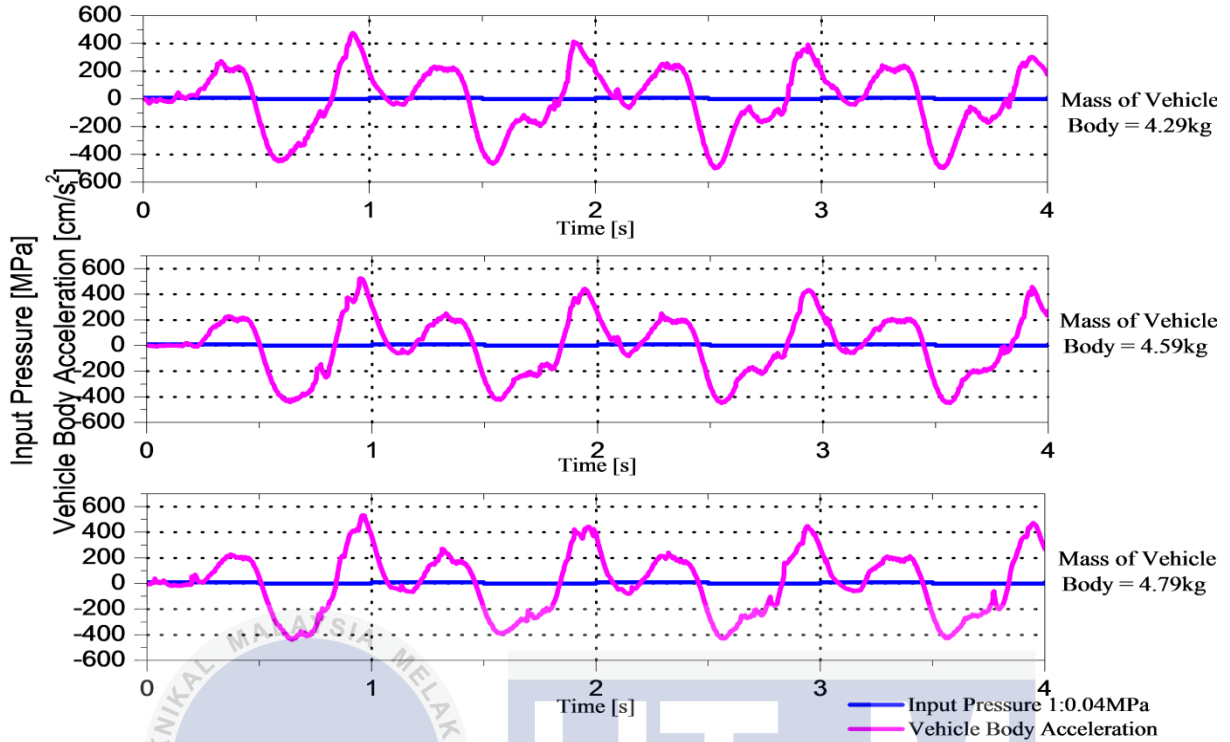
Figure C3: Vehicle body acceleration of Experiment A
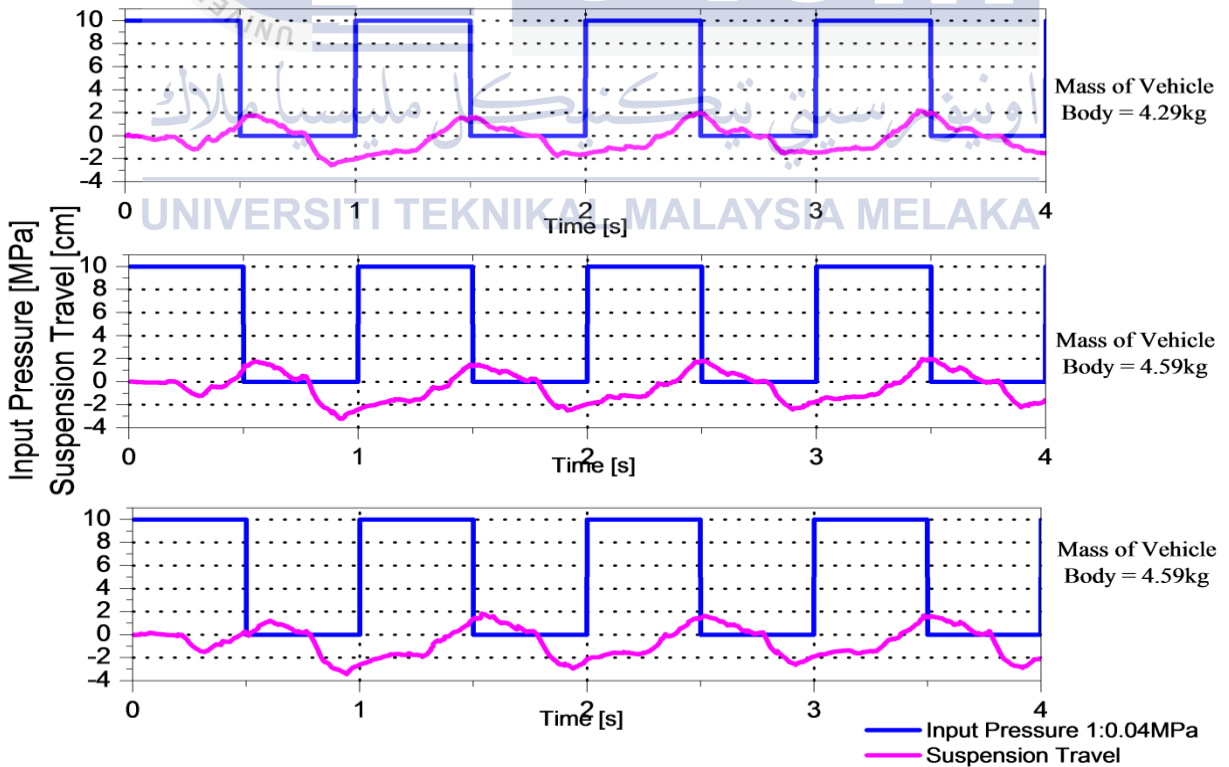
Figure C4: Suspension travel of Experiment A
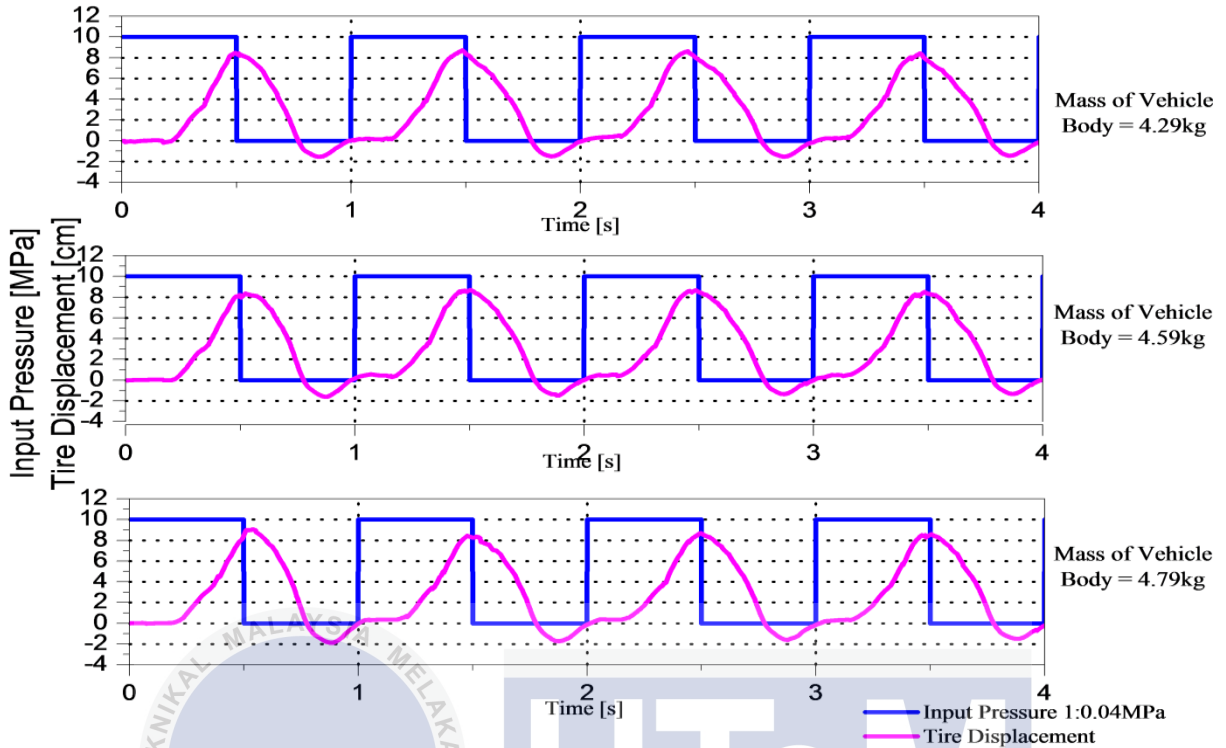
Figure C5: Tire displacement of Experiment A
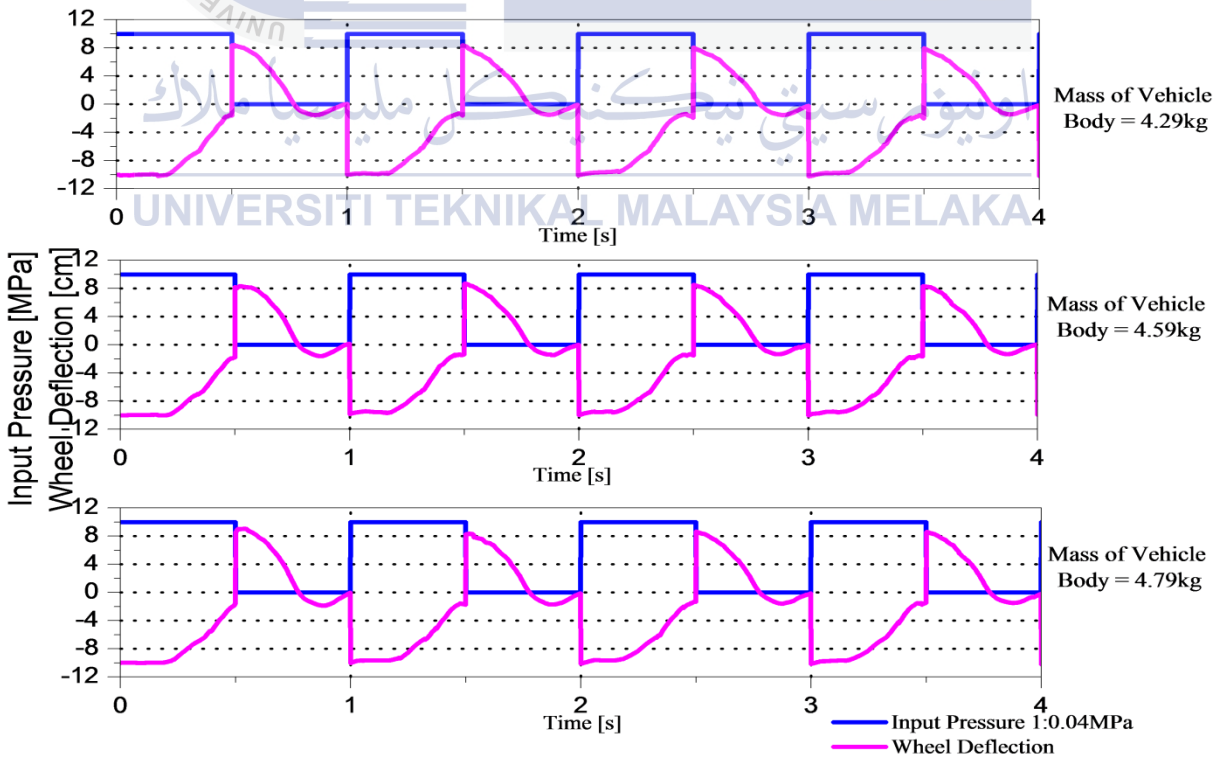
Figure C6: Wheel deflection of Experiment A

Experiment B
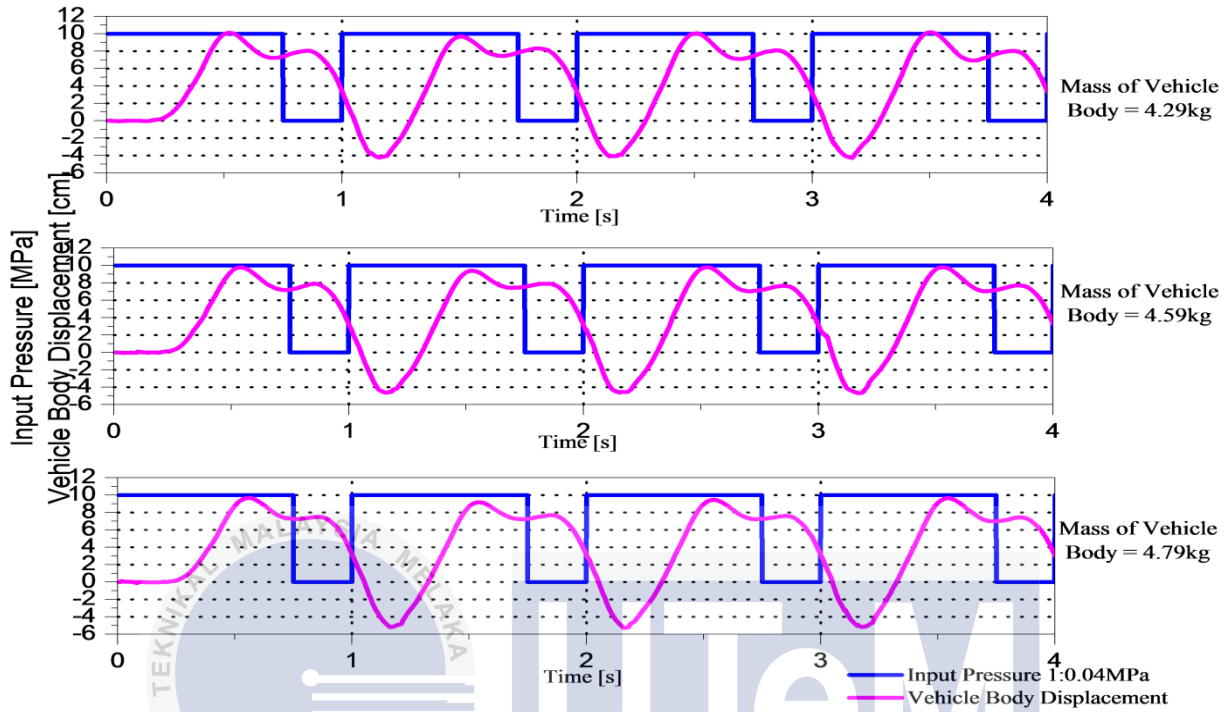
Figure C7: Vehicle body displacement of Experiment B
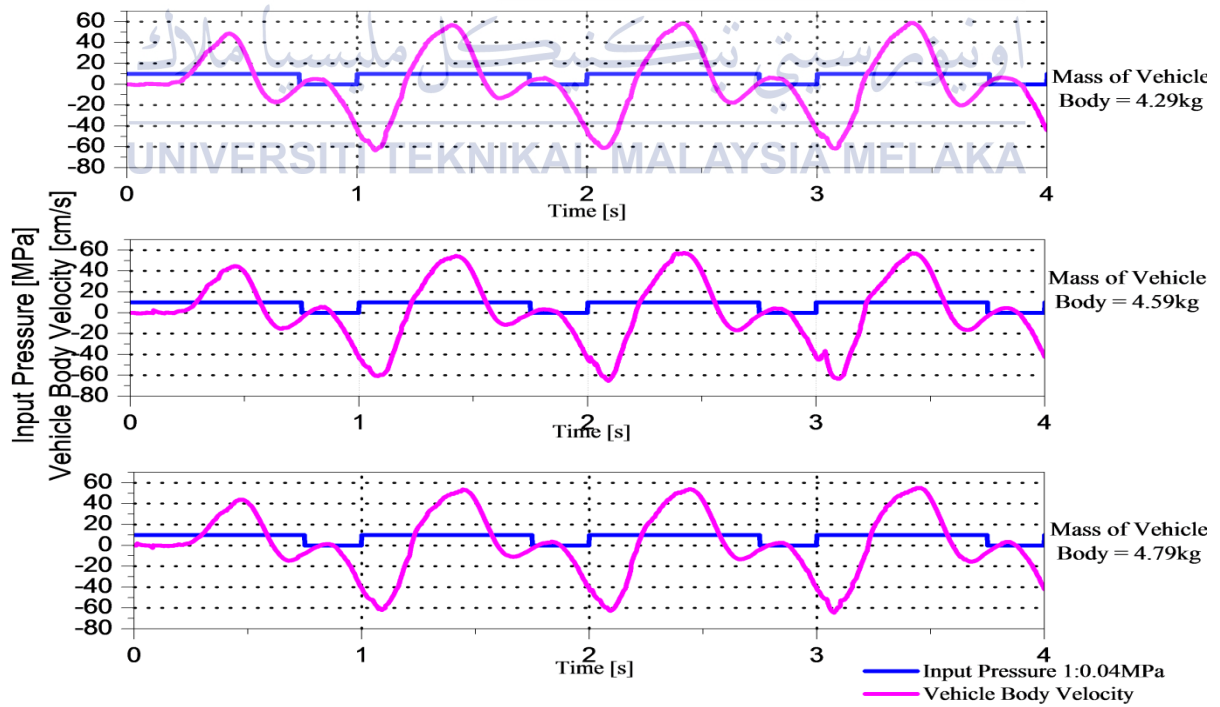
Figure C8: Vehicle body velocity of Experiment B
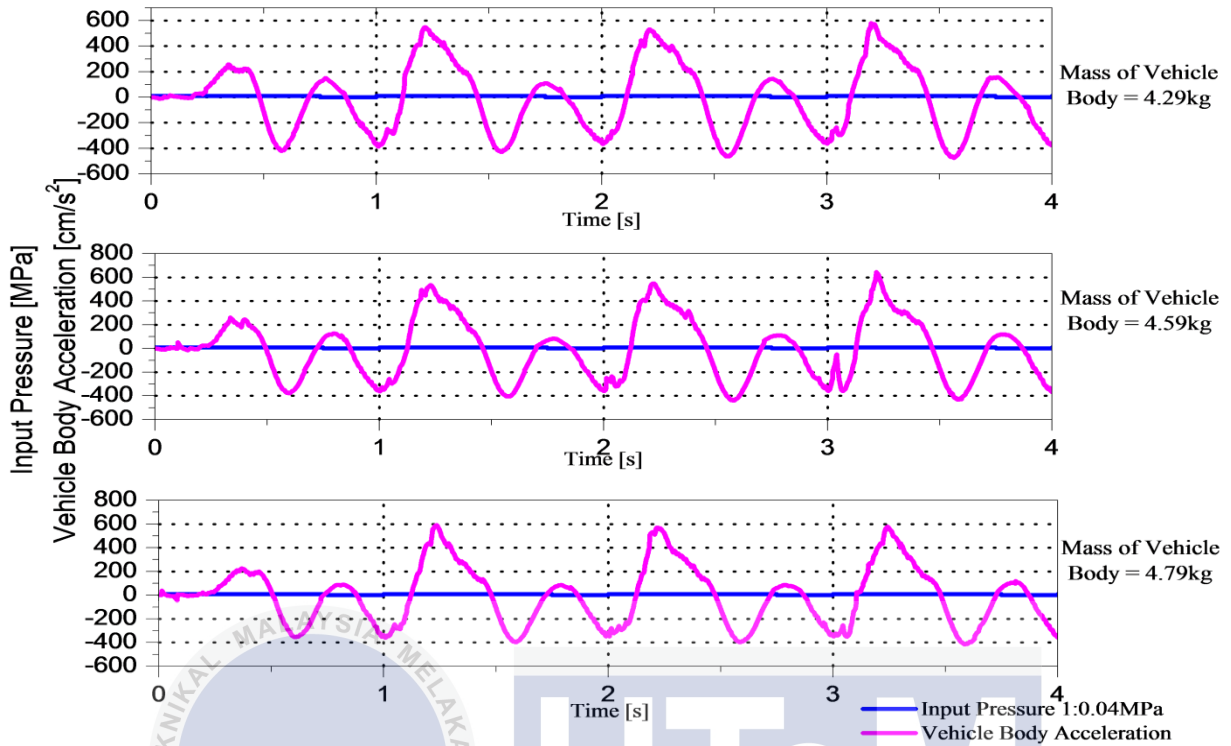
Figure C9: Vehicle body acceleration of Experiment B
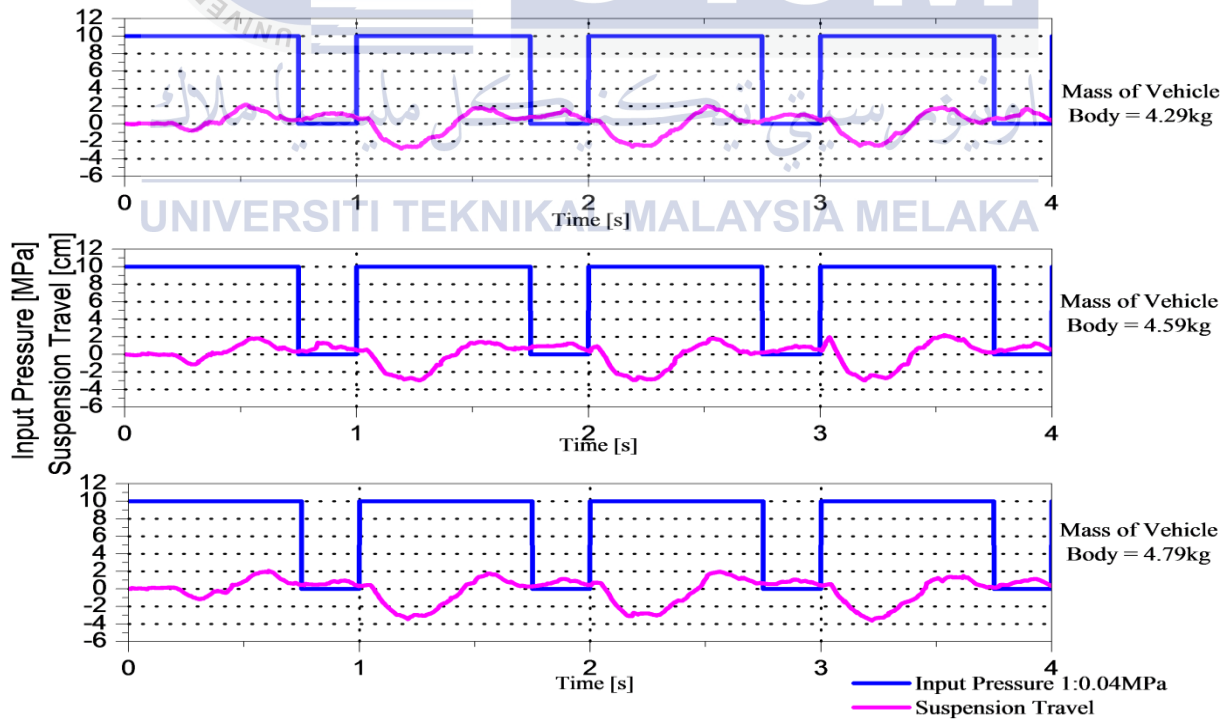
Figure C10: Suspension travel of Experiment B
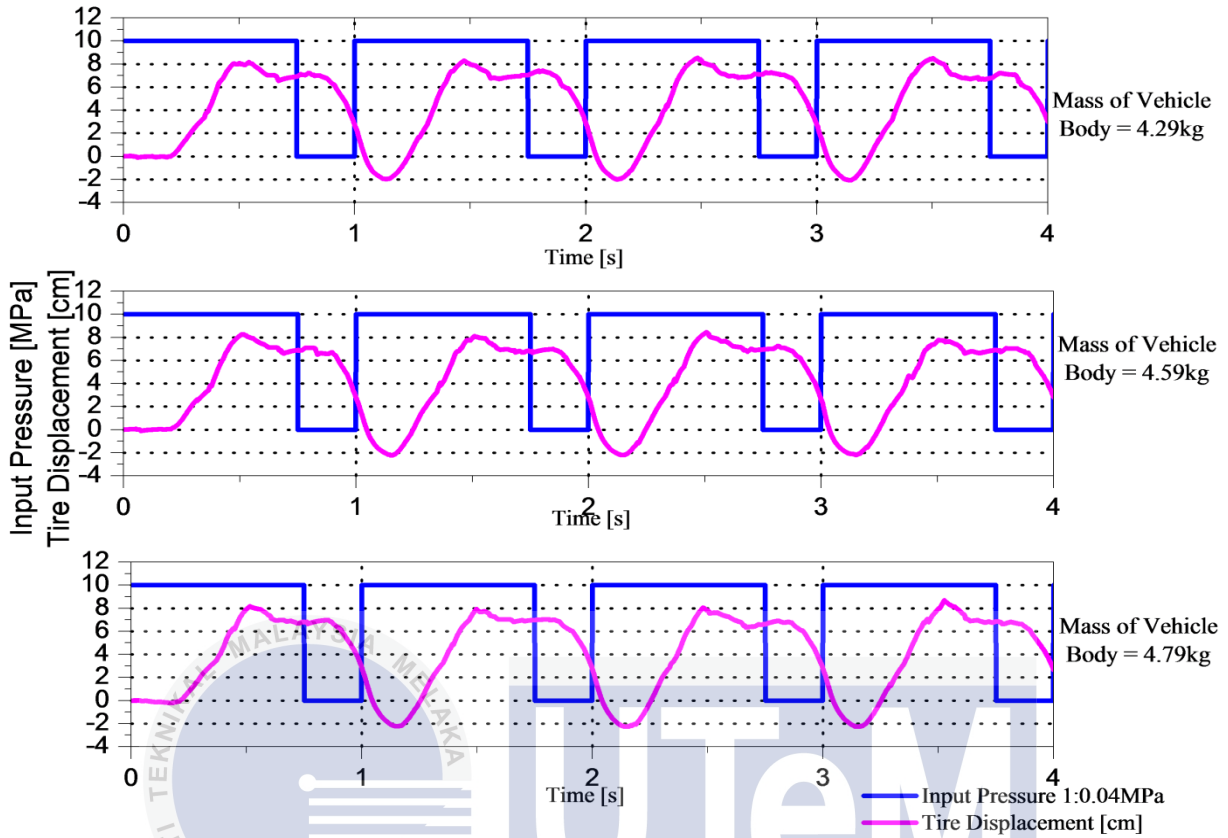
Figure C11: Tire displacement of Experiment B
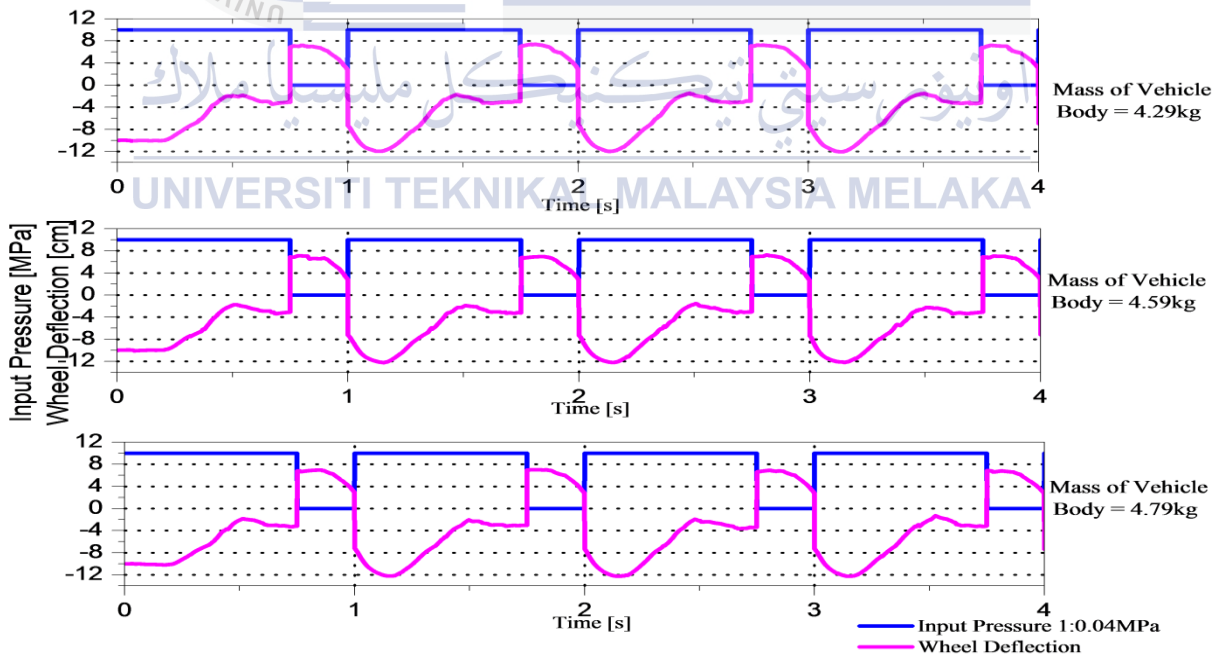
Figure C12: Wheel deflection of Experiment B

Experiment C
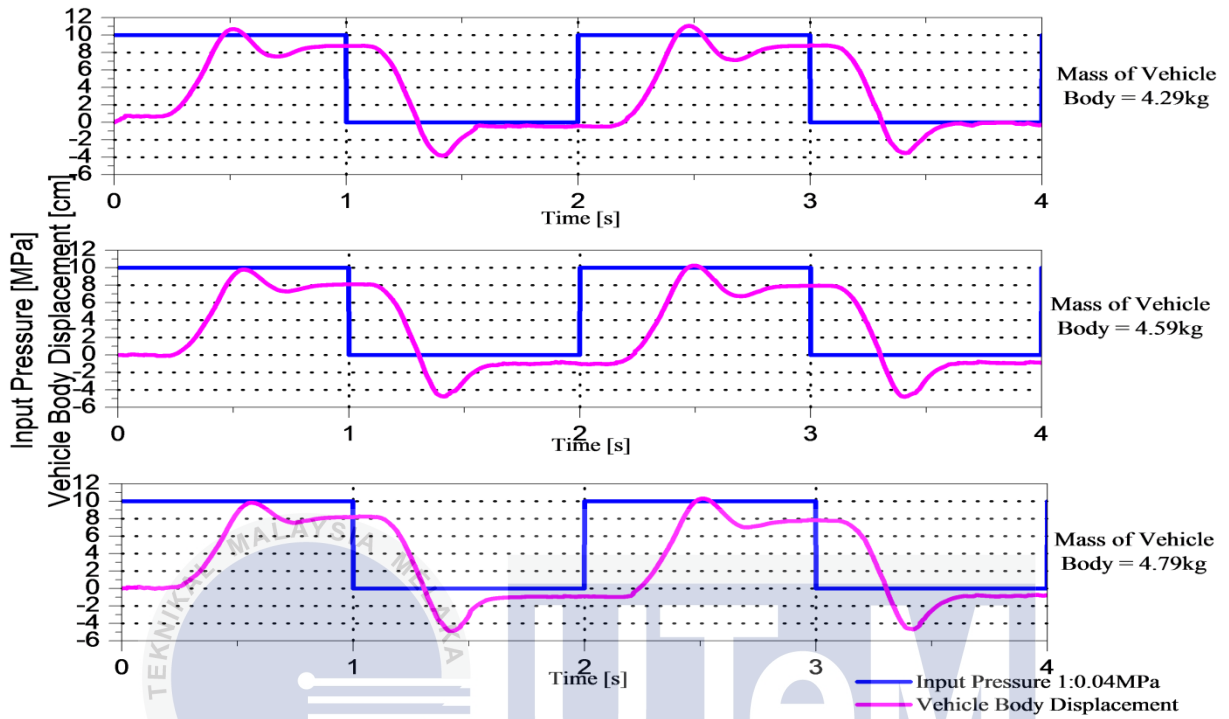
Figure C13: Vehicle body displacement of Experiment C
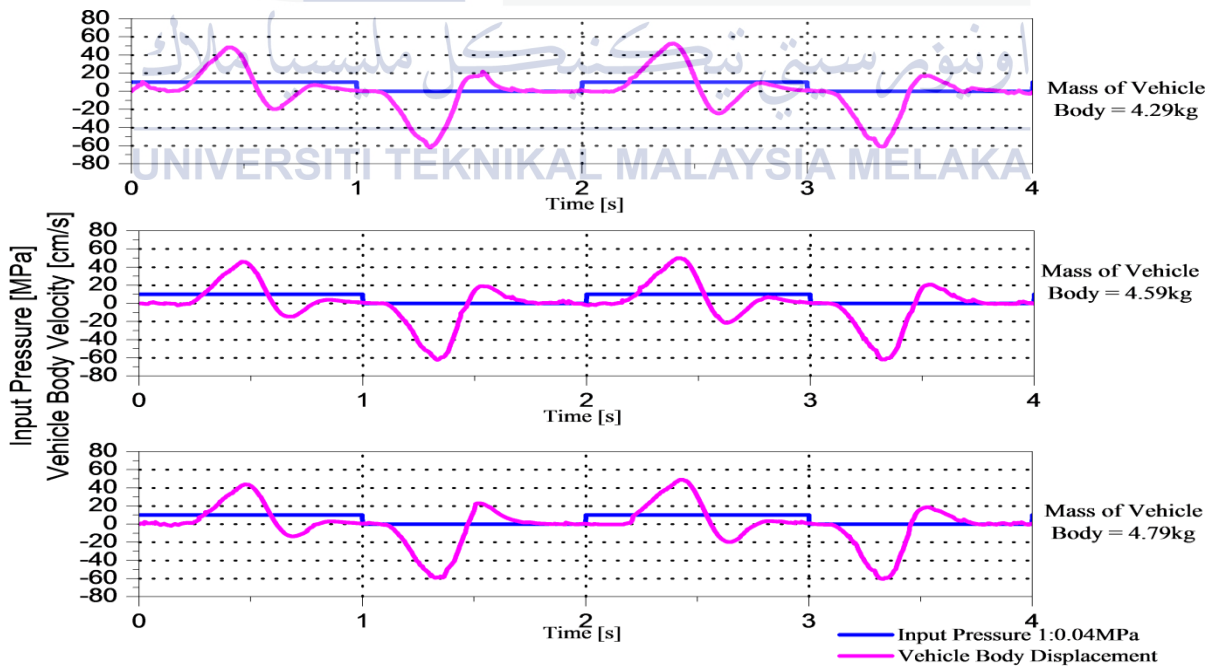
Figure C14: Vehicle body velocity of Experiment C
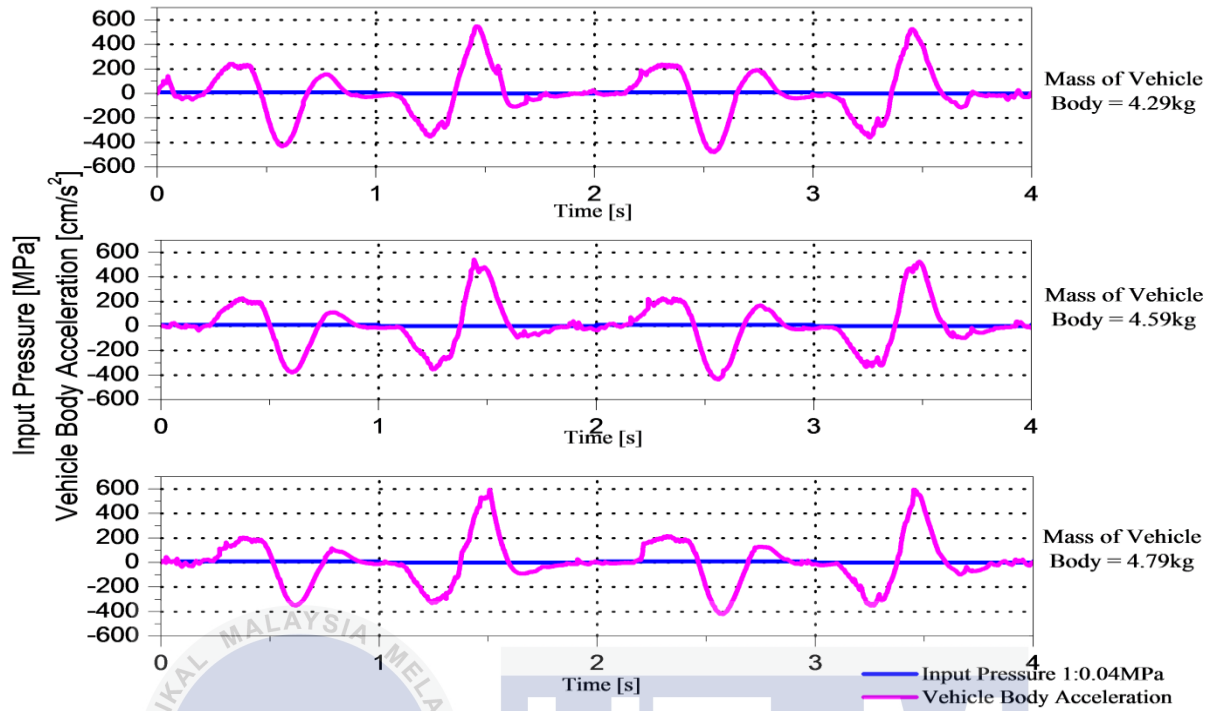
Figure C15: Vehicle body acceleration of Experiment C
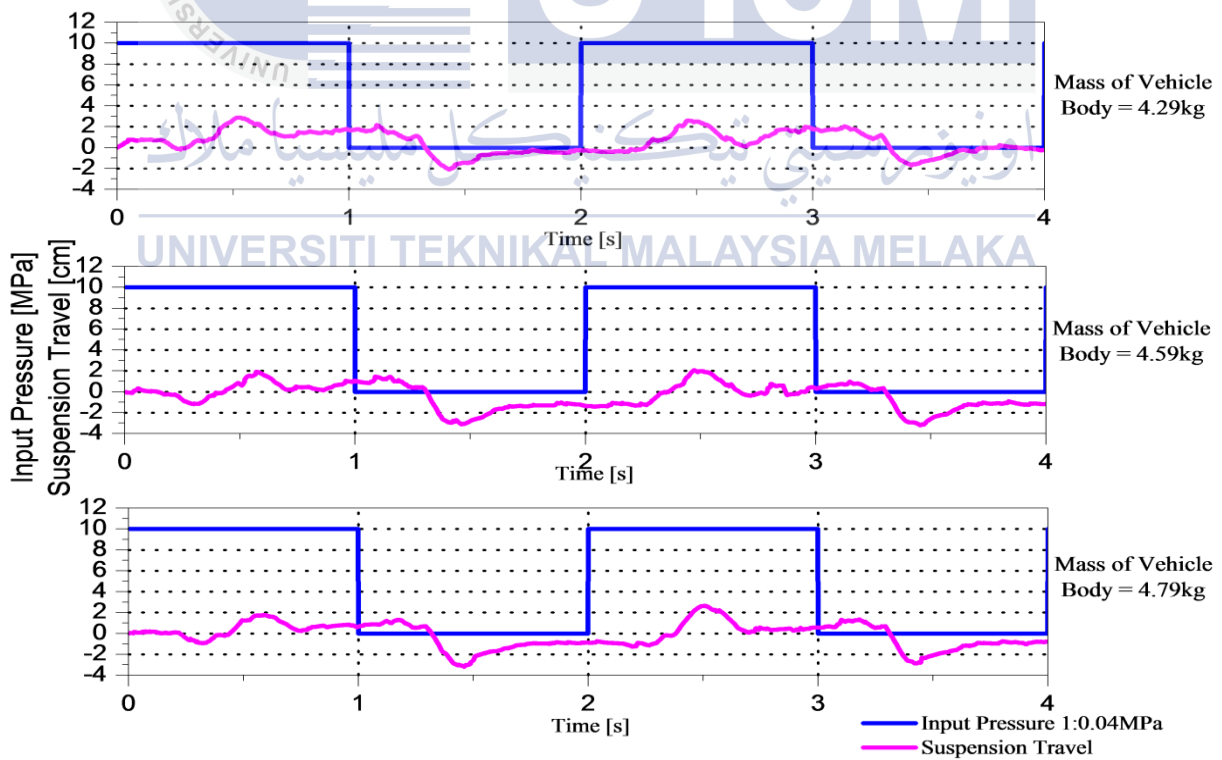
Figure C16: Suspension travel of Experiment C
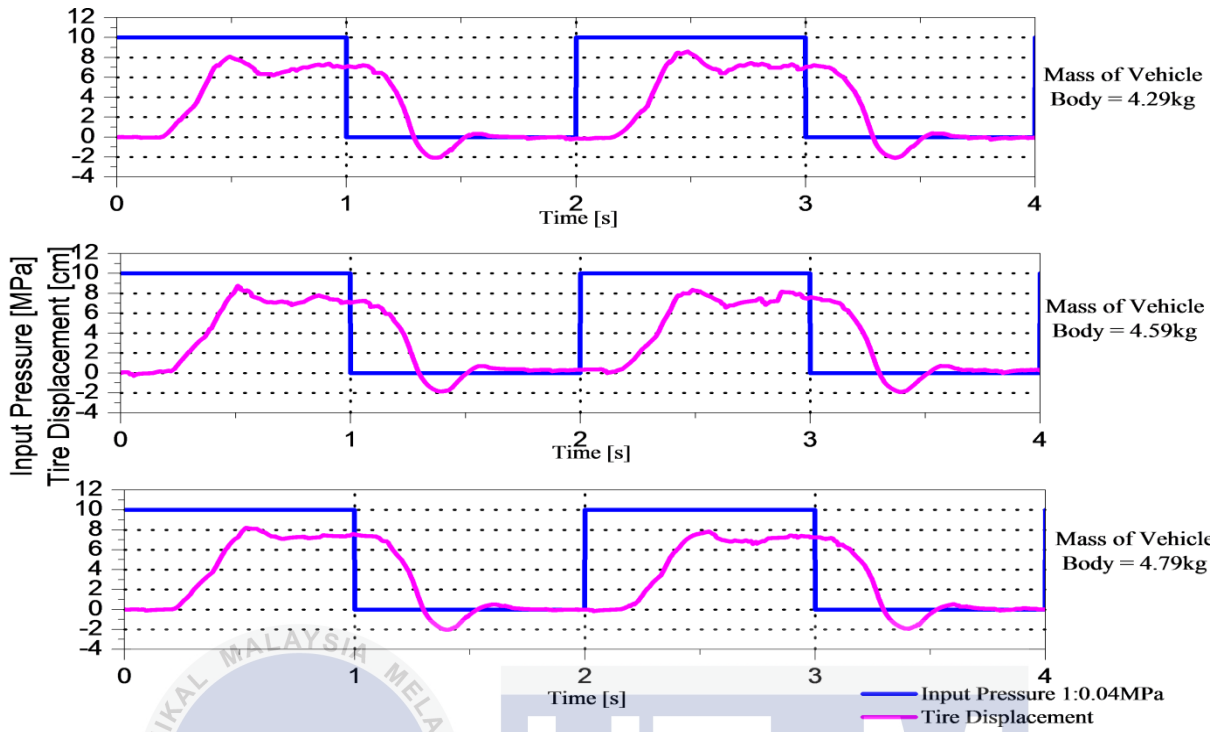
Figure C17: Tire displacement of Experiment C
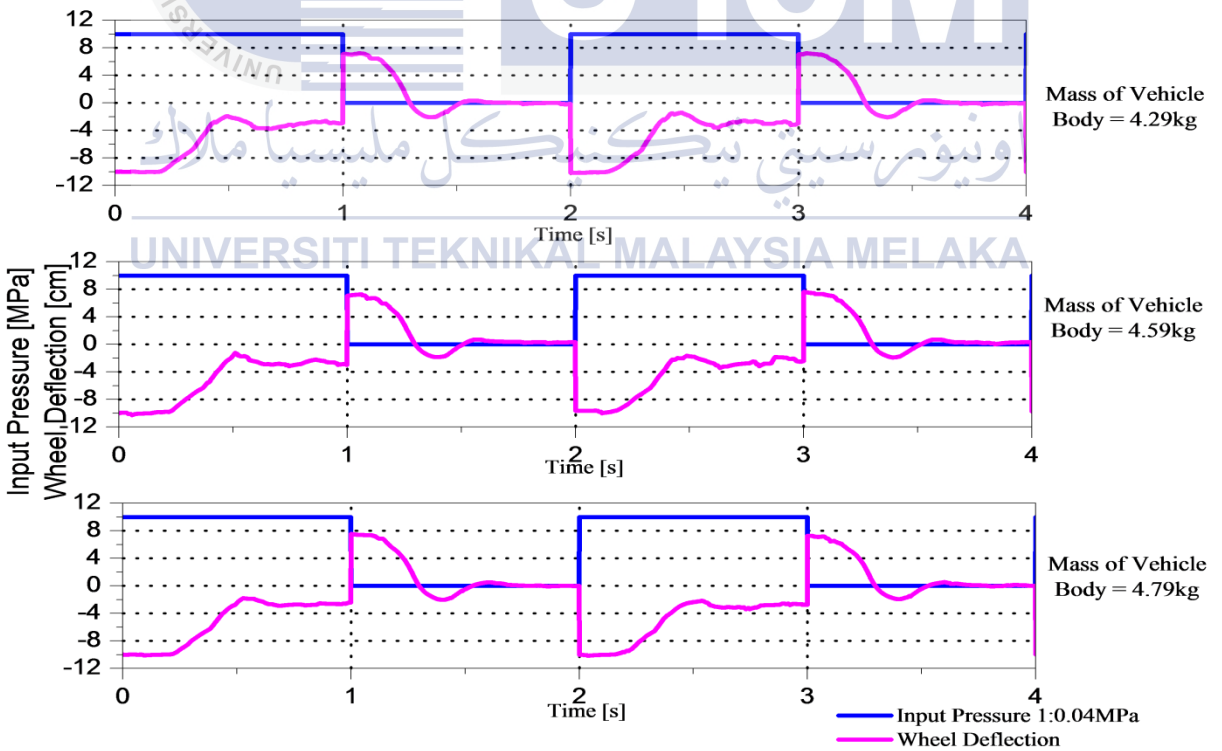
Figure C18: Wheel deflection of Experiment C

Experiment D
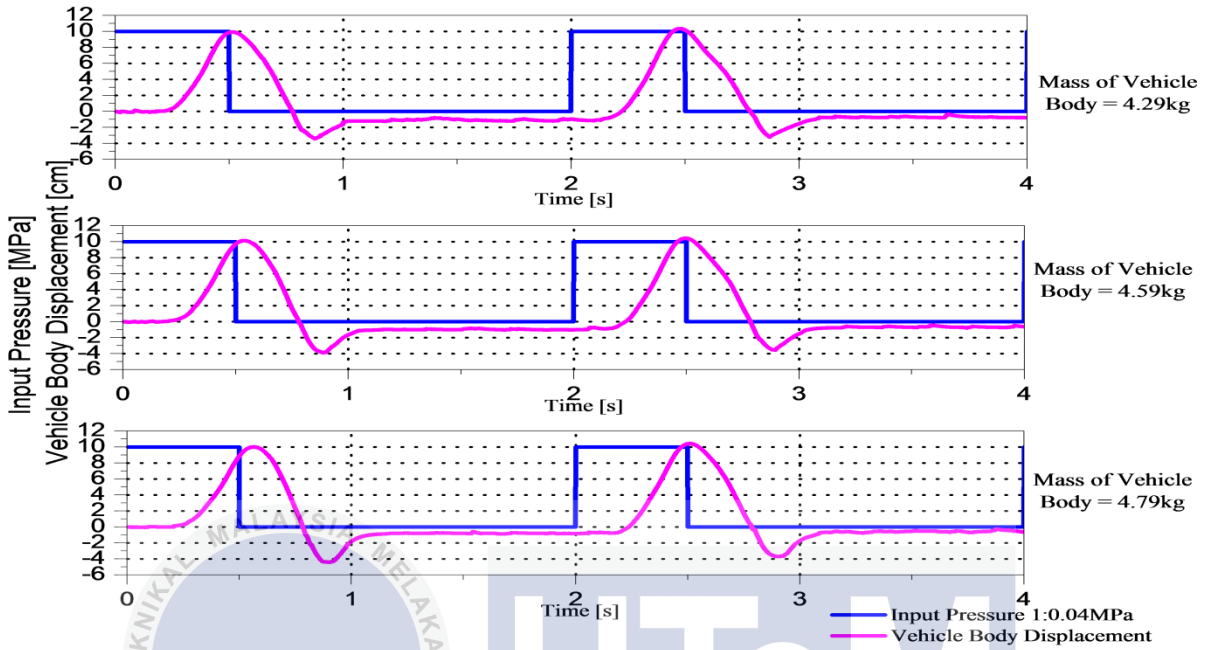
Figure C19: Vehicle body displacement of Experiment D
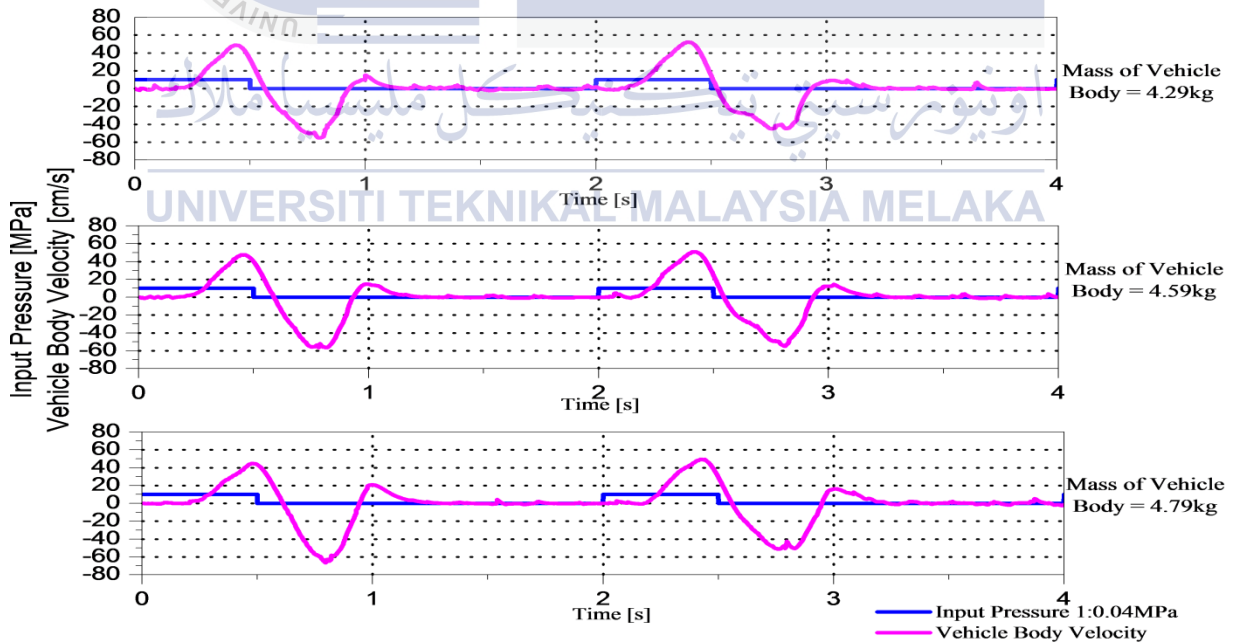
Figure C20: Vehicle body velocity of Experiment D
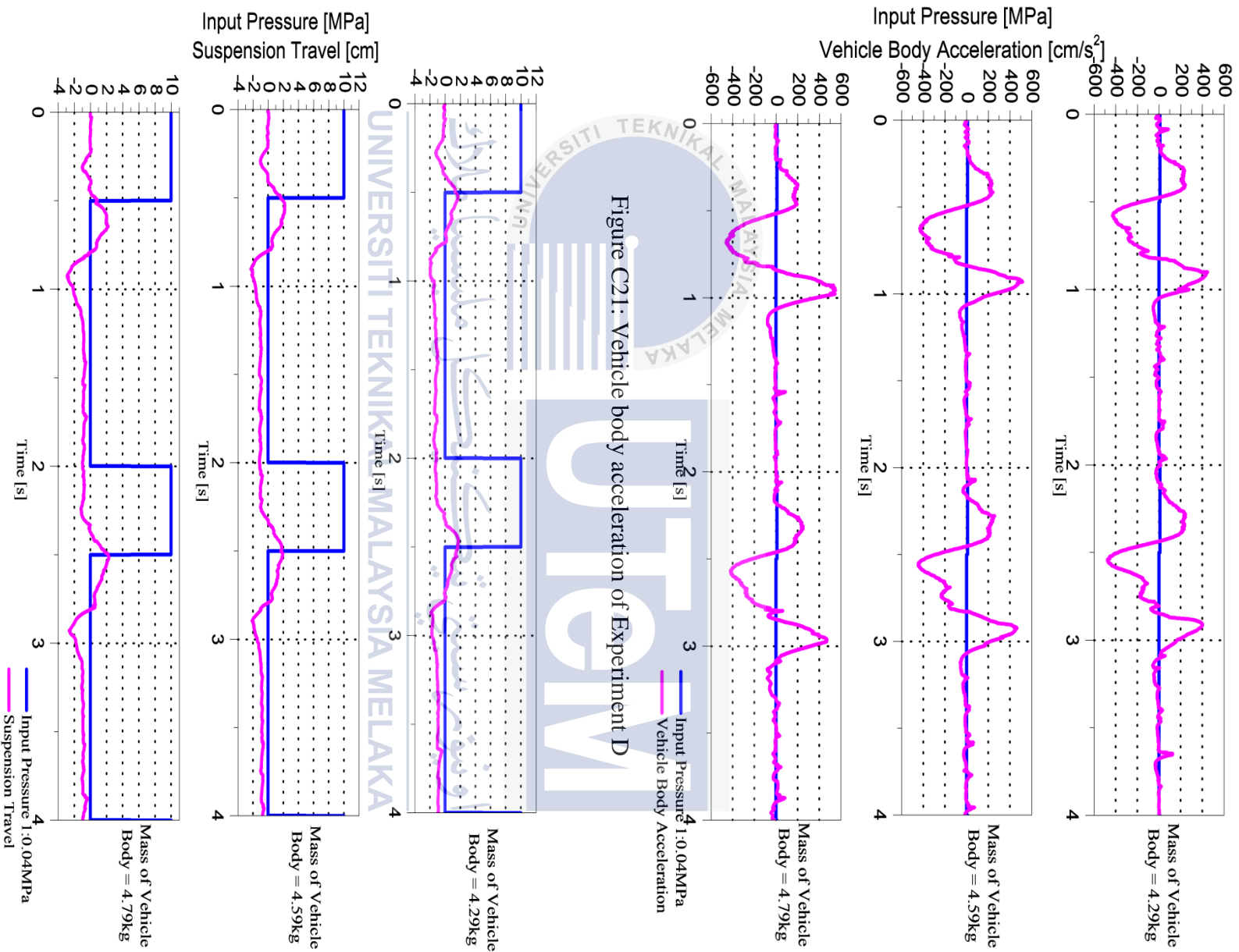
Figure C21: Vehicle body acceleration of Experiment D

Figure C22: Suspension travel of Experiment D
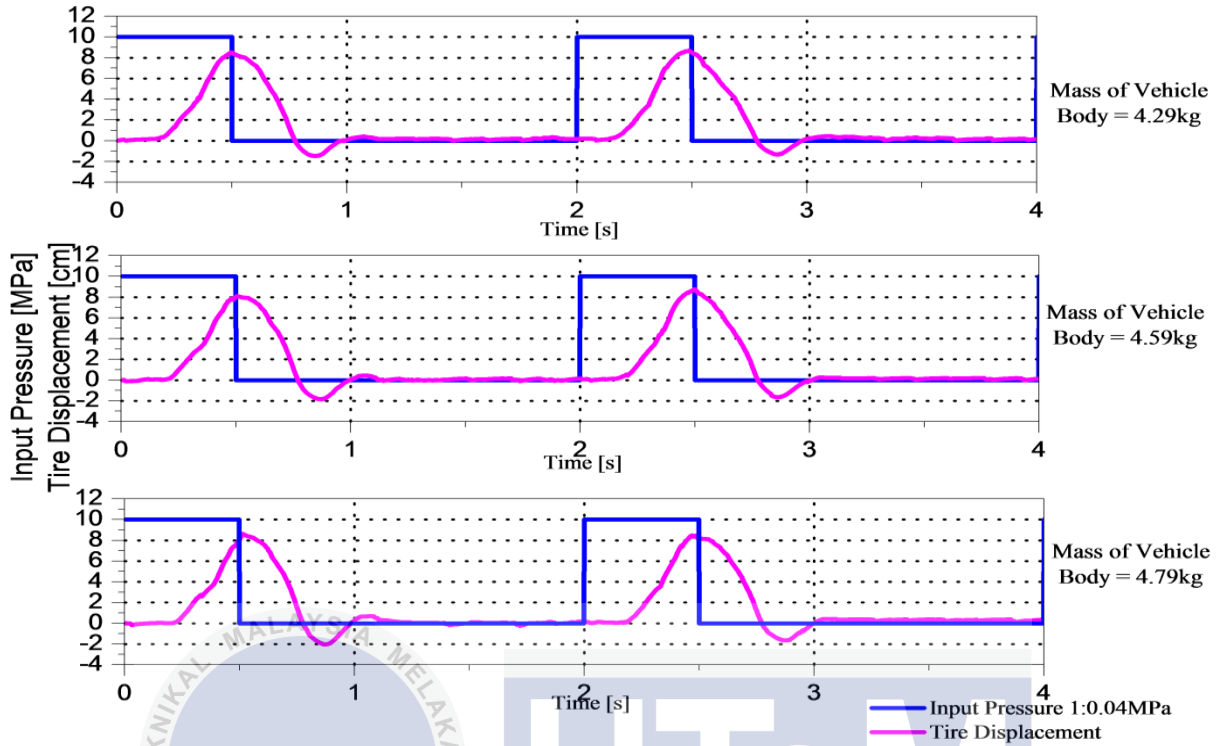
Figure C23: Tire deflection of Experiment D
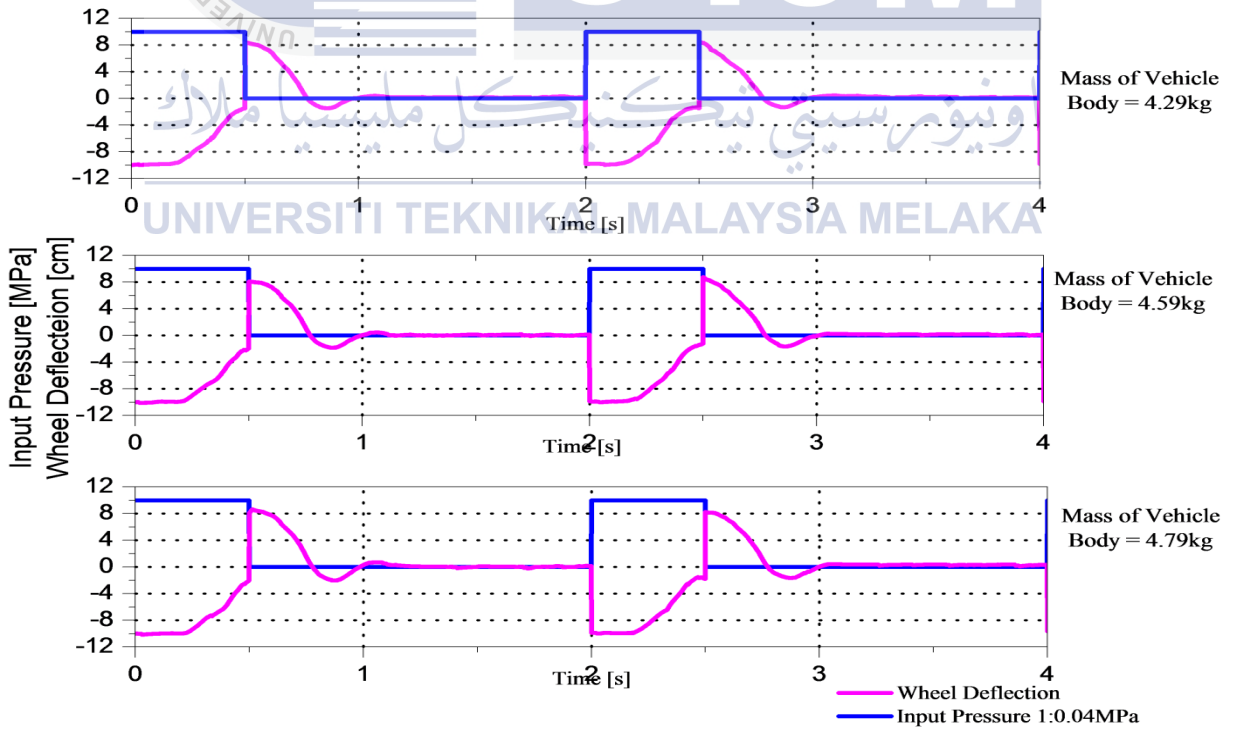
Figure C24: Wheel deflection of Experiment D